Thick braids and other non-trivial homotopy in configuration spaces of hard discs

Patrick Ramsey
School of Mathematical Sciences
Lancaster University

October 24, 2025

This thesis is submitted for the degree of *Doctor of Philosophy*.

Abstract

We study ordered configuration spaces of hard discs inside a unit disc, focusing in some cases on small numbers of discs, but generalising where possible. These are a natural generalisation of ordered configuration spaces of points inside the unit disc. As the radius of the hard discs increases, the homotopy-type is known to change at finitely many 'critical radii', and we classify the critical radii for between one and five discs. We study the configuration spaces just above the least critical radius through their homotopy groups (which are generated by non-contractible maps from the sphere into the configuration space). By observing that the disc centres cannot all lie on one line in the unit disc, we find a non-contractible S^{n-3} in the configuration space of n discs just beyond the first critical radius, which vanishes below this radius. In the case $n = 4$, we find a circle action on the configuration space beyond the first critical radius, and construct the quotient space. By retracting the quotient space onto a graph, we show that the configuration space is homotopy-equivalent to the product of a circle with a graph of Euler characteristic 11. We explore the persistence of the non-contractible S^{n-3} beyond the first critical radius as the unit disc is deformed into an ellipse, and demonstrate that there remains a non-contractible map from S^{n-3} into the configuration space of n hard discs inside an ellipse of any eccentricity. We consider the homotopy groups in dimension less than $n - 3$ of configuration spaces of hard discs inside a unit disc beyond the first critical radius. We conjecture that these are isomorphic to the homotopy groups in the same dimension of the configuration space of points. We suggest a method of proof by defining a flow on the configuration space with certain properties, and demonstrate such a flow on the configuration space of three points.

Contents

Acknowledgements

I would like to thank my supervisor, Dr. Jonny Evans, for his support and advice throughout the my research in the last four years, and for his flexibility in exploring a variety of research topics with me while I searched for an open question I was enthusiastic about. I am grateful for the advice of Dr. Hannah Alpert, who directed me towards the *Applied Algebraic Topology Research Network* and helped me to understand where my work sits in the field. I would also like to thank Matthew Buck for being available to discuss maths with, and anyone else in the School of Mathematical Sciences at Lancaster University who showed interest in my research or otherwise supported my mathematical development through organising or participating in seminars and reading groups. Finally, I would like to thank my friends, family and everyone else who has given me moral or practical support during my PhD.

Author's Declaration

I hereby declare that all work in this thesis is my own. This work has not been published in this form, nor submitted for assessment towards any other degree.

Chapter 1

Introduction

We consider $\mathrm{Conf}_{n,r}(U)$, the ordered configuration space of n hard discs of radius r in a (typically convex) subset $U \subset \mathbb{R}^2$. By hard discs, we mean non-intersecting open metric balls $B(x,r) \subset \mathbb{R}^2$ under the standard Euclidean metric. This is a natural generalisation of $\mathrm{Conf}_n(U)$, the ordered configuration space of n points in U. However, whereas the topological properties of $\mathrm{Conf}_n(U)$ are well-understood [10, 15, 21] when U is connected and simply-connected (indeed, then the space is homotopy-equivalent to $\mathrm{Conf}_n(\mathbb{R}^2)$, and homeomorphic if U is open), much less is known about $\mathrm{Conf}_{n,r}(U)$, which is topologically highly dependent both on r and U. Here, we use the notation $\mathcal{D} = (D_1, D_2, \ldots, D_n) \in \mathrm{Conf}_{n,r}(U)$ interchangeably with the underlying configuration $x = (x_1, \ldots, x_n) \in \mathrm{Conf}_n(U)$ (where $D_i = B(x_i, r)$), and we write $\bigcup x \coloneqq \bigcup_{i=1}^n \{x_i\}$, $\bigcup \mathcal{D} \coloneqq \bigcup_{i=1}^n D_i$. Throughout the thesis, we primarily consider the case where U is the unit disc D^2, in which case we drop U from the notation.

1.1 Development of the field from applied mathematics

Configuration spaces of hard discs were proposed as a model for understanding phase transitions by physicists in the mid 2000s [9, 31]. This model is based on the idea (summarised in [26]) that particles (i.e. atoms or molecules) in sufficiently close proximity exert a repulsive force on each other. This gives to each particle a 'potential energy' (which we can think of as the energy this particle would gain if we allowed the repulsive force to push it away to an infinite distance in the absence of other forces). Then each particle i generates a radial 'potential energy field' $V_i(r)$, in the sense that if another

particle j is at a distance r from i, then i contributes $V_i(r)$ to the total potential energy of j. A common model for this field is

$$V_i(r) = \begin{cases} \infty & : \ r < r_i \\ 0 & : \ \text{otherwise} \end{cases}$$

for some positive real r_i. Under this model, it is impossible for the distance between i and j to be less than r_i, since conservation of energy means that no particle can have infinite potential energy. If we choose some $r_0 > 0$ and assume $r_j = 2r_0$ for all particles j, then any two particles must be separated by a distance of at least $2r_0$ – equivalently, we can replace each particle by a hard disc of radius r_0. Thus the configuration space of particles is modelled by $\mathrm{Conf}_{n,r_0}(U)$ for some container U, where n is the number of particles. The free energy of the configuration is typically decreasing as r_0 increases; therefore, as the temperature (and thus the energy) increases (resp. decreases), r_0 must decrease (resp. increase). At low temperatures, r_0 is large and thus the particles obstruct each other significantly. This disconnects the configuration space, and forces the particles to lie in a near-lattice configuration, which is equivalent to the solid state. In the study of phase transitions, the configuration space is often studied in the 'thermodynamic limit' $n \to \infty$, $r^d = \frac{c}{n}$ with c a constant and d the dimension of U, which fixes the total volume of the discs.

Configuration spaces have also received some interest from the field of topological robotics [16]. Here, a configuration space may be used to model some physical area or volume, such as a warehouse, containing some autonomous robots which can move within this area. Much of the work here focuses on 'topological complexity'. Given a topological space X, consider the map $\pi\colon PX \to X \times X$, where PX is the path space on X (the set of continuous maps $[0,1] \to X$ given the compact-open topology) and $\pi(\gamma) \coloneqq (\gamma(0), \gamma(1))$. A motion planning algorithm is a section of π, that is, a map $s\colon X \times X \to PX$ such that $\pi \circ s = 1_{X \times X}$. It is natural to want the motion planning algorithm to be continuous, but this is not possible for all X. We measure how far away we are from having a continuous motion planning algorithm using the topological complexity of X, $TC(X)$. This is defined to be the least k such that there exists a motion planning algorithm s and a partition $X \times X = \bigsqcup_{i=1}^{k} F_i$ such that $s|_{F_i}$ is continuous for all i. Then the existence of a continuous motion planning algorithm is equivalent to $TC(X) = 1$. According to [16, Lemma 4.2], $TC(X) = 1$ if and only if X is contractible. In this thesis, we study the

homotopy groups of configuration spaces of hard discs (see §1.3). Since the homotopy groups count (in a crude sense) topological holes of each dimension, this work measures (crudely) how far the configuration spaces of discs are from having a continuous motion planning algorithm.

1.2 Homotopy type, Morse theory and critical radii

More recently, mathematicians have begun to explore these configuration spaces abstractly, seeking to derive information about them through topological invariants. The topological invariants of a space, which include topological complexity [16, Cor. 4.27], homotopy groups and (co)homology [22, §2.1, §3.1], are completely determined by its homotopy type, which is defined as follows.

Definition 1.2.1. Take topological spaces $A \subset X$ and Y. We say that two continuous maps $f\colon X \to Y$ and $g\colon X \to Y$ are homotopic, denoted $f \simeq g$, if there is a continuous map $H\colon [0,1] \times X \to Y$ such that $H(0,x) = f(x)$ and $H(1,x) = g(x)$ for all $x \in X$. We say furthermore $f \simeq g$ rel A if $H(t,x) = f(x) = g(x)$ for all $t \in [0,1], x \in A$.

Definition 1.2.2. Take topological spaces X, Y. We say these are homotopy equivalent (or, of the same homotopy type), denoted $X \simeq Y$, if there are continuous $f\colon X \to Y$, $g\colon Y \to X$ such that $g \circ f \simeq 1_X$ and $f \circ g \simeq 1_Y$; then, we say that g is a homotopy inverse to f.

Homotopy equivalence is commonly understood as equivalence up to deformation.

A major mathematical step in the understanding of configuration spaces was the application of 'min-type' Morse theory, an analogue to Morse theory developed for a certain class of non-smooth functions, to the problem. In classical Morse theory [27], we give to a manifold M a differentiable function $f\colon M \to \mathbb{R}$. Then we can find a vector field V on M (typically we choose the gradient field ∇f) such that the vector at each regular (i.e. non-critical) point of f is non-zero, and f increases along the flow lines of V. This allows us to understand M by looking at the superlevel sets $M^b \coloneqq f^{-1}[b,\infty)$ as b decreases. Specifically, if there is an interval $[a,b]$ containing no critical values, then we can define a flow which retracts the region $f^{-1}[a,b]$ onto $f^{-1}(b)$ by flowing each point in this region along the vector field, and fixes every point in M^b. We call such a flow a *strong deformation retraction*, and say that M^b is a *strong deformation retract* of M^a

[29, p. 30]. A strong deformation retraction is, in particular, a homotopy-equivalence $M^b \simeq M^a$ (although not all homotopy equivalences are strong deformation retractions). Thus, as b decreases, the homotopy type of M^b changes only at the critical values; if we can understand how the homotopy type changes at each critical point, then we can understand the whole manifold.

Min-type Morse theory extends the methods of Morse theory to min-type Morse functions: functions which are a minimum over some set of Morse functions. Baryshnikov *et al.* [11] developed the tautological function $\tau\colon \mathrm{Conf}_n(U) \to \mathbb{R}$ given by

$$\tau(x) = \min\left\{\min\left\{\frac{1}{2}|x_i - x_j| \mid i \neq j\right\}, \min\left\{\mathrm{dist}(x_i, \partial D^2) \mid 1 \leq i \leq n\right\}\right\}$$

where $\mathrm{dist}(x_i, \partial D^2) = \min\left\{|x_i - p| \mid p \in \partial D^2\right\}$. By construction, $\tau(x)$ is the greatest $r \in \mathbb{R}$ such that if we replace each x_i with the ball $B(x_i, r)$, the result $\mathcal{D}_r(x) \coloneqq (B(x_1, r), \ldots, B(x_n, r))$ is a valid configuration of $\mathrm{Conf}_{n,r}(U)$. Thus $\mathrm{Conf}_{n,r}(U) = \tau^{-1}[r, \infty)$. τ is a min-type Morse function, and the authors develop the notion of a *balanced stress graph* (see Figs. 1.1, 2.1) to play the role of a critical point.

Definition 1.2.3. Let $\mathcal{D} \in \mathrm{Conf}_{n,r}(U)$. The *stress graph* of $\mathcal{D}$, $N(\mathcal{D})$, consists of:

- A vertex at each x_i, called an *interior vertex*,
- A vertex at each point of contact between any disc and ∂U, called a *boundary vertex*,
- For each boundary vertex, a straight *boundary edge* joining it radially to the interior vertex of the disc on which the boundary vertex lies (this edge will be orthogonal to ∂U),
- For each pair of touching discs, a straight *interior edge* joining the corresponding interior vertices.

Let $x \in \mathrm{Conf}_n(U)$. The stress graph of x is $N(x) \coloneqq N\left(\mathcal{D}_{\tau(x)}(x)\right)$.

The edges of $N(x)$ correspond to the points x_i such that $\mathrm{dist}(x_i, \partial D^2) = \tau(x)$ and the pairs x_i, x_j such that $|x_i - x_j| = 2\tau(x)$. In order for τ to increase along the flow lines of a vector field V, each of these distances must be increasing along V near x. Conversely, Baryshnikov *et al.* show that if we can find a submanifold $M \subset \mathrm{Conf}_n(U)$ and a vector V_x at each $x \in M$ such that all the edge lengths of $N(x)$ are increasing along V_x locally,

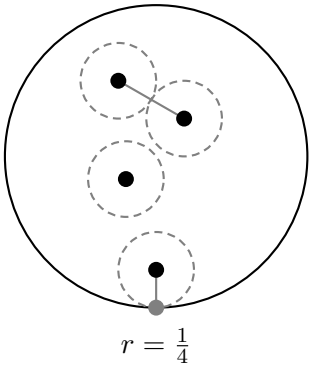

Figure 1.1: A configuration x of points in D^2 (black) with its stress graph (grey). Each point of x is contained in a circle (grey, dashed), where the radius of these discs is the greatest achievable without any discs overlapping each other or leaving the unit disc. At each point of contact between discs, or between a disc and ∂D^2, an edge joins the corresponding vertices.

then we can always construct a vector field V on M such that τ is increasing along V. Thus, for any $0 < r < s$, there are two possibilities:

1. $\tau^{-1}[r, s)$ admits a vector field V such that τ is strictly increasing along the trajectories of V everywhere. Hence we can retract $\tau^{-1}[r, s]$ onto $\tau^{-1}(s)$ along the flowlines of V, so $\mathrm{Conf}_{n,r}(U) \simeq \mathrm{Conf}_{n,s}(U)$.

2. There exists $x \in \tau^{-1}[r, s)$ such that there is no suitable choice of V_x. We call x a *critical configuration*, and $\tau(x)$ a *critical radius*.

In this way, stress graphs allow us to understand the critical configurations: these are the configurations where the edges of the stress graph push against each other and against ∂U in such a way that there is no room for all the edges to lengthen simultaneously. It turns out, by Farkas' Lemma from linear algebra, that if x is a critical configuration, then we can choose the magnitude of the force on each edge of $N(x)$ so that the total force on each vertex is 0, and so is the total force exerted on the boundary by each component.

Definition 1.2.4. Take $x \in \mathrm{Conf}_n$, and let E be the set of edges of $N(x)$. A *weighting* on $N(x)$ is a map $w\colon E \to [0, \infty)$, where $w_e \coloneqq w(e)$ defines the force with which each edge pushes on its endpoints. More precisely, given an edge e incident to x_i, let $v_{i,e}$ denote the other vertex on e – so $v_{i,e}$ is either x_j for some $j \neq i$, or $\frac{x_i}{|x_i|}$ if e is a boundary

edge. Then e exerts a force $w_e(x_i - v_{i,e})$ on x_i. If x_i is adjacent to the boundary via an edge e, then e exerts a force $w_e\left(\frac{x_i}{|x_i|} - x_i\right)$ on the boundary.

We say that w is *balanced* if the total force $F_i \coloneqq \sum_{e \text{ incident to } x_i} w_e(x_i - v_{i,e})$ on each interior vertex x_i is zero. $N(x)$ is a *balanced stress graph* if it has a non-trivial balanced weighting.

In [11], the authors give a second condition in the definition of a balanced weighting: in each connected component $G \subset N(x)$, the total force exerted on the boundary by the boundary edges is zero.. However, this condition is a consequence of the condition that $F_i = 0$ for all i. We will show this in Lemma 2.0.2.

We will typically use the term critical configuration to refer to all configurations with a balanced stress graph, and we will sometimes treat w as part of the information contained in the stress graph.

In summary, we obtain:

Fact 1.2.5. *If $[r, s)$ does not contain a critical radius of τ, then $\mathrm{Conf}_{n,r}(U) \simeq \mathrm{Conf}_{n,s}(U)$. The critical radii are characterised by balanced stress graphs.*

Around the same time as this Morse-theoretic approach was being developed, authors began trying to find these critical configurations for small n, e.g. [13], using numerical techniques. These approximate the repulsive forces from the stress graph by a smooth function inversely proportional to r^n, where r is the distance between two given points, using this to define a flow on the configuration space. The greater the value of n, the more like the hard disc case the simulation behaves. The authors aimed to find 'wells of attraction' - configurations where the total force on each particle is (nearly) zero, and where nearby configurations naturally flow towards these wells. These can then be confirmed as critical points analytically. However it is not certain that this technique finds all critical points.

The most significant research into the case $U = D^2$ comes from Alpert [1], who considers the natural inclusion $\iota\colon \mathrm{Conf}_{n,r} \to \mathrm{Conf}_n$ and its pullback to cohomology $\iota^*\colon H^*(\mathrm{Conf}_n) \to H^*(\mathrm{Conf}_{n,r})$. Using geometric arguments, Alpert proves:

Fact 1.2.6. *The least critical radius of Conf_n is $\frac{1}{n}$. The stress graph of the corresponding configuration is a diameter of D^2 containing all n points – that is, all the points lie*

on a common diameter, and there is some non-repeating sequence $i_1, \ldots, i_n$ *containing the integers in* $[1, n]$ *such that* x_{i_1} *and* x_{i_n} *are at distance* $\frac{1}{n}$ *from the boundary, and* $|x_{i_k} - x_{i_{k+1}}| = \frac{2}{n}$ *for all* $1 \leq k \leq n-1$.

Fact 1.2.7. *If* Conf_n *has a critical configuration whose stress graph is not just a diameter, then the corresponding radius is greater than* $\frac{3}{2n+3}$.

Alpert then considers the change in $\ker \iota^*$ as r increases. The author shows that $\ker \iota^*$ becomes non-trivial at the first critical radius, $\frac{1}{n}$, and in the case $n = 4$, it also increases in size at $r = \frac{1}{3}$ and $r = \sqrt{2} - 1$. We show in §2 that this is all the critical radii of Conf_4.

The majority of recent research in the area has focused broadly on finding additional structure in the homology and cohomology of the configuration spaces of hard discs inside an infinite strip [5, 3, 7, 32, 33], although some work has also looked at topological complexity [34]. There also exists some similar research into configuration space of polygons, primarily squares [2, 4, 6, 28].

1.3 Braids and homotopy groups of configuration spaces of points

In this thesis, we will derive information about the homotopy groups of $\mathrm{Conf}_{n,r}$ for different values of n and r. Here, we discuss these groups and, in particular, the homotopy groups of configuration spaces of points.

Let X be a topological space, and let $\Omega^m_x X$ be the set of maps of pairs $(I^m, \partial I^m) \to (X, \{x\})$, where $I = [0, 1]$. Since $S^m = I^m / \partial I^m$, it will often be easier to think of these as basepoint-preserving maps $(S^m, *) \to (X, x)$. The m-th homotopy group [22, pp. 25-28, 340-341] is $\pi_m(X, x) = \Omega^m_x X / \simeq$, where $\simeq$ represents homotopy rel $\{*\}$ (see Def. 1.2.1). We write $[\gamma]$ for the homotopy class containing $\gamma \colon (S^m, *) \to (X, x)$. It is common to drop x from the notation, especially where X is path-connected. $\pi_1(X, x)$ is called the fundamental group of X. We say a space X is aspherical if $\pi_m(X) = 0$ for all $m \geq 2$, and we call X an Eilenberg-MacLane space of type $K(G, k)$ (or just a $K(G, k)$) if $\pi_k(X) = G$ and $\pi_m(X) = 0$ for all $m \neq k$.

$\pi_m(X)$ has a well-defined group structure under concatenation. Given $[\gamma], [\delta] \in \pi_m(X)$, the concatenation $\delta \cdot \gamma$ is found as follows.

1. Take some equator S^{m-1} which passes through $*$ and collapse it to a point. S^m/S^{m-1} is a wedge of two spheres (i.e. a union where the intersection consists of precisely one point, $*$).

2. Apply γ to the first sphere of S^m/S^{m-1}, and δ to the second sphere.

Then we define $[\delta] \cdot [\gamma] = [\delta \cdot \gamma]$. The identity of $\pi_m(X)$ is $[c]$, where c is the constant function $p \mapsto x \ \forall p \in S^m$. The inverse of $[f] \in \pi_m(X)$ is found by the composition of f with some orientation-reversing map $S^m \to S^m$. Concatenation is abelian for $m \geq 2$. π_m is a homotopy-invariant, and we reproduce the proof below in Lemmas 1.3.1 and 1.3.2.

Lemma 1.3.1. *Let X, Y be topological spaces, $x \in X$, and $f\colon X \to Y$ a continuous map. Then f induces a homomorphism $f_*\colon \pi_m(X) \to \pi_m(Y)$ for all $m \in \mathbb{N}$.*

Proof. Let $\gamma\colon (S^m, *) \to (X, x)$ be a basepoint-preserving continuous map, which represents a class in $\pi_m(X, x)$. Then $f \circ \gamma\colon (S^n, *) \to (Y, f(x))$ is a basepoint-preserving continuous map.

We first check this descends to a well-defined map on homotopy classes. Suppose there is some $\gamma'\colon (S^m, *) \to (X, x)$ such that $\gamma \simeq \gamma'$. Then there is a homotopy rel basepoints, $H\colon [0,1] \times S^m \mapsto X$, between γ and γ'. Hence $f \circ H\colon [0,1] \times S^m \mapsto Y$ is a homotopy rel basepoints between $f \circ \gamma$ and $f \circ \gamma'$, as required. Thus f induces a map $f_*\colon \pi_m(X) \to \pi_m(Y)$ defined by $f_*[\gamma] = [f \circ \gamma]$.

If c is the constant map, then $f \circ c$ is also constant. Thus f_* preserves the identity.

Take $[\gamma], [\delta] \in \pi_m(X, x)$. If we choose the same equator S^{m-1} in each case, it is immediate that $f \circ (\delta \cdot \gamma)(p) = (f \circ \delta) \cdot (f \circ \gamma)(p)$ for all $p \in S^m$.

Finally, take $[\gamma] \in \pi_m(X, x)$. Both $f_*([\gamma]^{-1})$ and $(f_*[\gamma])^{-1}$ are represented by the map $S^m \to S^m \xrightarrow{\gamma} X \xrightarrow{f} Y$, where the first map is orientation-reversing, thus the maps are equal. □

Lemma 1.3.2. *Let X, Y be topological spaces such that $f\colon X \xrightarrow{\simeq} Y$, and let $x \in X$. Then $f_*\colon \pi_n(X, x) \cong \pi_n(Y, f(x))$.*

Proof. We aim to show that f_* is a bijection, and thus (by Lemma 1.3.1) an isomorphism.

Denote by $g\colon Y \to X$ a homotopy-inverse to f.

First, let $[\gamma], [\delta] \in \pi_m(X, x)$ be such that $f_*[\gamma] = f_*[\delta]$. Then $f \circ \gamma \simeq f \circ \delta$, and therefore $\gamma = \mathrm{id}_X \circ \gamma \simeq g \circ f \circ \gamma \simeq g \circ f \circ \delta \simeq \mathrm{id}_X \circ \delta = \delta$, that is $[\gamma] = [\delta]$. Thus f_* is injective.

Now, take $[\delta] \in \pi_m(Y, f(x))$, and let $\gamma = g \circ \delta$. Then $f \circ \gamma = f \circ g \circ \delta \simeq \mathrm{id}_Y \circ \delta = \delta$, that is $f_*[\gamma] = [\delta]$. Thus f_* is surjective. □

For sufficiently nice spaces, we also have the converse by Whitehead's theorem [22, Thm. 4.5]: if X, Y are CW-complexes and $f\colon X \to Y$ a continuous map such that f_* is an isomorphism in every dimension, then f is a homotopy equivalence.

We now consider $X = \mathrm{Conf}_n$ for some $n \in \mathbb{N}$. Conf_n is known to be aspherical (that is, it has trivial m-th homotopy group for all $m \geq 2$) [15, Cor. 2.2]. $\pi_1(\mathrm{Conf}_n)$ is known as the *pure braid group* on n strings PBr_n [21]. Given a pure braid $f\colon (I, \{0,1\}) \to (\mathrm{Conf}_n, \{x\})$, the associated geometric braid $\Gamma_f = \bigcup_{t\in[0,1]}(\{t\} \times \bigcup f(t)) \subset I \times D^2$ consists of n labelled, pairwise disjoint 'strings' (i.e. homeomorphic images of the closed unit interval), where each slice $\{t\} \times D^2$ is a picture of the configuration $f(t) \in \mathrm{Conf}_n$. The slices at $t = 0$ and $t = 1$ are identical, including labelling. Each string represents the path of one point in the configuration throughout the path f. We can show a geometric braid using a *braid diagram*.

Definition 1.3.3. Choose a (not necessarily orthogonal) projection $\pi\colon D^2 \to (-1,1) \times \{0\} \to (-1,1)$ from D^2 onto the x-axis. Let $f\colon (I, \{0,1\}) \to (\mathrm{Conf}_n, \{x\})$ be continuous. Then the braid diagram (Fig. 1.2) of f consists of two pieces of information:

1. The image of Γ_f under $\mathrm{id}_{[0,1]} \times \pi\colon [0,1] \times D^2 \to [0,1] \times (-1,1)$,
2. At each point where the images of two strings cross (intersect), we record which string passes in front and which passes behind. We show this on the braid diagram by omitting a short section of the string that passes behind on each side of the intersection.

Due to the symmetries of D^2, we will typically choose the basepoint of Conf_4 to be the configuration where the four points lie in a square, with x_1 top-left and the remaining points following in sequence anticlockwise, and we will choose our projection so that the positions of x_1, x_2, x_3, x_4 in the basepoint are projected onto the x-axis $(-1,1) \times \{0\}$ in order, left to right. In accordance with convention, we will draw our braid diagrams so

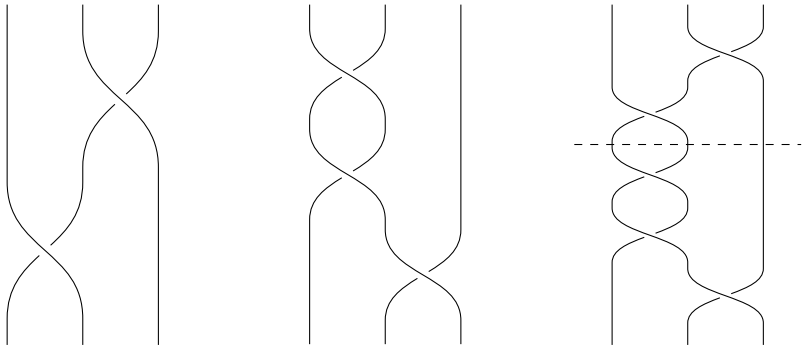

Figure 1.2: The diagrams of two braids α, β and their concatenation $\beta\alpha$. The horizontal dashed line shows where the braids are joined together

the time coordinate (in $[0, 1]$) is vertical, with the top line being 0 and the bottom being 1, and the space coordinate is displayed horizontally.

Conf_n has a natural action by the symmetric group S_n, $\varsigma \cdot (x_1, \dots x_n) = (x_{\varsigma(1)}, \dots, x_{\varsigma(n)})$. In order to understand the pure braid group, we introduce $\mathrm{UConf}_n \coloneqq \mathrm{Conf}_n / S^n$, the unordered configuration space of n points in D^2. As with Conf_n, each braid has an associated geometric braid; since the strings are no longer labelled, it is no longer required that each string return to its own starting point in D^2 (although it remains true that the slices at $t = 0$ and $t = 1$ are identical up to permutation of the labels, so each string ends at the start point of some string). We have $\pi_m(\mathrm{UConf}_n) = 0$ for $m \geq 2$ by [21, Thm. 3.2], and we call $\pi_1(\mathrm{UConf}_n)$ the *braid group* on n strings, Br_n. Each braid induces a permutation on the points – this is a homomorphism $Br_n \to S_n$ – then $PBr_n = \ker(Br_n \to S_n)$ consists of precisely those braids where every string returns to its own starting point. In a braid diagram, the concatenation of braids $\beta\alpha$ is drawn by drawing α, then drawing β directly below it so that the ends of the strings in α line up with the start of the strings in β, and finally rescaling vertically so the braid has height 1 (see Fig. 1.2).

The most common presentation is due to Artin. Consider a geometric braid and associated diagram. Given any braid, we can always obtain a homotopic braid such that no two crossings in the braid diagram take place at the same t. Then we can choose $0 = t_0 < t_1 \dots < t_k = 1$, where k is the number of crossings, such that the slice $[t_i, t_{i+1}] \times (-1, 1)$ contains only one crossing for each $i \in \{0, 1, \dots, k-1\}$ (see Fig. 1.3).

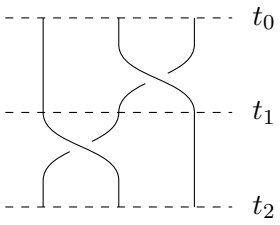

Figure 1.3: A braid diagram on 3 strings. A homotopy on the braid allows us to ensure that only one crossing takes place on each horizontal. Then we can choose some times $t_0 = 0, t_1, \ldots, t_k = 1$ (indicated as dashed lines – here $k = 2$) such that precisely one crossing takes place in each period $[t_i, t_{i+1}]$.

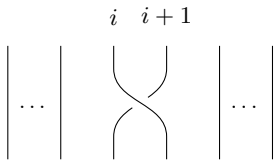

Figure 1.4: The generator σ_i for Br_n

We can further choose our homotopy such that each of these slices is the diagram of a braid – that is, so that the positions of our n points in $\{t_i\} \times (-1, 1)$ are the same, up to reordering, for all i. Thus the braid group is generated by crossings of pairs of strings, where the two strings lie next to each other in the braid diagram. We denote by σ_i ($i \in \{1, \ldots, n-1\}$) (see Fig. 1.4) the crossing where the string in the i-th position crosses in front of the string in the $(i+1)$-th position – that is, where the points in positions i and $i+1$ swap positions by moving anticlockwise around each other. These generators are related by

$$\begin{aligned} \sigma_i \sigma_j &= \sigma_j \sigma_i && \text{if } |i-j| \geq 2 \\ \sigma_i \sigma_{i+1} \sigma_i &= \sigma_{i+1} \sigma_i \sigma_{i+1} && \text{for all } i \in \{1, \ldots, n-1\} \end{aligned}$$

The generators of PBr_n, $s_{ij} = s_{ji}$ ($i < j$), are the braids in which strings i and j wind round each other anticlockwise then return to their own start positions, passing behind any intermediate strings (Fig. 1.5). This can be described, for any $i \leq k < j$, as $s_{ij} = \sigma_i \ldots \sigma_{k-1} \sigma_{j-1}^{-1} \ldots \sigma_{k+1}^{-1} \sigma_k^2 \sigma_{k-1}^{-1} \ldots \sigma_i^{-1} \sigma_{k+1} \ldots \sigma_{j-1}$. In particular,

$$s_{ij} = \sigma_i \ldots \sigma_{j-2} \sigma_{j-1}^2 \sigma_{j-2}^{-1} \ldots \sigma_i^{-1} = \sigma_{j-1}^{-1} \ldots \sigma_{i+1}^{-1} \sigma_i^2 \sigma_{i+1} \ldots \sigma_{j-1}$$

where string i crosses under all the intermediate strings and string j under none in the first expression, and vice versa in the second.

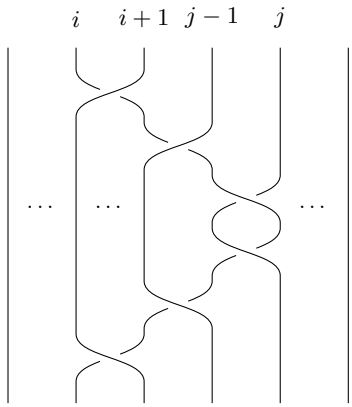

Figure 1.5: The generator $s_{ij} = \sigma_i \dots \sigma_{j-2}\sigma_{j-1}^2\sigma_{j-2}^{-1}\dots\sigma_i^{-1}$ for PBr_n.

We include the following calculation as proof, inductively, that all expressions $\sigma_i \dots \sigma_{k-1}\sigma_{j-1}^{-1}\dots\sigma_{k+1}^{-1}\sigma_k^2\sigma_{k-1}^{-1}\dots\sigma_i^{-1}\sigma_{k+1}\dots\sigma_{j-1}$ $(i \le k < j)$ represent the same braid.

$$\begin{aligned}
&\sigma_i \dots \sigma_{k-1}\sigma_{j-1}^{-1}\dots\sigma_{k+1}^{-1}\sigma_k^2\sigma_{k-1}^{-1}\dots\sigma_i^{-1}\sigma_{k+1}\dots\sigma_{j-1} \\
&\qquad = \sigma_i \dots \sigma_{k-1}\sigma_{j-1}^{-1}\dots\sigma_{k+1}^{-1}\sigma_k^2\sigma_{k+1}\dots\sigma_{j-1}\sigma_{k-1}^{-1}\dots\sigma_i^{-1} \\
&\qquad = \sigma_i \dots \sigma_{k-1}\sigma_{j-1}^{-1}\dots\sigma_{k+2}^{-1}\sigma_{k+1}^{-1}\sigma_k^2\sigma_{k+1}\sigma_{k+2}\dots\sigma_{j-1}\sigma_{k-1}^{-1}\dots\sigma_i^{-1} \\
&\qquad = \sigma_i \dots \sigma_{k-1}\sigma_{j-1}^{-1}\dots\sigma_{k+2}^{-1}\sigma_{k+1}^{-1}\sigma_k\sigma_{k+1}\sigma_{k+1}^{-1}\sigma_k\sigma_{k+1}\sigma_{k+2}\dots\sigma_{j-1}\sigma_{k-1}^{-1}\dots\sigma_i^{-1} \\
&\qquad = \sigma_i \dots \sigma_{k-1}\sigma_{j-1}^{-1}\dots\sigma_{k+2}^{-1}\sigma_k\sigma_{k+1}\sigma_k^{-1}\sigma_k\sigma_{k+1}\sigma_k^{-1}\sigma_{k+2}\dots\sigma_{j-1}\sigma_{k-1}^{-1}\dots\sigma_i^{-1} \\
&\qquad = \sigma_i \dots \sigma_{k-1}\sigma_{j-1}^{-1}\dots\sigma_{k+2}^{-1}\sigma_k\sigma_{k+1}^2\sigma_k^{-1}\sigma_{k+2}\dots\sigma_{j-1}\sigma_{k-1}^{-1}\dots\sigma_i^{-1} \\
&\qquad = \sigma_i \dots \sigma_k\sigma_{j-1}^{-1}\dots\sigma_{k+2}^{-1}\sigma_{k+1}^2\sigma_k^{-1}\dots\sigma_i^{-1}\sigma_{k+2}\dots\sigma_{j-1}
\end{aligned}$$

The pure braid relations are simplified in [24] to

$$\begin{aligned}
s_{ij}s_{rs} &= s_{rs}s_{ij} && \text{if } r < s < i < j \text{ or } i < r < s < j \quad , \\
s_{rj}s_{ir}s_{ji} = s_{ji}s_{rj}s_{ir} &= s_{ir}s_{ji}s_{rj} && \text{if } r < i < j \quad , \\
s_{js}s_{ji}s_{jr}s_{rs} &= s_{rs}s_{js}s_{ji}s_{jr} && \text{if } r < i < s < j \quad .
\end{aligned}$$

1.4 Contents and structure of the thesis

In §2, we calculate the critical configurations and radii of $\tau\colon \mathrm{Conf}_n \to \mathbb{R}$ for $n \in \{2,3,4,5\}$.

Theorem A. *The full set of pairs (n,r), where $n \in \{1,2,3,4,5\}$ and r is a critical radius of* Conf_n*, is given by*

n	r
1	1
2	$\frac{1}{2}$
3	$\frac{1}{3}$, $2\sqrt{3}-3$
4	$\frac{1}{4}$, $\frac{1}{3}$, $\sqrt{2}-1$
5	$\frac{1}{5}$, $\frac{1}{4}$, $\frac{1}{3}$, $\frac{\sin\frac{\pi}{5}}{1+\sin\frac{\pi}{5}}$

This is seen in Prop. 2.0.7, 2.0.8, 2.0.9, 2.0.10, and 2.0.11.

In §3, we look just beyond the first critical radius for topological features which vanish in Conf_n when pushed forward through the inclusion $\iota\colon \mathrm{Conf}_{n,r} \to \mathrm{Conf}_n$. Thm. 3.1.1 and 3.2.1 show

Theorem B. *Let $n \geq 4$, and $r = \frac{1}{n} + \varepsilon$ for sufficiently small $\varepsilon > 0$. $\pi_{n-3}(\mathrm{Conf}_{n,r})$ contains a non-trivial element which lies in $\ker(\iota_*\colon \pi_{n-3}(\mathrm{Conf}_{n,r}) \to \pi_{n-3}(\mathrm{Conf}_n))$.*

In particular, for $n = 4$ we demonstrate a non-trivial 'thick braid' which vanishes as a braid in the (pure) braid group. We then explore the possibility of adding more discs into the unused space in D^2, in such a way that the extra discs do not play a part in the non-contractible loop, in order to probe higher critical radii for large n.

In §4, we calculate the full homotopy type of $\mathrm{Conf}_{4,r}$ just beyond the first critical radius, culminating in Thm. 4.0.1, which says:

Theorem C. *There is a 1-dimensional cell complex Y of Euler characteristic 11 such that $\mathrm{Conf}_{4,r} \simeq Y \times S^1$ for all $r \in \left(\frac{1}{4}, \frac{1}{3}\right]$.*

We use this to calculate $\pi_1(\mathrm{Conf}_{4,r})$ beyond the first critical radius, showing that it contains two elements for every generator of the pure braid group, and most of the pure braid relations break down (Prop. 4.4.2, Table 4.2).

In §5, we explore deformations of the unit disc. In particular, we consider the change in homotopy-type as we deform the disc into an ellipse, which we classify by its eccentricity $e = \sqrt{1 - \frac{b^2}{a^2}}$, where a and b are the semi-major and semi-minor radii respectively. In Thm. 5.0.4 and 5.0.7, we show

Theorem D. *Let $n \geq 4$, and E be the ellipse with semi-major radius a, semi-minor radius b and eccentricity e. Then $\mathrm{Conf}_{n,r}(E)$ contains a non-contractible $(n-3)$-sphere of the same construction as that in Thm. B for $r = \frac{1}{n} + \varepsilon$, $\varepsilon > 0$ sufficiently small, when*

either:

i. $b \in \left(\frac{1}{\sqrt{n}}, 1\right]$ *and* $a = 1$, *or*

ii. $b \in \left(\frac{1}{n}, \sqrt{r}\right]$ *and* $e^2 = \frac{(1-r)^2}{b^2 - r^2 + (1-r)^2}$.

In case *ii*, we show that the homotopy class remains for e arbitrarily close to 1, or equivalently for a arbitrarily large.

Finally, in §6, we consider the homotopy groups of dimension less than $n-3$ just beyond the first critical radius. In this exploration, we define a gradient-like flow for τ on Conf_n which preserves the stress graph $N(x)$ (in the sense that no edges or vertices are lost along a flowline, but more may be added).

Chapter 2

The critical radii for small numbers of discs

Recall that, for fixed n, the homotopy-type of $\mathrm{Conf}_{n,r}$ changes at finitely many values of r as r increases, and these are characterised by balanced stress graphs (Def. 1.2.4). Later, in §6, we will require a generalisation of these graphs which allow for negative weights.

Definition 2.0.1. Take $x \in \mathrm{Conf}_n$. Let E be the set of edges of $N(x)$. A *generalised weighting* on $N(x)$ is a map $w\colon E \to \mathbb{R}$, where $w_e \coloneqq w(e)$ defines the force with which each edge pushes on its endpoints, as described in Def. 1.2.3.

Then w is *generalised balanced* if the total force F_i on each interior vertex x_i is zero. $N(x)$ is a *generalised balanced stress graph* if it has a non-trivial generalised balanced weighting. If, in this case, $N(x)$ has no non-trivial balanced weighting, then we may also call it a *phantom balanced stress graph.*

In this chapter, we find the generalised balanced configurations for Conf_n, $n \in \{2, 3, 4, 5\}$ and the associated generalised critical radii. We start with some lemmas which define how our generalised balanced stress graphs may appear. The critical radii found below are summarised in Fig. 2.1 with the corresponding configurations.

Lemma 2.0.2. *Let w be a generalised balanced weighting on some $x \in \mathrm{Conf}_n$. Then in each connected component $G \subset N(x)$, the total force exerted on the boundary by the boundary edges is zero.*

Proof. First, observe that each edge of G exerts force on both its vertices, and these two forces are equal and opposite. Hence, the sum of all forces exerted by the edges of G is 0. Next, taking the sum of all forces acting on the interior vertices, we have $\sum_{x_i \text{ in } G} F_i = 0$. Therefore, the sum of all forces acting on the boundary vertices of G is also 0. □

Given a generalised weighted graph (G, w), we denote by $Z(G) \subset G$ the subgraph containing all vertices of G and the edges of G with non-zero weight. $Z(G)$ is thus empty if and only if w is trivial.

Lemma 2.0.3. *Let G be a generalised balanced stress graph, and suppose $Z(G)$ has an interior vertex, v, of degree at most 1. Then v is isolated in $Z(G)$.*

In particular, if v is a leaf of G, then the unique incident edge has weight 0.

Proof. Let G be a generalised weighted stress graph, v a vertex with $\deg_{Z(G)}(v) = 1$, and e an edge incident to v in $Z(G)$. Then the magnitude of the force on v is equal to w_e, so this force is non-zero. Therefore, G is not generalised balanced. □

Lemma 2.0.4. *Let G be a generalised balanced stress graph, and v a vertex of G with $\deg_{Z(G)}(v) = 2$. Then the two incident edges of v in $Z(G)$ are collinear.*

Proof. Let G be a generalised weighted stress graph, v a vertex with $\deg_{Z(G)}(v) = 2$, and e, e' the edges incident to v in $Z(G)$. Suppose e, e' are not collinear, and therefore not parallel. Any non-trivial linear combination of the two edge vectors is therefore non-zero, and thus G is not generalised balanced. □

We define the interior of a stress graph to be the full subgraph induced by the interior vertices. The following lemmas will be used implicitly to reduce repetition in the calculations of the critical radii.

Lemma 2.0.5. *Take $n > 1$, $x \in \text{Conf}_n$, and w a generalised weighting on $N(x)$. If the interior of $Z(N(x))$ is trivial, then w is not generalised balanced.*

Proof. By assumption, all edges of $Z(N(x))$ are boundary edges. Since $n > 1$, there is at least one x_i not at the origin, so $\tau(x) < 1$. Then each vertex has at most one

incident boundary edge in $N(x)$. Therefore, for all j, $\deg_{Z(N(x))}(x_j) \leq 1$, and thus $\deg_{Z(N(x))}(x_j) = 0$ by Lemma 2.0.3. Thus w is the trivial weighting. □

Lemma 2.0.6. *Take $n > 2$ and let $x \in \mathrm{Conf}_n$ be generalised balanced. Then the interior of $N(x)$ contains no components with only one edge, unless this edge has trivial weight.*

Proof. Take $x \in \mathrm{Conf}_n$ and choose a generalised balanced weighting w on $N(x)$. Let the vertices x_i, x_j be adjacent along an edge e with non-zero weight, and suppose this component of the interior stress graph contains no other vertices. By Lemma 2.0.4, both x_i and x_j have a second incident edge in the stress graph, collinear with e. By assumption, these are boundary edges. Therefore, this component of the stress graph is a diameter of D^2, and $\tau(x) = \frac{1}{2}$. However, it is impossible to fit a third point $y \in D^2$ such that $\mathrm{dist}(y, \partial D^2) \geq \frac{1}{2}$ and $\mathrm{dist}(y, x_i), \mathrm{dist}(y, x_j) \geq 1$. □

Proposition 2.0.7. *The unique critical radius of* Conf_1 *is $r = 1$.* Conf_1 *has no other generalised critical radii.*

Proof. If $x_1 \neq 0$, then there is a unique closest point to x_1 on ∂D^2. Then $N(x)$ contains exactly one edge, and the vertex at x_1 is a leaf. Thus the only generalised balanced choice of weights is trivial by Lemma 2.0.3. Conversely, if $x_1 = 0$, then there is an edge of length 1 joining x_1 to each $p \in \partial D^2$, and these are balanced by giving every edge weight 1. □

Proposition 2.0.8. *The unique critical radius of* Conf_2 *is $r = \frac{1}{2}$.* Conf_2 *has no other generalised critical radii.*

Proof. Let $x \in \mathrm{Conf}_2$ be a generalised critical configuration and choose a generalised balanced weighting on $N(x)$. By Lemma 2.0.5, $N(x)$ has an interior edge joining x_1 and x_2 with non-zero weight. By Lemma 2.0.3, neither x_1 nor x_2 can be a leaf in $Z(N(x))$, so each must be incident to a boundary edge with non-zero weight. Then Lemma 2.0.4 implies these edges are all collinear. Thus $N(x)$ is a diameter of D^2. We can balance this by giving the interior edge weight 1 and the boundary edges weight 2, and the associated critical radius is $\frac{1}{2}$. □

We denote by P_n the path on n vertices (and $n-1$ edges), and by C_n ($n \geq 3$) the cyclic graph on n vertices.

Proposition 2.0.9. *The critical radii of* Conf_3 *are* $\frac{1}{3}, 2\sqrt{3}-3$. Conf_3 *has no other generalised critical radii.*

Proof. Let $x \in \mathrm{Conf}_3$ be a generalised critical configuration and choose a generalised balanced weighting on $N(x)$. By Lemmas 2.0.5 and 2.0.6, each component in the interior of $Z(N(x))$ has at least two edges. Then the interior part of $Z(N(x))$ is P_3 or C_3.

If the interior of $Z(N(x))$ is C_3, then Lemma 2.0.4 implies that each vertex must be adjacent to a boundary vertex. Since all interior edges have the same length, C_3 is realised as an equilateral triangle. Since the boundary edges all have the same length, the triangle must be centred at the origin. We can balance this configuration by giving the interior edges weight 1 and the boundary edges weight $2\sqrt{3}$. This configuration corresponds to the critical radius $2\sqrt{3}-3$.

If the interior of $Z(N(x))$ is P_3, then Lemma 2.0.3 implies that the two vertices of degree 1 must be adjacent to a boundary vertex, and the incident edge must have non-zero weight. Moreover, Lemma 2.0.4 implies that the edges must all be collinear. Then $N(x)$ is a diameter of D^2. We can balance this by giving the interior edges weight 1 and the boundary edges weight 2, and the associated radius is $\frac{1}{3}$. □

Proposition 2.0.10. *The critical radii of* Conf_4 *are* $\frac{1}{4}, \frac{1}{3}, \sqrt{2}-1$. Conf_4 *also has a generalised critical radius* $\frac{\sqrt{3}-1}{2}$.

Proof. Let $x \in \mathrm{Conf}_4$ be a generalised critical configuration and choose a generalised balanced weighting on $N(x)$. By Lemmas 2.0.5 and 2.0.6, each component in the interior of $Z(N(x))$ contains a P_3. We consider the following cases.

Suppose the interior of $Z(N(x))$ contains a copy of C_4. Then this appears as a non-degenerate parallelogram. By Lemma 2.0.4, each vertex must have a third incident edge in $Z(N(x))$, and there are two possibilities.

1) Each of these is a boundary edge. Then $N(x)$ must be a square centred at the origin. This can be balanced by giving the interior edges weight 1 and the boundary edges weight $2\sqrt{2}$, and corresponds to the critical radius $\sqrt{2}-1$.

2) $Z(N(x))$ contains an edge across a diagonal of the parallelogram, splitting it into two equilateral triangles. The remaining two vertices have boundary edges. If these are the only two boundary vertices, the boundary vertices must be antipodal by Lemma 2.0.2, so the centre of the diagonal is at the origin. If we consider one of the vertices incident to the diagonal, we see that its three incident edges lie in a half plane, so this configuration can't be balanced. However, it can be generalised balanced by giving weight $2\sqrt{3}$ to the boundary edges, 1 to the outer edges of the parallelogram, and -1 to the diagonal. The associated radius is $\frac{\sqrt{3}-1}{2}$. Otherwise, if one of the vertices on the diagonal is adjacent to the boundary, then other vertex on the diagonal must be at the origin. Then this configuration lies in the family of generalised critical configurations in which one point is at the origin, with radius $r = \frac{1}{3}$, which is discussed in the final paragraph.

Next suppose the interior of $Z(N(x))$ contains a C_3 (in an equilateral triangle) but no C_4. Assume without loss of generality that the C_3 contains x_1, x_2, x_3. By Lemma 2.0.4, each vertex of the C_3 must have a third incident edge in $Z(N(x))$. These cannot all be boundary edges, since these three vertices would form the critical configuration of radius $2\sqrt{3} - 3$ from Conf_3, and then there is insufficient space to fit the fourth point. Therefore x_4 is adjacent to exactly one vertex, say x_3, by an edge of non-zero weight. x_4 is also adjacent to a boundary vertex by Lemma 2.0.3, and the two edges incident to x_4 are collinear by Lemma 2.0.4. Then there are two possibilities:
1) $x_3 = 0$. Then the edge connecting x_1 to x_3 is collinear with the boundary edge incident to x_1. But the edge connecting x_1 to x_2 applies a non-zero force to x_1 and this has a component orthogonal to the line containing the other two edges, so this configuration is never balanced.
2) $x_3 \neq 0$. Since x_1 and x_2 are both at distance r from the boundary, it follows that the line containing x_3 and x_4 is a line of symmetry for the configuration, whence we derive that r satisfies $r^2 + \left(\left(3 + \sqrt{3}\right) r - 1\right)^2 = (1 - r)^2$. This has solutions $r \in \{0, \frac{1}{3}\}$, but $0 \notin \tau(\mathrm{Conf}_4)$, so $r = \frac{1}{3}$. Thus $x_3 = 0$, a contradiction.

Finally, suppose the interior of $Z(N(x))$ has no C_3 or C_4. If it is P_4, then the two end vertices each have an incident boundary edge with non-zero weight by Lemma 2.0.3 and thus $N(x)$ is a diameter containing all four points by repeated applications of Lemma 2.0.4. This is balanced by giving the interior edges weight 1 and the boundary edges weight 2, and has associated radius $\frac{1}{4}$. If the interior of $Z(N(x))$ consists of a P_3 and

an isolated point, then $Z(N(x))$ is a diameter containing three points by the same arguments, corresponding to radius $\frac{1}{3}$. Otherwise, the interior of $Z(N(x))$ consists of one vertex of degree 3, and three leaves. Then each leaf is incident to a boundary edge, which is collinear with its other incident edge, by Lemmas 2.0.3 and 2.0.4. This means that the vertex of degree 3 lies on three radii and is thus at the origin, so this corresponds to radius $\frac{1}{3}$ again. Any such configuration can be at least generalised balanced. □

Proposition 2.0.11. *The critical radii of* Conf_5 *are* $\frac{1}{5}, \frac{1}{4}, \frac{1}{3}, \frac{\sin\frac{\pi}{5}}{1+\sin\frac{\pi}{5}}$. Conf_5 *also has generalised critical radii* $\frac{41-6\sqrt{3}}{121}, 2-\sqrt{3}, \frac{1}{3}$.

Proof. Let $x \in \mathrm{Conf}_5$ be a generalised critical configuration and choose a generalised balanced weighting on $N(x)$. By Lemmas 2.0.5 and 2.0.6, each component in the interior of $Z(N(x))$ contains a P_3. We consider the following cases.

First, suppose the interior of $Z(N(x))$ contains a C_5. This is a pentagon with 5 equal edges. By Lemma 2.0.4, each vertex must have a third incident edge in $Z(N(x))$, and these can be boundary edges or diagonals within the pentagon.

1) If there are no diagonals, then the C_5 is a regular pentagon centred at the origin. This is balanced by giving each interior edge weight 1, and each boundary edge weight $4\cos\frac{3\pi}{10}$, and corresponds to a critical radius $r = \frac{\sin\frac{\pi}{5}}{1+\sin\frac{\pi}{5}}$.

2) If there are two diagonals in the pentagon, then the graph is constrained to a trapezium with one edge of side length $4r$ and three edges of side length $2r$. The vertices at the ends of the long edge must be adjacent to a boundary vertex by Lemma 2.0.4. If these are the only two boundary vertices in $Z(N(x))$, these must be antipodal by Lemma 2.0.2. Otherwise, the vertex at the centre of the long edge lies on three radii. In each case, the vertex at the centre of the long edge miust be the origin. Then this configuration lies in the family of generalised critical configurations in which one point is at the origin, with radius $r = \frac{1}{3}$, which is discussed in the final paragraph.

3) If there is one diagonal, this splits the pentagon into a parallelogram and a triangle, with one shared edge. The three vertices not on this edge are adjacent to boundary vertices. This yields a family of configurations with associated radius $\frac{1}{3}$. This can always be generalised balanced (but not balanced) – for example, when the parallelogram is a square, we give weight -1 to the shared edge, $\sqrt{3}$ to the edges of the square and the boundary edge incident to the triangle, 2 to the edges of the triangle, and $2\sqrt{6}$ to the

boundary edges incident to the square.

Next, suppose the interior of $Z(N(x))$ contains a C_4, but no C_5. Denote the vertices of the C_4 as x_1, x_2, x_3, x_4 in anticlockwise order. If the fifth point is not in the same component of $Z(N(x))$, then the C_4 would have to be one of the critical configurations from the case $n = 4$ – however, this is impossible as the fifth point will not fit at a sufficient distance from the C_4 and the boundary. Therefore, the interior part of $Z(N(x))$ consists of the C_4 and a vertex, say x_5, which is adjacent to exactly one vertex in the cycle, say x_4. Then x_5 must have a boundary edge collinear with the edge between x_4 and x_5 by Lemmas 2.0.3 and 2.0.4, and each of the remaining three vertices must have a third incident edge. This yields three subcases:

1) x_1 and x_3 are each adjacent to a boundary vertex and $x_4 = 0$. This configuration lies in the family of generalised critical configurations in which one point is at the origin, with radius $r = \frac{1}{3}$, which is discussed in the final paragraph.

2) x_1 and x_3 are each adjacent to a boundary vertex and $x_4 \neq 0$. Since $\text{dist}(x_1, \partial D^2) = \text{dist}(x_3, \partial D^2)$ and $|x_1 - x_4| = |x_3 - x_4|$, it follows that x_1 and x_3 are equidistant from the diameter containing x_4 and x_5, and so x_2 lies on this diameter. Then by summing distances along this diameter, we have

$$2 = \text{dist}(x_5, \partial D^2) + |x_4 - x_5| + |x_2 - x_4| + \text{dist}(x_2, \partial D^2) \geq 6r$$

However, since the edge from x_4 to x_3 is not radial and therefore not collinear with the boundary edge incident to x_3, we have

$$\text{dist}(x_4, \partial D^2) < |x_3 - x_4| + \text{dist}(x_3, \partial D^2) = 3r$$

x_4 lies on a diameter at a distance $3r$ from one end, so $\text{dist}(x_4, \partial D^2) = \min\{3r, 2 - 3r\}$. Therefore $2 - 3r < 3r$, which is a contradiction – this case does not correspond to the stress graph of any generalised critical $x \in \text{Conf}_5$.

3) x_1 and x_3 are adjacent to each other, while x_2 is adjacent to the boundary. If x_2 and x_5 are the only boundary vertices, they are antipodal by Lemma 2.0.2. The configuration can be generalised balanced by giving weight $2\sqrt{3}$ to the boundary edges, $\sqrt{3}$ to the edge between x_4 and x_5, 1 to the outer edges of the parallelogram, and -1 to the edge between x_1 and x_3, and corresponds to radius $r = 2 - \sqrt{3}$. Otherwise, either x_1 or x_3 is adjacent to the boundary. Then the other of these vertices must be at the origin, so this

configuration lies in the family of generalised critical configurations in which one point is at the origin, with radius $r = \frac{1}{3}$, which is discussed in the final paragraph.

Next, suppose the interior of $Z(N(x))$ contains a C_3, but no C_4 or C_5. Denote the vertices of the C_3 as x_1, x_2, x_3 in anticlockwise order, and the remaining vertices x_4, x_5. If the C_3 is an entire component in the interior of $Z(N(x))$, then we obtain the critical configuration of radius $2\sqrt{3} - 3$ from Conf_3, but this is too big to fit the remaining points. If the component containing C_3 contains 4 vertices, then the fourth must be adjacent to exactly one vertex of the C_3. But we argue in the proof for Conf_4 that this configuration is never critical. Therefore, this component contains all 5 vertices. The graphs of this type can be considered in three cases.

1) C_3 contains a vertex, say x_3, which is adjacent x_4 and x_5. Then both are adjacent to a boundary vertex, and the two incident edges at each vertex are collinear, by Lemmas 2.0.3 and 2.0.4. Therefore x_3 lies either on two non-collinear radial lines, or at the centre of a diameter, so $x_3 = 0$. This configuration lies in the closure of the stratum where the interior of $Z(N(x))$ is a tree containing a P_3 but no P_4, with associated radius $r = \frac{1}{3}$, discussed in the final paragraph.

2) One of the vertices of C_3, say x_3, is adjacent to one vertex, say x_4, and x_4 is adjacent to x_5. Then x_5 is adjacent to a boundary vertex, and the section of graph between x_3 and this boundary vertex is a straight line by Lemmas 2.0.3 and 2.0.4; moreover, x_1 and x_2 are adjacent to boundary vertices. This latter is impossible if $x_3 = 0$; therefore, x_1 and x_2 are equidistant from the line passing through x_3 and x_5. The edges at x_1 lie in a half-plane, so this graph cannot be balanced. However, it can be generalised balanced by giving weight $2\sqrt{3}$ to all edges incident to x_4 or x_5, 2 to the edges of the triangle adjacent to x_3, $2\sqrt{3} - 1$ to the boundary edges incident to the triangle, and $-\frac{4+8\sqrt{3}}{11}$ to the remaining edge of the triangle. If the boundary vertex adjacent to x_5 is placed at $(0, 1)$, then $x_2 = \big(r, 1 - 5r - \sqrt{3}r\big)$. We solve $|x_2| = 1 - r$ to find that the associated radius is $\frac{41-6\sqrt{3}}{121}$.

3) Two vertices of the triangle, say x_2 and x_3, are each adjacent to one of theremaining vertices, say x_4, x_5 respectively. Then x_4, x_5 are each adjacent to a boundary vertex, and the edge joining them to x_2 and x_3 respectively is collinear with their boundary edge by Lemmas 2.0.3 and 2.0.4, so $\mathrm{dist}(x_2, \partial D^2) = \mathrm{dist}(x_3, \partial D^2) = 3r$. However, we also have $\mathrm{dist}(x_2, \partial D^2) \leq |x_2 - x_1| + \mathrm{dist}(x_1, \partial D^2) = 3r$ and $\mathrm{dist}(x_3, \partial D^2) \leq |x_3 - x_1| +$

$\text{dist}(x_1, \partial D^2) = 3r$. At least one of these is not a straight line distance, and so the inequality is strict, which is a contradiction. Therefore this case does not correspond to the stress graph of a generalised critical $x \in \text{Conf}_5$.

Finally, suppose the interior of $Z(N(x))$ contains no cycles. Using arguments from the proof for Conf_4, we can say that if it is a P_5, then this is a diameter of D^2, corresponding to $r = \frac{1}{5}$; if it is a P_4 and an isolated vertex, then this is a diameter of D^2, corresponding to $r = \frac{1}{4}$; if the longest path is a P_3, then there is a vertex and the origin and the corresponding radius is $r = \frac{1}{3}$. The only remaining configuration is a P_4 where the remaining vertex is adjacent to one of the middle vertices. By Lemma 2.0.3, each of the leaves of this graph has an incident boundary edge, so then by repeated applications of Lemma 2.0.4, we see that the vertex of degree 3 lies on three radial lines, and thus lies at the origin. However, the paths from the boundary vertices to this vertex do not all have the same length, which is a contradiction. □

Remark 2.0.12. Consider the family of critical configurations of Conf_5 at $r = \frac{1}{3}$ with one point at the origin, and the family of generalised critical configurations of Conf_5 at $r = \frac{1}{3}$ where the interior part of the stress graph is a parallelogram with a triangle on one edge. These families meet at the configuration where the stress graph is a trapezium with an edge from the centre of the long side to each opposite corner.

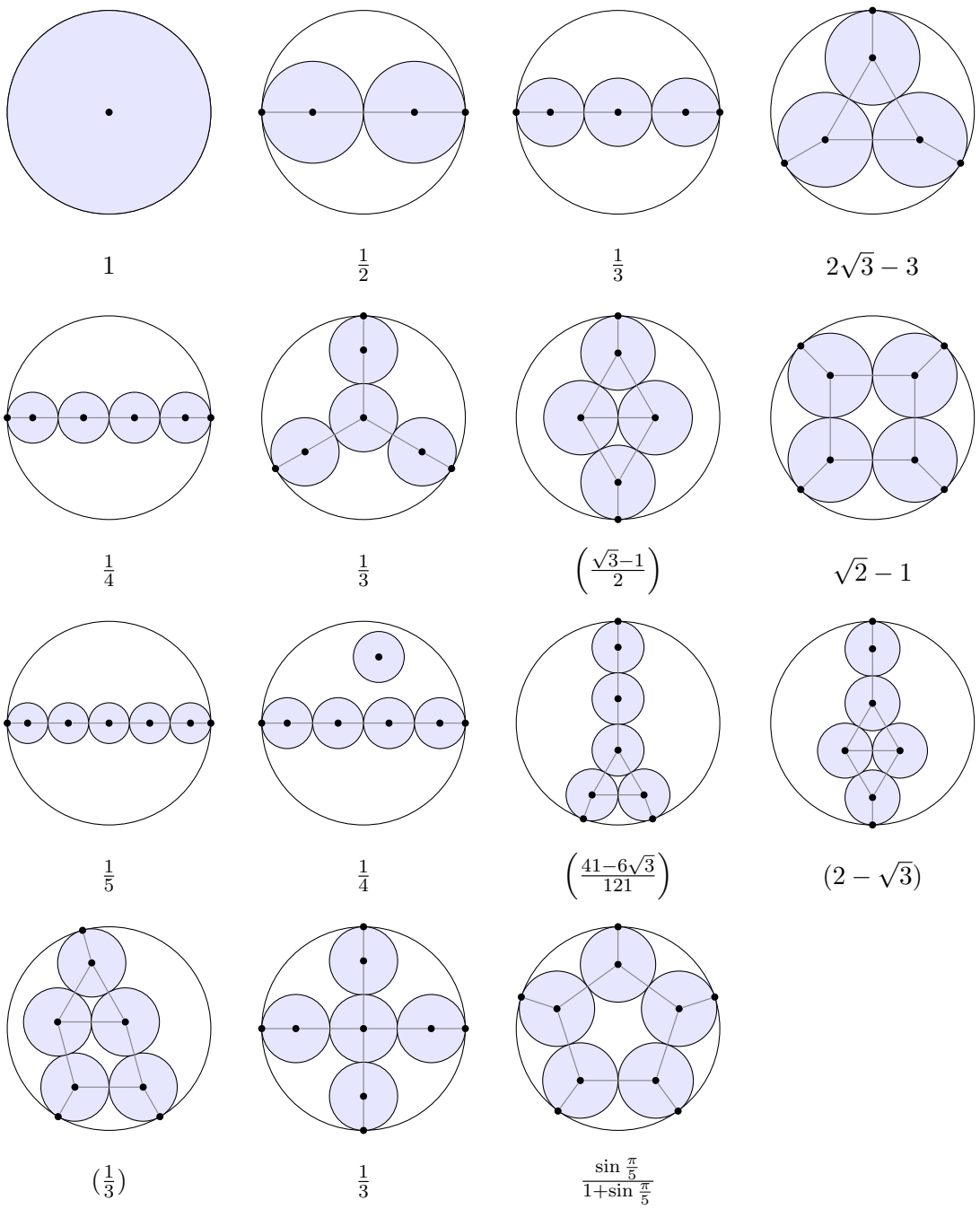

Figure 2.1: The generalised critical configurations of Conf_n, $n \in \{1,2,3,4,5\}$, with the underlying stress graphs. The associated critical radius r is written below each configuration. Brackets indicate that the configuration is not balanced using only non-negative weights. For most pairs (n,r) shown, there is a unique generalised balanced stress graph up to rotation of the unit disc. The exceptions are $\left(5,\frac{1}{4}\right)$, where the isolated disc may move freely; $\left(4,\frac{1}{3}\right)$ and $\left(5,\frac{1}{3}\right)$, where the outer discs may move freely; and $\left(5,\left(\frac{1}{3}\right)\right)$, where there is a family of generalised balanced stress graphs, parametrised by an internal angle of the rhombus.

Chapter 3

A new homotopy class beyond the first critical radius

3.1 Four discs, and braids of thick strings

For $n = 4$, understanding the spaces $\mathrm{Conf}_{n,r}$ as r changes is comparatively simple, as there are only three critical radii (see Prop. 2.0.10). For $r > \sqrt{2} - 1$, the configuration space is empty. For $\frac{1}{3} < r \leq \sqrt{2} - 1$, the configuration space is homotopy equivalent to $\mathrm{Conf}_{4,\sqrt{2}-1}$, in which there is only one configuration up to rotation of the unit disc and permutation of the four discs, so the configuration space is a disjoint union of six circles. For $r \leq \frac{1}{4}$, it is the configuration space of points. Thus, it only remains to check $\frac{1}{4} < r \leq \frac{1}{3}$. In this case we will demonstrate the existence of a 'thick braid': a non-trivial loop in $\mathrm{Conf}_{4,r}$ which is trivial in Conf_4 when the discs of each configuration are replaced by their centres. This immediately shows that the radius of the discs affects the homotopy-type of the space: for $r \leq \frac{1}{4}$, $\mathrm{Conf}_{n,r}$ is a $K(PBr_4, 1)$, whereas this is no longer the case for $r > \frac{1}{4}$.

Theorem 3.1.1. *Let $\frac{1}{4} < r \leq \frac{1}{3}$. Then $\mathrm{Conf}_{4,r}$ contains a non-trivial loop which is homotopic to $\sigma_3\sigma_1^{-1}\sigma_3^{-1}\sigma_1$ in the standard representation of the braid group, and therefore trivial when the disc radii are reduced below $\frac{1}{4}$.*

A realisation of this loop is depicted in Figure 3.2.

A key piece of the proof comes in proving that the given loop is non-contractible. This

will rely on the following map (inspired by [1]) and lemma, which will be used in this chapter and again in §5.

Definition 3.1.2. Given some $\mathcal{D} \in \mathrm{Conf}_{n,r}(U)$, and some non-repeating sequence $I = (i_k)$ of integers $1 \leq i_k \leq n$, let $\theta_k := \theta_k(\mathcal{D})$ be the anticlockwise angle from the vector $(1,0)$ to the vector $x_{i_{k+1}} - x_{i_k}$ for all k. Let $\phi_k = \theta_k - \theta_{k-1}$ for $2 \leq k \leq n-1$. Then the *angle map* is $\mathrm{ang}_I \colon \mathrm{Conf}_{n,r}(U) \to T^{n-2}$, $\mathcal{D} \mapsto (\phi_2(\mathcal{D}), \ldots, \phi_{n-1}(\mathcal{D}))$. If I is the sequence $1, 2, \ldots, n$, then we write $\mathrm{ang}(\mathcal{D}) := \mathrm{ang}_I(\mathcal{D})$.

We may think of ϕ_k as a turning angle: if we walk along a straight path from $x_{i_{k-1}}$ to x_{i_k}, and then from x_{i_k} to $x_{i_{k+1}}$, then ϕ_k is the angle through which we turn at x_{i_k} (see Fig. 3.1).

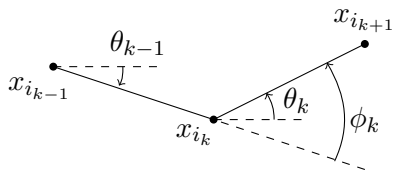

Figure 3.1: The angles θ_k and ϕ_k used to construct the map ang in Def. 3.1.2. Angles are taken to be anticlockwise from the dotted line to the solid line, so $\theta_{k-1} < 0$ and $\theta_k, \phi_k > 0$ in this diagram.

Lemma 3.1.3. *Let $n, k \in \mathbb{N}$, $r > \frac{1}{k}$ and $U \subset \mathbb{R}^2$ a connected, codimension zero submanifold such that any disc of radius r in U is contained in D^2. Let T be some m-dimensional manifold, $f \colon \mathrm{Conf}_{n,r}(U) \to T$ be a continuous map, and $p \in T$ be such that if $f(\mathcal{D}) = p$, then some k discs in $\mathcal{D}$ lie on a straight line. Let S be an $(m-1)$-sphere in $T \backslash \{p\}$ such that $[S] \neq 0 \in \pi_{m-1}(T \backslash \{p\})$ and $\mathcal{S} \colon S \to \mathrm{Conf}_{n,r}(U)$ a local section of f. Then $\mathcal{S}$ represents a non-trivial class in $\pi_{m-1}(\mathrm{Conf}_{n,r}(U))$.*

Proof. First, we note that $\mathcal{S}$ is an $(m-1)$-sphere inside $\mathrm{Conf}_{n,r}(U)$, so represents some class in $\pi_{m-1}(\mathrm{Conf}_{n,r}(U))$. Since $r > \frac{1}{k}$, we cannot fit k discs of radius r on one straight line inside D^2, nor therefore inside U, so $f(\mathrm{Conf}_{n,r}(U)) \subset T \backslash \{p\}$. Given that $S = f(\mathcal{S})$, we have $f_*[\mathcal{S}] = [S] \neq 0 \in \pi_{m-1}(T \backslash \{p\})$, and the result follows by Lemma 1.3.1. □

Once a choice of $S, \mathcal{S}$ is made, this lemma can be used to prove that $\mathcal{S}$ is non-trivial in its homotopy group. We will typically apply this lemma with $f = \mathrm{ang}_I$ for some appropriate choice of I, $T = T^{n-2}$, and $p = 0$, since $p = 0$ is often missing from the

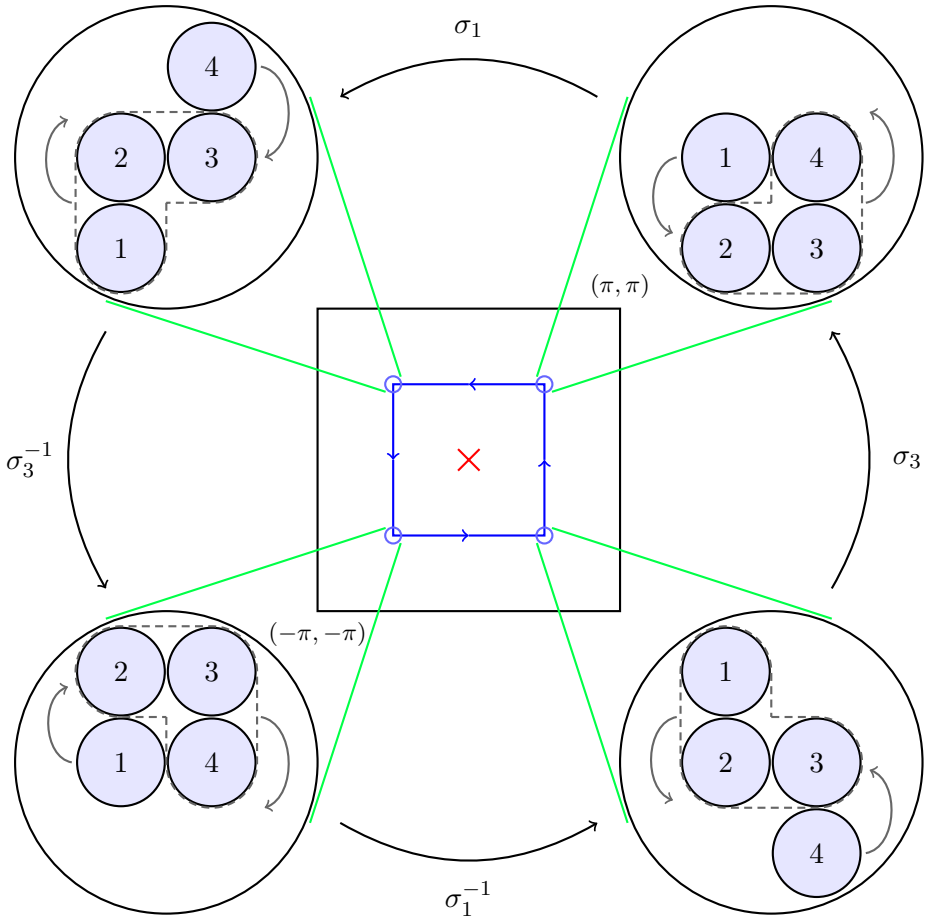

Figure 3.2: A loop of configurations of four discs of radius 0.29 inside the unit disc, starting at the top right, which is homotopic to the sequence $\sigma_3\sigma_1^{-1}\sigma_3^{-1}\sigma_1$ in the standard representation of the braid group. This descends to the loop $\partial\left[-\frac{\pi}{2}, \frac{\pi}{2}\right]^2 \subset T^2$ (blue) under the map ang. The blue loop is non-contractible in $T^2\backslash\{0\}$; then since $0 \notin \text{ang}(\text{Conf}_{4,0.29})$, the loop of configurations is also non-contractible. This homotopy class persists for $\frac{1}{4} < r \leq \frac{1}{3}$.

image of ang if the disc radius is large enough.

Proof of Theorem 3.1.1. Consider the loop $S = \partial\left(\left[-\frac{\pi}{2}, \frac{\pi}{2}\right]^2\right) \subset T^2$. We can then define a local section $\mathcal{S}\colon S \to \mathrm{Conf}_{4,r}$ for any $r \leq \frac{1}{2+\sqrt{2}}$ by

$$(\phi_2, \phi_3) \mapsto \frac{1}{2+\sqrt{2}} \begin{pmatrix} (-1 - \cos\phi_2 - \cos\phi_3, \sin\phi_2 - \sin\phi_3) \\ (-1 + \cos\phi_2 - \cos\phi_3, -\sin\phi_2 - \sin\phi_3) \\ (1 + \cos\phi_2 - \cos\phi_3, -\sin\phi_2 - \sin\phi_3) \\ (1 + \cos\phi_2 + \cos\phi_3, -\sin\phi_2 + \sin\phi_3) \end{pmatrix}$$

where the rows are the coordinates of the centres, denoted x_i ($i \in \{1,2,3,4\}$), of the four discs.

It is possible from the given coordinates to check $\mathcal{S}$ is well-defined. First note that on S, there is always one $\phi_j = \pm\frac{\pi}{2}$. Then $\sin\phi_j = \pm 1$ and $\cos\phi_j = 0$, so letting ϕ represent the other coordinate, $|x_i|^2 = \left(\frac{1}{2+\sqrt{2}}\right)^2 \left((1 \pm \cos\phi)^2 + (1 \pm \sin\phi)^2\right) \leq \left(\frac{1+\sqrt{2}}{2+\sqrt{2}}\right)^2 \leq (1-r)^2$. Therefore, $D_i \subset D^2$ for each i. We may check similarly that any two disc centres are separated by a distance at least $2r$.

By construction, discs 2 and 3 lie on the same horizontal line at all values of $\mathcal{S}$, while the coordinates of discs 1 and 4 are chosen to satisfy $\mathrm{ang} \circ \mathcal{S} = \mathrm{id}_S$, so this is indeed a local section to ang.

Consider $\{\mathcal{S}(\phi_2, \phi_3) \mid (\phi_2, \phi_3) \in S\}$. At each corner of S, the four disc centres of $\mathcal{S}(\phi_1, \phi_2)$ form a parallelogram. Along the first edge, $\{(\frac{\pi}{2} - t\pi, \frac{\pi}{2}) \mid t \in [0,1]\}$, we can check from the coordinates that D_1 moves half a turn anticlockwise around D_2, while the three other discs stay in the same position relative to one another. This causes D_1 and D_2 to switch positions in the parallelogram; therefore the underlying path in Conf_4 traced out by the disc centres along this side is homotopic to the braid σ_1. Similarly, the remaining sides of S yield the braids σ_3^{-1}, σ_1^{-1}, σ_3.

If $\mathrm{ang}(\mathcal{D}) = 0$, then the four discs lie on a straight line. Furthermore, $[S] \neq 0 \in \pi_1(T^2 \backslash \{0\})$. Therefore $\mathcal{S}$ represents a non-trivial class in $\pi_1(\mathrm{Conf}_{4,r})$ by Lemma 3.1.3.

Finally, this homotopy class persists until the second critical radius by Fact 1.2.5, which is $r = \frac{1}{3}$ (see Prop. 2.0.10). □

3.2 More discs yields a higher-dimensional homotopy class

It is well-known [15, Cor. 2.2] that the configuration space of n points in any codimension-zero subset of the plane (and in particular the open unit disc) is aspherical – that is, its homotopy groups in dimension 2 or greater are trivial. Here, we generalise the work of §3.1 to demonstrate a non-trivial element of $\pi_{n-3}(\mathrm{Conf}_{n,\frac{1}{n}+\varepsilon})$ for all $n \geq 5$, provided ε is suitably small, showing that this property is lost beyond the first critical radius.

Theorem 3.2.1. *There is a non-trivial element in $\pi_{n-3}(\mathrm{Conf}_{n,r})$ for all $n \geq 5$ and $\frac{1}{n} < r \leq \frac{1}{n-1}$.*

To prove this theorem, we will construct a sphere of configurations for sufficiently small $r > \frac{1}{n}$. The following lemma is used to prove that the configurations in the constructed sphere lie inside D^2.

Lemma 3.2.2. *Let $\mathcal{D} = (D_1, D_2, \ldots, D_n)$ be a configuration of open unit discs such that D_k is in contact with D_{k+1} for all $1 \leq k \leq n-1$ and $\phi_l = \pm\xi$ for some $2 \leq l \leq n-1$, $0 < \xi \leq \frac{\pi}{2}$. Then $\bigcup \mathcal{D} \subset B\left(\frac{x_1+x_n}{2}, n - 4\sin^2\frac{\xi}{4}\right)$.*

Proof. Let $z = \frac{x_1+x_n}{2}$. The claim is equivalent to proving $x_i \in B\left(z, n - 4\sin^2\frac{\xi}{4} - 1\right)$, or equivalently $|z - x_i| \leq n - 4\sin^2\frac{\xi}{4} - 1 = n - 3 + 2\cos\frac{\xi}{2}$, for all i. We have two cases:

$\boldsymbol{i \neq l}$: By the triangle inequality, $|z - x_i| \leq \frac{1}{2}(|x_1 - x_i| + |x_i - x_n|)$. Then, assuming (by reversing the labelling if necessary) that $i > l$, we have

$$\begin{aligned}
|x_1 - x_i| &\leq \sum_{k=1}^{l-2} |x_k - x_{k+1}| + |x_{l-1} - x_{l+1}| + \sum_{k=l+1}^{i-1} |x_k - x_{k+1}| \\
&= 2(l-2) + 4\cos\frac{\xi}{2} + 2(i-1-l) \\
&= 2(i-3) + 4\cos\frac{\xi}{2} \\
|x_i - x_n| &\leq \sum_{k=i}^{n-1} |x_k - x_{k+1}| \\
&= 2(n-i)
\end{aligned}$$

Thus $|z - x_i| \leq n - 3 + 2\cos\frac{\xi}{2}$, as required.

$\boldsymbol{i = l}$: First, consider our configuration placed in the plane with x_{l-1} and x_{l+1} equidistant from the origin along the x-axis. Then (up to reflection) $x_{l-1} = (-c, 0)$, $x_l = (0, -s)$,

$x_{l+1} = (c, 0)$, where $c = 2\cos\frac{\xi}{2}$ and $s = 2\sin\frac{\xi}{2}$. As in the first case, we have $|x_1 - x_{l-1}| \leq \sum_{i=1}^{l-2} |x_i - x_{i+1}| = 2(l-2)$, $|x_n - x_{l+1}| \leq \sum_{i=l+1}^{n-1} |x_i - x_{i+1}| = 2(n-l-1)$, so there are $A \in [0, l-2]$, $B \in [0, n-l-1]$, and angles α, β such that $x_1 = (-c - 2A\sin\alpha, 2A\cos\alpha)$ and $x_n = (c + 2B\sin\beta, 2B\cos\beta)$. Then $z - x_l = (B\sin\beta - A\sin\alpha, A\cos\alpha + B\cos\beta + s)$. Therefore

$$\begin{aligned}
|z - x_l|^2 &= (B\sin\beta - A\sin\alpha)^2 + (A\cos\alpha + B\cos\beta + s)^2 \\
&= B^2\sin^2\beta - 2AB\sin\alpha\sin\beta + A^2\sin^2\alpha \\
&\quad + B^2\cos^2\beta + 2AB\cos\alpha\cos\beta + A^2\cos^2\alpha + s^2 + 2sA\cos\alpha + 2sB\cos\beta \\
&= B^2 + 2AB\cos(\alpha+\beta) + A^2 + s^2 + 2sA\cos\alpha + 2sB\cos\beta \\
&\leq B^2 + 2AB + A^2 + s^2 + 2sA + 2sB \\
&= (A + B + s)^2 \\
&\leq \left(n - 3 + 2\sin\frac{\xi}{2}\right)^2
\end{aligned}$$

We complete our proof by noting that $\sin\frac{\xi}{2} \leq \cos\frac{\xi}{2}$. □

Remark 3.2.3. This maximum is sharp, as it is attained by discs 1 and n in the configuration in which all discs except l are collinear.

Proof of Theorem 3.2.1. First, consider the case $\frac{1}{n} < r \leq \frac{1}{n - 4\sin^2(\frac{\pi}{2n})}$. We take the $(n-3)$-sphere $S = \partial\left[-\frac{2\pi}{n}, \frac{2\pi}{n}\right]^{n-2}$, and claim that the following algorithm defines a local section $\mathcal{S}\colon S \to \mathrm{Conf}_{n,r}$. We construct the configuration $(D_1, \ldots, D_n) \coloneqq \mathcal{S}(\phi_2, \ldots, \phi_{n-1})$ as follows:

1. Place D_1 centred at the origin of the plane and D_2 in contact with it, centred at $(2r, 0)$.
2. Place each subsequent disc D_i in contact with D_{i-1}, such that x_i lies on the ray from x_{i-1} at angle ϕ_{i-1}.
3. Translate all discs by $-\frac{x_1 + x_n}{2}$.

$\mathrm{ang} \circ \mathcal{S} = \mathrm{id}_S$ by construction (step 2). The placement of D_i at step 2 is continuous with respect to ϕ_i, and the translation in step 3 is continuous with respect to x_1 and x_n, so $\mathcal{S}$ is continuous. Thus, we prove our claim if we show that $\mathcal{S}(\Phi) \in \mathrm{Conf}_{n,r}$ for all $\Phi \in S$.

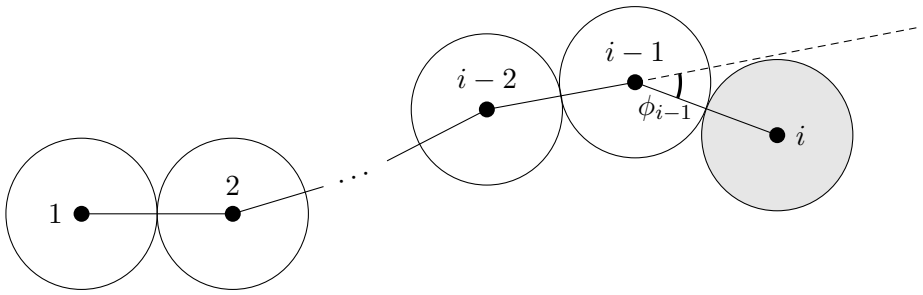

Figure 3.3: The placement of the i-th disc in the construction of the configurations of Theorem 3.2.1.

At the placement of D_i in step 2, consider the two regular n-gons which have $\overline{x_{i-1}x_i}$ as one of their sides. Since $|\phi_k| \leq \frac{2\pi}{n}$, the external angle of a regular n-gon, for all k, the sequence of edges

$$x_1 \longrightarrow x_2 \longrightarrow \ldots \longrightarrow x_{i-1} \longrightarrow x_i$$

lies outside or on the boundary of these two n-gons. Thus, since $i-1 < n$, $D_i \cap D_j = \emptyset$ for $j \in \{1, 2, \ldots, i-1\}$. Therefore no two discs in $\mathcal{S}(\phi_2, \ldots, \phi_{n-1})$ overlap. Since every point in S has at least one coordinate equal to $\pm\frac{2\pi}{n}$ and D_{i+1} touches D_i for all i, we can apply Lemma 3.2.2 with $\xi = \frac{2\pi}{n}$ to show that $\bigcup \mathcal{S}(\phi_2, \ldots, \phi_{n-1}) \subset B\left(0, \left(n - 4\sin^2\frac{\pi}{2n}\right) r\right) \subset D^2$, which completes the proof of our claim.

Next, we note that if $\mathrm{ang}(\mathcal{D}) = 0$, then the n discs lie on one straight line. Moreover, $[S] \neq 0 \in \pi_{n-3}(T^{n-2}\backslash\{0\})$. Therefore we may apply Lemma 3.1.3 to show that $\mathcal{S}$ represents a non-trivial class in $\pi_{n-3}(\mathrm{Conf}_{n,r})$.

Finally, this non-trivial class persists up to the second critical radius by Fact 1.2.5. This is $\frac{1}{n-1}$ – when $n \in \{4, 5\}$, this is Prop. 2.0.10 and 2.0.11, while for $n \geq 6$, we note that $\frac{3}{2n+3} \geq \frac{1}{n-1}$, and so this must be the second critical radius by Fact 1.2.7. □

Remark 3.2.4. While we are able to extend the existence of a homotopic sphere in $\mathrm{Conf}_{n,r}$ to radii up to $r = \frac{1}{n-1}$ in the proof of Thm. 3.2.1, Remark 3.2.3 shows this will not project to $\partial\left([-\frac{2\pi}{n}, \frac{2\pi}{n}]^{n-2}\right)$ for radii above $\frac{1}{n-4\sin^2(\frac{\pi}{2n})}$: for these radii, any configuration with angles $(0, \ldots, 0, -\frac{\pi}{n}, \frac{2\pi}{n}, -\frac{\pi}{n}, 0, \ldots, 0)$ has diameter greater than 2, so does not lie in the unit disc.

Remark 3.2.5. This algorithm allows us to construct explicit coordinates for our configuration in terms of $\theta_i = \sum_{j=1}^{i} \phi_j$. At step 2, $x_i = 2r(\sum_{j=1}^{i-1} \cos\theta_j, \sum_{j=1}^{i-1} \sin\theta_j)$ for

$i \geq 2$, with $\theta_1 = 0$. After translation by $-\frac{1}{2}(x_1 + x_n) = -r(\sum_{j=1}^{n-1} \cos\theta_j, \sum_{j=1}^{n-1} \sin\theta_j)$, we have $x_i = r(\sum_{j=1}^{i-1} \cos\theta_j - \sum_{j=i}^{n-1} \cos\theta_j, \sum_{j=1}^{i-1} \sin\theta_j - \sum_{j=i}^{n-1} \sin\theta_j)$.

Remark 3.2.6. We can construct a sphere of the same homotopy class by lifting $S = \partial\left([-\xi,\xi]^{n-2}\right)$ to $\mathrm{Conf}_{n,r}$ by the same algorithm for all $0 < \xi \leq \frac{2\pi}{n}$ and $\frac{1}{n} < r \leq \frac{1}{n-4\sin^2(\frac{\xi}{4})}$. Then, by Remark 3.2.5, $x_i \to \left(\frac{2i-n-1}{n}, 0\right)$ as $\xi \to 0$ for all configurations of the sphere. That is to say, the configurations of the sphere are constrained increasingly close to the critical configuration.

Remark 3.2.7. This construction gives rise to many distinct homotopy classes in $\pi_{n-3}(\mathrm{Conf}_{n,r})$ for $\frac{1}{n} < r \leq \frac{1}{n-1}$. Given $r \leq \frac{1}{n-4\sin^2\frac{\pi}{2n}}$, take $\varsigma \in S_n$, and let $\mathcal{S}' = \varsigma \cdot \mathcal{S}$, where the action of ς on $\mathrm{Conf}_{n,r}$ permutes the discs in the natural way. It can be shown that there is a path $\gamma\colon [0,1] \to \mathrm{Conf}_{n,r}$ such that $\gamma(0) \in \mathcal{S}$ and $\gamma(1) = \varsigma \cdot \gamma(0)$, so we can consider $[\mathcal{S}']$ in the same homotopy group as $[\mathcal{S}]$. Then $\mathrm{ang}(\mathcal{S}')$ encircles some $0 \neq \Phi \in \{(\phi_2, \ldots, \phi_{n-1}) \in T^{n-2} \mid \forall_i\ \phi_i \in \{0, \pi\}\}$, where Φ corresponds to n discs lying on a line. Hence $\mathrm{ang}_*([\mathcal{S}']) \neq [S]$, so $[\mathcal{S}'] \neq [\mathcal{S}]$.

3.3 Higher critical radii: a parametric packing problem

It is natural to consider whether similar constructions might work beyond higher critical radii. The most accessible critical configurations of $\mathrm{Conf}_{n,r}$ for this question are the configurations where k discs of radius $\frac{1}{k}$ ($k < n$) lie on some diameter of D^2. If we 'forget' the remaining $n-k$ discs, then we know that this critical configuration exists in $\mathrm{Conf}_{k,\frac{1}{k}}$, and we have shown (Thm. 3.2.1) that there is a corresponding non-contractible $(k-3)$-sphere in $\mathrm{Conf}_{k,r}$ for $r \in \left(\frac{1}{k}, \frac{1}{k-1}\right]$. We want to know whether the 'same' non-trivial π_{k-3}-class exists in $\mathrm{Conf}_{n,\frac{1}{k}+\varepsilon}$ for sufficiently small ε. In the sphere representing this class, we would expect to see some k discs which wind round the line $x = 0$ as described in the algorithm of Thm. 3.2.1, while the remaining $n-k$ discs would move only as much as necessary to avoid intersections between discs.

We formalise the notion of forgetting, and explore this type of question for all critical radii and non-trivial homotopy classes, as follows. Take $n \geq k$ and let $F_{n,k}\colon \mathrm{Conf}_{n,r} \to \mathrm{Conf}_{k,r}$ be the forgetful map $(D_1, \ldots, D_n) \mapsto (D_1, \ldots, D_k)$. Then we ask:

Question 3.3.1. Take $m, k \in \mathbb{N}$. Let r_0 be a critical radius of $\mathrm{Conf}_k(U)$, and take some non-trivial $\gamma \in \pi_m(\mathrm{Conf}_{k,r_0+\varepsilon}(U))$. What is the largest $n \in \mathbb{N}$ such that, for all

sufficiently small $\varepsilon > 0$, there exists $\gamma' \in \pi_m(\mathrm{Conf}_{n,r_0+\varepsilon})$ with $(F_{n,k})_*(\gamma') = \gamma$?

Having found some n and γ' satisfying the above conditions, we therefore have a non-zero π_m-class in $\mathrm{Conf}_{n,r_0+\varepsilon}(U)$, where r_0 is a higher critical radius for n discs. Furthermore, since $F_{n,k} = F_{n,n'} \circ F_{n',k}$ for every $k \leq n' \leq n$, this also yields a non-trivial π_m-class in each $\mathrm{Conf}_{n',r_0+\varepsilon}(U)$, where r_0 is a higher critical radius for every $k < n' \leq n$.

For the remainder of this section, we consider the π_{k-3}-class in $\mathrm{Conf}_{k,\frac{1}{k}+\varepsilon}$ from §3.2. It is easy to find a lower bound on our question for these. By Remark 3.2.6, for any $\varepsilon' > 0$ and sufficiently small $\varepsilon > 0$, we can construct a non-contractible sphere in $\mathrm{Conf}_{k,\frac{1}{k}+\varepsilon}$ whose configurations are contained in $H_{\varepsilon'} \coloneqq \bigcup_{i=1}^{k} B\left(\left(\frac{2i-k-1}{k}, 0\right), \frac{1}{k} + \varepsilon'\right)$. Therefore, if we can fit l discs of radius $\frac{1}{k} + \varepsilon$ in $D^2 \backslash H_{\varepsilon'}$, then we have a lower bound $n \geq k + l$.

We illustrate this with an example.

Proposition 3.3.2. *Consider the non-trivial class $[\mathcal{S}] \in \pi_2(\mathrm{Conf}_{5,\frac{1}{5}+\varepsilon})$ constructed in §3.2. Then for $5 \leq n \leq 19$, there is $[\mathcal{S}'] \in \pi_2(\mathrm{Conf}_{n,\frac{1}{5}+\varepsilon})$ such that $(F_{n,5})_*([\mathcal{S}']) = [\mathcal{S}]$.*

This is inspired by the packing of 19 discs in [17].

Proof. Consider the configuration $(D_1, \ldots, D_{19}) \in \pi_2(\mathrm{Conf}_{19,\frac{1}{5}})$ in Fig. 3.4, in which $x_i = (\frac{-6+2i}{5}, 0)$ for $1 \leq i \leq 5$ (five discs lined up across the horizontal diameter), and the remaining 14 discs are centred at the coordinates of form $\frac{2}{5}\left(\cos\frac{\pi j}{3}, \sin\frac{\pi j}{3}\right)$ or $\frac{4}{5}\left(\cos\frac{\pi j}{6}, \sin\frac{\pi j}{6}\right)$, j an integer.

We now adjust the configuration as follows, for some $\varepsilon > 0$.

1. Roll $D_{11}, D_{13}, D_{16}, D_{18}$ along ∂D^2 towards the horizontal diameter, so they no longer touch D_6, D_7, D_8, D_9. Stop before they make contact with $D_{10}, D_{14}, D_{15}, D_{19}$.
2. Move D_6, D_7, D_8, D_9 away from the horizontal diameter. Stop before they make contact with any other discs.
3. Enlarge D_6, D_7 about their point of contact until they have radius $\frac{1}{5} + \varepsilon$. Do the same for D_8, D_9.
4. Enlarge D_j about its point of contact with ∂D^2 until it has radius $\frac{1}{5} + \varepsilon$ for each $10 \leq j \leq 19$.

If ε is chosen to be sufficiently small, then the discs D_j $(6 \leq j \leq 19)$ do not overlap each

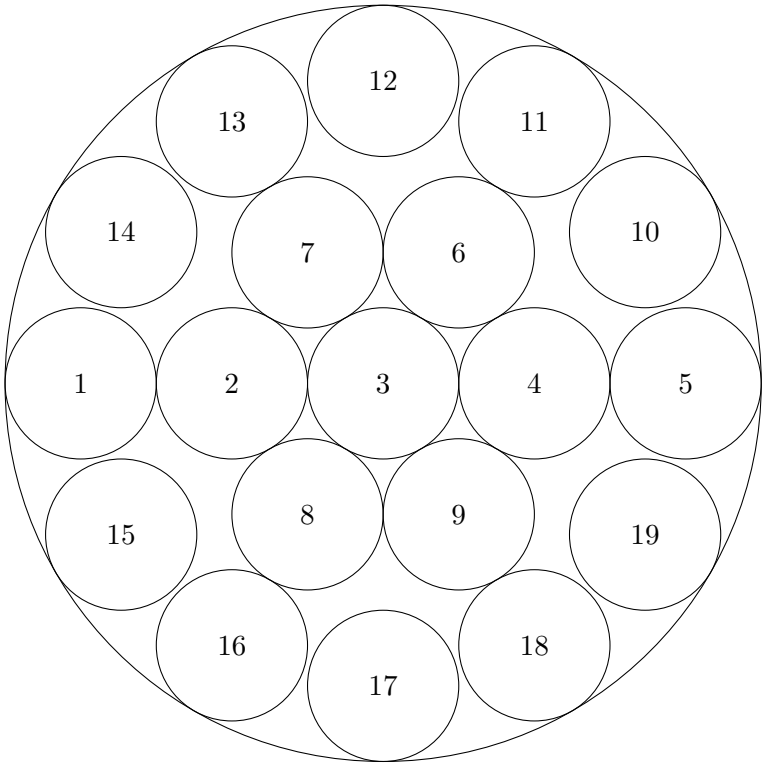

Figure 3.4: A configuration in $\mathrm{Conf}_{19,\frac{1}{5}}$. The positions of D_i for $6 \leq i \leq 19$ can be adjusted so that none are in contact with discs D_i for $1 \leq i \leq 5$. This allows the D_i, $1 \leq i \leq 5$, to trace out the non-trivial element of $\pi_2(\mathrm{Conf}_{5,\frac{1}{5}+\varepsilon})$ from §3.2.

other and remain within D^2. Furthermore, there is some ε' and some non-contractible 2-sphere γ in $\mathrm{Conf}_{5,\frac{1}{5}+\varepsilon}$ such that the configurations of γ are contained in $H_{\varepsilon'}$ and $H_{\varepsilon'} \cap D_j = \emptyset$ for all $6 \leq j \leq 19$.

Thus by choosing a representation of $[\mathcal{S}]$ such that the discs of each configuration fit inside $H_{\varepsilon'}$, and placing $n-5$ additional discs in some of the positions D_j $(6 \leq j \leq 19)$, we construct $[\mathcal{S}'] \in \pi_2(\mathrm{Conf}_{n,\frac{1}{5}+\varepsilon})$ such that $(F_{n,5})_*([\mathcal{S}']) = [\mathcal{S}]$ for $5 \leq n \leq 19$. □

Since the best known packing of 20 discs into D^2 has disc radius 0.19522 (see [30]), it appears likely that 19 is the best possible value of n for $k = 5$, as it is likely impossible to fit 20 discs of radius $\frac{1}{5}+\varepsilon$ in D^2 at all. On the other hand, it is not necessarily true that this technique gives the best possible lower bound for general n, since this construction depends on a specific choice of representative of the homotopy class. However, in most representatives $\mathcal{S}$ of this class, the variation of $\bigcup \mathcal{D}$ over all $\mathcal{D} \in \mathcal{S}$ is much greater. This means that the additional discs must be able to fit into many differently-shaped regions (given by $D^2 \setminus \bigcup \mathcal{D}$ for each $\mathcal{D}$), and must do so continuously, and without intersecting with each other. The configurations we constructed in §3 consist of an unbroken line of discs, in which the variation of $\bigcup \mathcal{D}$ is symmetric about the x-axis. If the positions of the first k discs vary more, we see that for some $\mathcal{D} \in \mathcal{S}$, there is more space above the configuration, and for other $\mathcal{D} \in \mathcal{S}$, there is more space below, so some of the additional discs must move from one side of the configuration to the other. This may not be possible in a continuous way without intersecting other discs when we are near the packing limit. Thus it seems reasonable to conjecture the following:

Conjecture 3.3.3. *Let $0 \neq \gamma \in \pi_{k-3}(\mathrm{Conf}_{k,\frac{1}{k}+\varepsilon})$ be the sphere found in §3.2. Let $H := \bigcup_{i=1}^{k} B\left(\left(\frac{2i-k-1}{k}, 0\right), \frac{1}{k}\right)$, H_ε its ε-thickening, and m be the greatest number of discs of radius $\frac{1}{k}$ which fit in $D^2 \setminus H_\varepsilon$ for some $\varepsilon > 0$. Then the answer to Question 3.3.1 is $k+m$.*

In complete generality, an upper bound is given by the maximal packing of discs of radius $r_0 + \varepsilon$ into D^2 ($\varepsilon > 0$ arbitrarily small).

Chapter 4

The full homotopy type for four discs

In §3.1, we determine the homotopy type of $\mathrm{Conf}_{4,r}$ for $r \leq \frac{1}{4}$ and $r > \frac{1}{3}$. We also show that there exists a non-trivial 'thick braid' in $\pi_1(\mathrm{Conf}_{4,r})$ for $\frac{1}{4} < r \leq \frac{1}{3}$ which vanishes under the inclusion $\mathrm{Conf}_{n,r} \to \mathrm{Conf}_n$. In this chapter, we develop a full picture of the homotopy type of $\mathrm{Conf}_{4,r}$ when $\frac{1}{4} < r \leq \frac{1}{3}$. We start by noting that $\mathrm{Conf}_{4,r} \simeq \mathrm{Conf}_{4,\frac{1}{3}} = \tau^{-1}[\frac{1}{3}, \infty)$ by Fact 1.2.5.

Let Y be the 1-dimensional cell complex consisting of

- a set, V_1, of 0-cells, indexed over the 6 vertices of an octahedron,
- a set, V_2, of 0-cells, indexed over the 8 faces of an octahedron, and
- a set, E, of 1-cells, in which $v_1 \in V_1$ and $v_2 \in V_2$ bound a 1-cell if and only if the vertex corresponding to v_1 is on the boundary of the face corresponding to v_2.

We will prove the following.

Theorem 4.0.1. *Let* $r \in \left(\frac{1}{4}, \frac{1}{3}\right]$. *Then* $\mathrm{Conf}_{4,r} \simeq Y \times S^1$.

We will prove that $\mathrm{Conf}_{4,\frac{1}{3}}$ is a trivial circle bundle (a topological space of the form $X \times S^1$ for some space X) in §4.1. Then, we will show how the quotient $\mathrm{Conf}_{4,\frac{1}{3}}/S^1$ sits naturally on the surface of an octahedron in §4.2. Finally, we will retract $\mathrm{Conf}_{4,\frac{1}{3}}/S^1$ onto Y in §4.3. We will then use this in §4.4 to understand the homotopy groups of $\mathrm{Conf}_{4,r}$, $r \in \left(\frac{1}{4}, \frac{1}{3}\right]$, in particular studying how the elements of the fundamental group

can be considered as 'thick braids', in comparison to the pure braid group on 4 strings PBr_4.

Throughout this chapter, we will denote an ordering of m numbers from the set $\{1, 2, \ldots, n\}$ by $(i_1\ i_2\ \ldots\ i_m)$, and a cyclic ordering by $[i_1\ i_2\ \ldots\ i_m]$, where $i_1, i_2, \ldots, i_m$ are distinct elements of $\{1, 2, \ldots, n\}$. Then for a cyclic ordering ς, denote $\hat{\varsigma}_{i_k} \coloneqq (i_{k+1}\ \ldots\ i_m\ i_1\ \ldots\ i_{k-1})$ for any $1 \leq k \leq m$. For an ordering ρ, we will denote the corresponding cyclic ordering (where we forget the start point) by $[\rho]$. Furthermore, we will sometimes borrow from the language of the permutation group and write $i_{k+1} = \varsigma(i_k)$ for $1 \leq k \leq m-1$ (and $i_1 = \varsigma(i_m)$ in the case that ς is a cyclic ordering).

We also, given distinct points P, Q, R, denote by $\angle PQR$ the anti-clockwise angle (taken in $[0, 2\pi)$) from the line segment $\overline{QP}$ to the line segment $\overline{QR}$ about Q. This means that $\angle PQR + \angle RQP = 2\pi$. Sometimes, we will be interested in the smaller of the two angles $\angle PQR, \angle RQP$, in which case we will write $|\angle PQR| = \min\{\angle PQR, \angle RQP\}$.

The proof will also require the following claims about configurations of discs.

Lemma 4.0.2. *Take $R \in (0, \infty)$, and let $x, y \in \overline{B(0,R)}$ be such that $|x - y| \geq R$. Then for all $\lambda, \mu \in [1, \infty)$, we have $|\lambda x - \mu y| \geq R$.*

Proof. The hypotheses of the lemma are equivalent to the claim $x \in \overline{B(0,R)} \backslash B(y,R)$. Take $t \in [1, \lambda]$. Since x lies on the line segment joining 0 and λx, with $0 \in \overline{B(y,R)}$ and $x \notin B(y,R)$, it follows that $tx \notin B(y,R)$ by convexity of the ball. Therefore $y \notin \bigcup_{t\in[1,\lambda]} B(tx,R)$. Since $0 \in \bigcup_{t\in[1,\lambda]} B(tx,R)$, it follows by convexity that $\mu y \notin \bigcup_{t\in[1,\lambda]} B(tx,R)$; in particular, $|\lambda x - \mu y| \geq R$. □

Lemma 4.0.3. *Let $\mathcal{D} \in \mathrm{Conf}_{n,\frac{1}{3}}$ for some $n \in \mathbb{N}$, $x, y \neq 0$ be the centres of some discs in $\mathcal{D}$. Then $\angle x0y \geq \frac{\pi}{3}$.*

Proof. Let $x, y \neq 0$ be the centres of two discs in $\mathcal{D}$. Then $|x-y| \geq \frac{2}{3}$ and $x, y \in \overline{B\left(0, \frac{2}{3}\right)}$. Let $\hat{x} = \frac{2}{3|x|}x$, $\hat{y} = \frac{2}{3|y|}y$, from which $|\hat{x}| = |\hat{y}| = \frac{2}{3}$ and $\angle\hat{x}0\hat{y} = \angle x0y$. Then by Lemma 4.0.2, we have $|\hat{x} - \hat{y}| \geq \frac{2}{3}$. At equality, we have the triangle with vertices $0, \hat{x}, \hat{y}$ is equilateral; thus $\angle\hat{x}0\hat{y} \geq \frac{\pi}{3}$. □

As one disc approaches the origin, however, we can strengthen this claim to show that the angle of separation to another disc must be at least $\frac{\pi}{2}$ in the limit.

Lemma 4.0.4. *Let $\mathcal{D} \in \mathrm{Conf}_{n,\frac{1}{3}}$ for some $n \in \mathbb{N}$, and let $x, y \neq 0$ be the centres of some discs in $\mathcal{D}$. Then $\angle x0y \geq \arccos\left(\frac{3}{4}|x|\right)$.*

Proof. Let $\theta = \angle x0y$ be the angle subtended at the origin by x and y. Denote $a = |x|, b = |y|, c = |x - y|$. Then $c^2 = a^2 + b^2 - 2ab\cos(\theta)$ by the cosine rule. We further note $c^2 \geq \frac{4}{9}$.

By Lemma 4.0.3, we have $\frac{\pi}{3} \leq \theta \leq \frac{5\pi}{3}$, from which we see that $2a\cos(\theta) \leq a \leq \frac{2}{3} + b$. Now,

$$\begin{aligned} 2a\cos(\theta) \leq \frac{2}{3} + b \Rightarrow \quad & 2a\left(\frac{2}{3} - b\right)\cos(\theta) \leq \frac{4}{9} - b^2 \\ \Rightarrow \quad & b^2 - 2ab\cos(\theta) \leq \frac{4}{9} - \frac{4}{3}a\cos\theta \\ \Rightarrow \quad & a^2 + b^2 - 2ab\cos(\theta) \leq a^2 + \frac{4}{9} - \frac{4}{3}a\cos\theta \quad . \end{aligned}$$

Therefore, we have shown that

$$\frac{4}{9} \leq a^2 + \frac{4}{9} - \frac{4}{3}a\cos\theta \quad .$$

Thus $\cos(\theta) \leq \frac{3}{4}a$, as required. □

4.1 The configuration space as a trivial circle bundle

Let $n \geq 2$, and consider the free continuous S^1-action on $\mathrm{Conf}_{n,r}$ given by rotating a configuration about the origin, resulting from the rotational symmetry of D^2. Take the projection $q\colon \mathrm{Conf}_{n.r} \to \overline{\mathrm{Conf}}_{n,r} \coloneqq \mathrm{Conf}_{n,r}/S_1$, which is a principal S^1-bundle, and choose any section $s\colon \overline{\mathrm{Conf}}_{n,r} \to \mathrm{Conf}_{n,r}$. Let $\Theta\colon \mathrm{Conf}_{n,r} \to S^1$ map each $\mathcal{D} \in \mathrm{Conf}_{n,r}$ to the unique $\theta \in S^1$ such that $\mathcal{D} = \theta \cdot s[\mathcal{D}]$. This yields the following.

Proposition 4.1.1. *$p\colon \mathrm{Conf}_{n,r} \to \overline{\mathrm{Conf}}_{n,r} \times S^1,\ \mathcal{D} \mapsto (q(\mathcal{D}), \Theta(\mathcal{D}))$ is a homeomorphism with inverse $\left(\bar{\mathcal{D}}, \theta\right) \mapsto \theta \cdot s\left(\bar{\mathcal{D}}\right)$. Furthermore, s is a homeomorphism onto its image.*

Here, we will use the section mapping each $\bar{\mathcal{D}} \in \overline{\mathrm{Conf}}_{n,r}$ to the unique representative in which $x_3 - x_2$ points in the positive x-direction (i.e. $x_3 - x_2 = (|x_3 - x_2|, 0)$ in Cartesian coordinates). Then $\Theta(\mathcal{D})$ is the anticlockwise angle from the vector $(1, 0)$ to the vector $x_3 - x_2$.

4.2 The geometric structure of the quotient space

Prop. 4.1.1 shows that $\overline{\mathrm{Conf}}_{4,\frac{1}{3}}$ has the same homotopy-type as $s\left(\overline{\mathrm{Conf}}_{4,\frac{1}{3}}\right) = \{\mathcal{D} \in \mathrm{Conf}_{4,\frac{1}{3}} \mid \Theta(\mathcal{D}) = 0\}$. Let $\bar{\tau} = \tau|_{s\left(\overline{\mathrm{Conf}}_n\right)}$ for all $n \in \mathbb{N}$. Then $s\left(\overline{\mathrm{Conf}}_{4,\frac{1}{3}}\right) = \bar{\tau}^{-1}\left[\frac{1}{3}, \infty\right)$.

If $x \in \mathrm{Conf}_4$ has some point at the origin, then $\tau(x) \leq \frac{1}{3}$. Therefore, we may begin by writing $\bar{\tau}^{-1}\left[\frac{1}{3}, \infty\right) = A \cup B \cup C$, where

$$A = \left\{ x \in \bar{\tau}^{-1}\left[\frac{1}{3}, \infty\right) : \ \forall_j \ |x_j| > 0 \right\},$$
$$B = \left\{ x \in \bar{\tau}^{-1}\left(\frac{1}{3}\right) : \ \exists_i \ |x_i| = 0 \text{ and all } x_j \text{ lie in some closed semidisc} \right\}, \text{ and}$$
$$C = \left\{ x \in \bar{\tau}^{-1}\left(\frac{1}{3}\right) : \ \exists_i \ |x_i| = 0 \text{ and no open semidisc contains all } x_j \neq 0 \right\}.$$

Moreover, in $\bar{\tau}^{-1}\left[\frac{1}{3}, \infty\right)$, no two points can lie on the same radius of the unit disc unless one is at the origin; then in A, the four points have a well-defined cyclic ordering ς (taken anticlockwise) about the origin, so we may write $A = \bigsqcup_\varsigma A_\varsigma$. Similarly, $B = \bigsqcup_{(i,\rho)} B_{i,\rho}$, where $i \in \{1,2,3,4\}$ is the index of the point at the origin and ρ is an ordering of the remaining three points (this is not a cyclic ordering, since the empty open semi-disc gives a well-defined starting point), and $C = \bigsqcup_{(i,\rho')} C_{i,\rho'}$, where in this case ρ' is a cyclic ordering of the remaining three points.

We also define $S_\varsigma = A_\varsigma \cup \bigcup_{i \in \{1,2,3,4\}} B_{i,\hat{\varsigma}_i}$.

Proposition 4.2.1. *S_ς is the closure of A_ς in $\bar{\tau}^{-1}\left[\frac{1}{3}, \infty\right)$.*

Proof. Let $(x^m)_{m \in \mathbb{N}}$ be a sequence in A_ς converging to some $x \in \bar{\tau}^{-1}\left[\frac{1}{3}, \infty\right)$. In particular, $x_i^m \to x_i$ for each $i \in \{1,2,3,4\}$. If there is no i such that $x_i = 0$, then $x \in A_\varsigma$.

Otherwise suppose $x_i = 0$ for some $i \in \{1,2,3,4\}$, and write $\varsigma = [i\ i_1\ i_2\ i_3]$. Take $\varepsilon > 0$. Then for all sufficiently large m, we have $|x_j^m - x_j| < \varepsilon$ for all $j \in \{1,2,3,4\}$. Therefore, we can choose some $\delta > 0$, where $\delta \to 0$ as $\varepsilon \to 0$, such that $|\angle x_j 0 x_j^m| < \delta$ for all $j \neq i$. Combining this with Cor. 4.0.4, we have

$$\angle x_i^m 0 x_{i_1} \geq \angle x_i^m 0 x_{i_1}^m - |\angle x_{i_1} 0 x_{i_1}^m| \geq \arccos \frac{3}{4}|x_i^m| - \delta$$

and similarly $\angle x_{i_3} 0 x_i^m \geq \arccos \frac{3}{4}|x_i^m| - \delta$.

The radii through $x_{i_1}, x_{i_2}, x_{i_3}$ split the unit disc into three sectors. Since $|\angle x_j 0 x_j^m| < \delta$ for all $j \neq i$, the points $x_{i_1}, x_{i_2}, x_{i_3}$ retain the cyclic order $[i_1\ i_2\ i_3]$, and x_i^m is in the

sector between x_{i_3} and x_{i_1}. This sector has angular extent

$$\angle x_{i_3} 0 x_i^m + \angle x_i^m 0 x_{i_1} \geq 2\left(\arccos\frac{3}{4}|x_i^m| - \delta\right) \to \pi \qquad \text{as } m \to \infty \quad .$$

Therefore, $x \in B_{i,\hat{\varsigma}_i}$.

Conversely, every $x \in A_\varsigma$ is the limit of a constant sequence in A_ς, and every $x \in B_{i,\hat{\varsigma}_i}$ is the limit of the sequence $(x^m)_{m\in\mathbb{N}}$ in A_ς given by $x_j^m = x_j$ for all m and all $j \neq i$, and $x_i \to 0$ along the radius which bisects the largest sector not containing any other x_j. □

Proposition 4.2.2. *$C_{i,\rho'}$ is parametrised by the hexagon*

$$\left\{(\phi_1,\phi_2) \in \mathbb{R}^2 \colon \frac{\pi}{3} \leq \phi_1 \leq \pi, \frac{\pi}{3} \leq \phi_2 \leq \pi, \pi \leq \phi_1 + \phi_2 \leq \frac{5\pi}{3}\right\} \quad .$$

$S_\varsigma \cap C_{i,\rho'}$ is one of the edges $\phi_1 = \pi$, $\phi_2 = \pi$, $\phi_1 + \phi_2 = \pi$ if $\rho' = [\hat{\varsigma}_i]$; otherwise, it is empty.

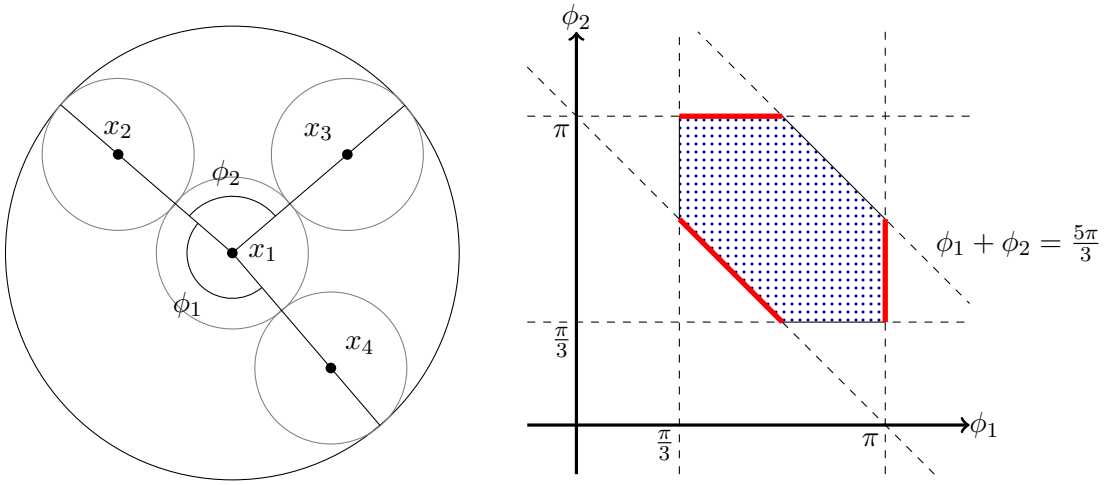

Figure 4.1: Left: A configuration in one of the connected components, $C_{1,[2\ 4\ 3]}$, of the critical locus of τ at $r = \frac{1}{3}$. Right: A coordinate parametrisation of $C_{1,[2\ 4\ 3]}$, using the angles shown on the configuration, given by the blue dotted area including boundary. The thick red line segments denote the intersection with the pieces S_ς.

Proof. Let $\rho' = [j\ k\ l]$. Then let $\hat{x} = (1, 0)$, $\phi_1 = \angle x_j 0 x_k$, $\phi_2 = \angle x_l 0 x_j$. A configuration in $\{x \in \tau^{-1}\left[\frac{1}{3}, \infty\right) \mid \exists_i |x_i| = 0$ and no open semidisc contains all $x_j \neq 0\}$ is uniquely determined by the triple $(\angle \hat{x} 0 x_j, \phi_1, \phi_2)$. Furthermore, $\angle \hat{x} 0 x_j$ is uniquely determined by the pair (ϕ_1, ϕ_2) and the condition $\Theta(x) = 0$. Thus, a configuration in $C_{i,\rho'}$ is uniquely determined by (ϕ_1, ϕ_2).

$\phi_1, \phi_2 \geq \frac{\pi}{3}$ and $\phi_1 + \phi_2 \leq \frac{5\pi}{3}$ by Cor. 4.0.3. $\phi_1, \phi_2 \leq \pi$ and $\phi_1 + \phi_2 \geq \pi$ by the condition that the remaining points are not contained in an open semidisc. When the three latter inequalities are all strict, then $x \notin A \cup B$. On the other hand, if $\phi_1 = \pi$, then x_j, x_i, x_k lie on some common diameter, so $x \in B_{i,(k\ l\ j)} \subset S_{[i\ k\ l\ j]}$. Similarly, $x \in B_{i,(j\ k\ l)} \subset S_{[i\ j\ k\ l]}$ if $\phi_2 = \pi$, and $x \in B_{i,(l\ j\ k)} \subset S_{[i\ l\ j\ k]}$ if $\phi_1 + \phi_2 = \pi$. □

Thus, $\overline{\mathrm{Conf}}_{4,\frac{1}{3}}$ consists of the six pieces S_ς and the eight hexagonal pieces $C_{i,\rho'}$. By the arguments of Prop. 4.2.2, S_ς is connected to each of the four pieces $C_{i,\rho'}$ where $i \in \{1,2,3,4\}$ and ρ' is the cyclic ordering $\hat{\varsigma_i}$ obtained by removing i from ς. Geometrically, $\hat{\varsigma_i}$ is the cyclic ordering of the remaining points when x_i flows to the origin. Conversely, each $C_{i,\rho'}$ is connected to three pieces S_ς, depending on which position you insert i into ρ'; and geometrically, the insertion of i between j and k inside ρ' corresponds to moving the outer discs until the empty arc between x_j and x_k is at least π radians, and then flowing x_i orthogonally to $x_j - x_k$ into this empty region. Each intersection between some S_ς and some $C_{i,\rho'}$ is a submersion of an interval. This is depicted in Fig. 4.2.

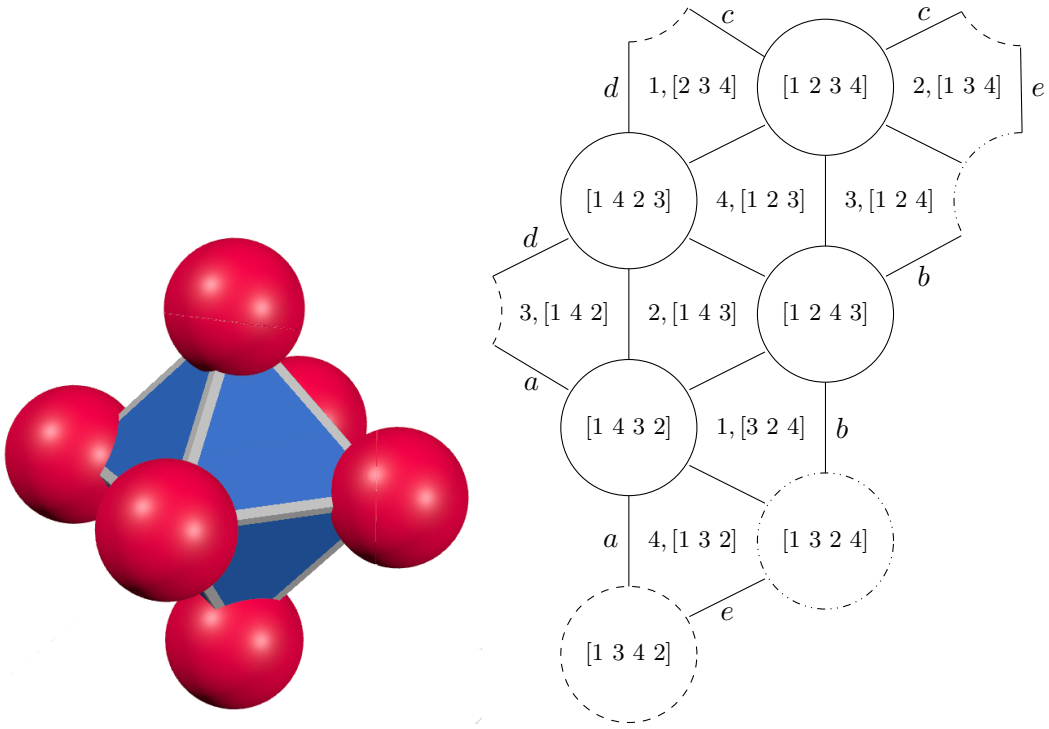

Figure 4.2: Left: The structure of $\mathrm{Conf}_{4,\frac{1}{3}}/S^1$, shown on the surface of an octahedron (grey). On the faces are the connected components, $C_{i,\rho'}$ (blue), of the critical locus at $r = \frac{1}{3}$, represented as hexagons due to Prop. 4.2.2. At the vertices are the connected components, S_ς (red), of the non-critical subset of $\mathrm{Conf}_{4,\frac{1}{3}}/S^1$. Right: A net/schematic for $\mathrm{Conf}_{4,\frac{1}{3}}/S^1$. The circle containing the cyclic ordering ς represents the set S_ς, and the hexagon containing a pair i, ρ represents the critical component $C_{i,\rho}$. The straight outer edges are labelled with letters to show how they are glued. The boundary arcs are glued to the circles of the same line style.

4.3 Contracting the configuration space

We note that C is the closure of the locus of critical configurations $x \in s\left(\overline{\mathrm{Conf}}_4\right)$ with $\bar{\tau}(x) = \frac{1}{3}$ – that is, there is no local flow at any $x \in C$ such that τ is increasing to first order. Conversely, if $x \in B$, then we may immediately flow the disc at the origin outwards as follows (see Fig. 4.3). The rays from the origin through the three other disc centres divides the boundary of the unit disc into three arcs. Since all discs lie in a closed semidisc, precisely one of these arcs is at least a semicircle. Then the disc at the origin may move radially outwards towards the point bisecting this arc. We use this idea to retract $\hat{\tau}^{-1}\left[\frac{1}{3}, \infty\right)$ onto the 1-skeleton Y from Thm. 4.0.1 by first contracting each S_ς to a point and then retracting each $C_{i,\rho'}$ onto a 1-skeleton.

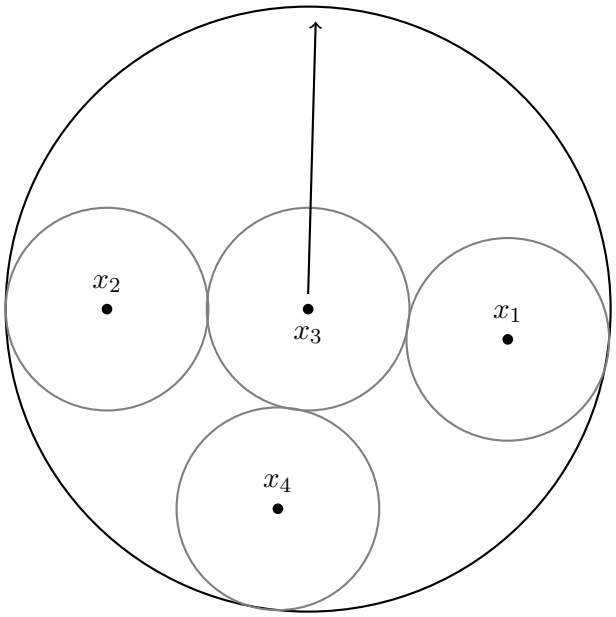

Figure 4.3: An example of a non-critical configuration in $s\left(\overline{\mathrm{Conf}}_{4,\frac{1}{3}}\right)$ with one disc centred at the origin. Since there is an empty sector of at least π radians anticlockwise from x_1 to x_2, it is possible for disc 3 to move into this gap along some radius (e.g. the radius bisecting this sector), thus increasing the value of τ on the underlying configuration of points.

Let $s_\varsigma \in S_\varsigma$ be the unique configuration in which $|x_i| = \frac{2}{3}$ for all $i \in \{1, 2, 3, 4\}$ and

$$\angle x_1 0 x_{\varsigma(1)} = \angle x_{\varsigma(1)} 0 x_{\varsigma^2(1)} = \angle x_{\varsigma^2(1)} 0 x_{\varsigma^3(1)} = \frac{\pi}{2}$$

– that is, if we consider s_ς as an element of $\mathrm{Conf}_{4,\frac{1}{3}}$, then it is the unique configuration in which all discs touch the boundary with cyclic order ς, the disc centres lie on the

corners of a square, and $x_3 - x_2$ points in the positive x-direction.

Proposition 4.3.1. *$\{s_\varsigma\}$ is a strong deformation retract of S_ς.*

This claim is proven by the following three lemmas. Take $\varepsilon \in \left(0, \frac{1}{3}\right)$, and consider the sets

$$S'_\varsigma = \{x \in S_\varsigma \mid \forall_i \ |x_i| \geq \varepsilon\},$$
$$T_\varsigma = \left\{x \in S_\varsigma \mid \forall_i \ |x_i| = \frac{2}{3}\right\}.$$

Lemma 4.3.2. *S'_ς is a strong deformation retract of S_ς.*

Proof. We start by defining our retraction. For any $x \in \mathrm{Conf}_{4,\frac{1}{3}}$, there is at most one i such that $|x_i| \leq \varepsilon$ by the triangle inequality. In the case that such i exists, the radii through the remaining three points split the unit disc into three sectors. If $x_i = 0$, one arc is at least a semicircle. Otherwise, the sector containing x_i has extent at least $2\arccos\frac{3}{4}|x_i|$ by Cor. 4.0.4, while the other two sectors each have extent at least $\frac{\pi}{3}$ by Cor. 4.0.3, and therefore their extent is at most $\frac{5\pi}{3} - 2\arccos\frac{3}{4}|x_i|$. Given that $|x_i| \leq \frac{1}{3}$, we have

$$2\arccos\frac{3}{4}|x_i| > 2\arccos\frac{1}{4} > \frac{5\pi}{3} - 2\arccos\frac{1}{4} > \frac{5\pi}{3} - 2\arccos\frac{3}{4}|x_i| \quad .$$

Therefore there is a unique largest sector, so we may define the following: let v be the point which bisects the arc bounding the largest sector, and l be the unique positive real number such that $|x_i + lv| = \varepsilon$ (where this equation treats v as a vector with $|v| = 1$). Then we can define a continuous map $\chi\colon [0,1] \times S_\varsigma \to \mathrm{Conf}_4$ (shown in Fig. 4.4), given by

$$\chi(t,x) \coloneqq \chi_t(x_1,x_2,x_3,x_4) = \left(\begin{cases} x_j + tlv & : |x_j| \leq \varepsilon \\ x_j & : \text{otherwise} \end{cases}\right)_{j\in\{1,2,3,4\}} \quad .$$

χ_t also preserves the cyclic order ς, since x_i flows in the direction of the angle bisector of the sector it lies in. We want to find a flow on S_ς, that is, a continuous map $[0,1] \times S_\varsigma \to S_\varsigma$. To do this, we will first show that $\chi([0,1] \times S_\varsigma) \subset \tau^{-1}\left[\frac{1}{3}, \infty\right)$, and then modify χ so that $\Theta(\chi_t(x)) = 0$ for all $t \in [0,1]$, $x \in S_\varsigma$.

We claim that $\chi([0,1] \times S_\varsigma) \subset \tau^{-1}\left[\frac{1}{3}, \infty\right)$. $\chi_t(x_j)$ is stationary for any $|x_j| \geq \varepsilon$, so we only need to check the case that $|x_i| \leq \varepsilon$ for some i, and moreover, in this case, $|\chi_t(x_i)| \leq \varepsilon < \frac{2}{3}$ for all $t \in [0,1]$. Then it remains to show that $|\chi_t(x_i) - x_j| \geq \frac{2}{3}$ for all

$j \neq i$. Now suppose by symmetry that x_i is anticlockwise of v inside the sector bounded by $x_{\varsigma^3(i)}$ and $x_{\varsigma(i)}$. We have

$$\begin{aligned}|\chi_t(x_i) - x_j|^2 &= |x_i - x_j + tlv|^2 \\ &= |x_i - x_j|^2 + 2tl(x_i - x_j)\cdot v + t^2l^2|v|^2 \\ &= |x_i - x_j|^2 + 2tl\left(|x_i|\cos(\angle v0x_i) - |x_j|\cos(\angle v0x_j)\right) + t^2l^2\end{aligned}$$

We bound this below by the following inequalities. By Cor. 4.0.3, we have

$$\angle x_{\varsigma(i)}0x_{\varsigma^2(i)} \geq \frac{\pi}{3}, \quad \angle x_{\varsigma^2(i)}0x_{\varsigma^3(i)} \geq \frac{\pi}{3} \tag{4.1}$$

hence

$$\angle v0x_{\varsigma(i)} = \frac{1}{2}\left(2\pi - \angle x_{\varsigma(i)}0x_{\varsigma^2(i)} - \angle x_{\varsigma^2(i)}0x_{\varsigma^3(i)}\right) \leq \frac{1}{2}\left(2\pi - 2\frac{\pi}{3}\right) = \frac{2\pi}{3} \tag{4.2}$$

By Cor. 4.0.4, we have

$$\angle x_i0x_{\varsigma(i)} \geq \arccos\frac{3}{4}|x_i| \geq \arccos\frac{1}{4} \geq \frac{5\pi}{12} \tag{4.3}$$

and therefore

$$\angle x_{\varsigma^3(i)}0v = \angle v0x_{\varsigma(i)} = \angle v0x_i + \angle x_i0x_{\varsigma(i)} \geq \angle v0x_i + \arccos\frac{3}{4}|x_i| \geq \angle v0x_i + \frac{5\pi}{12} \tag{4.4}$$

hence

$$\angle v0x_i \leq \frac{2\pi}{3} - \frac{5\pi}{12} = \frac{\pi}{4} \tag{4.5}$$

For $j = \varsigma(i)$, we have by (4.4) and (4.2)

$$0 < \arccos\frac{3}{4}|x_i| \leq \angle v0x_{\varsigma(i)} \leq \pi$$

Therefore, since cos is decreasing on $[0, \pi]$ and $|x_{\varsigma(i)}| \leq \frac{2}{3}$, and applying (4.5), we get

$$|x_{\varsigma(i)}|\cos(\angle v0x_{\varsigma(i)}) \leq \frac{2}{3}\cos\left(\arccos\frac{3}{4}|x_i|\right) = \frac{1}{2}|x_i| < |x_i|\cos(\angle v0x_i)$$

For $j = \varsigma^2(i)$, we have by (4.1) and (4.3)

$$\angle v0x_{\varsigma^2(i)} = \angle v0x_i + \angle x_i0x_{\varsigma(i)} + \angle x_{\varsigma(i)}0x_{\varsigma^2(i)} \geq 0 + \frac{5\pi}{12} + \frac{\pi}{3} > \frac{\pi}{2}$$

and by (4.1) and (4.4)

$$\angle v0x_{\varsigma^2(i)} = 2\pi - \angle x_{\varsigma^2(i)}0v = 2\pi - \angle x_{\varsigma^2(i)}0x_{\varsigma^3(i)} - \angle x_{\varsigma^3(i)}0v \leq 2\pi - \frac{\pi}{3} - \frac{5\pi}{12} < \frac{3\pi}{2}$$

Therefore,

$$|x_{\varsigma^2(i)}|\cos(\angle x_{\varsigma^2(i)}0v) < 0 < |x_i|\cos(\angle v0x_i)$$

For $j = \varsigma^3(i)$, we have $\cos\angle v0x_{\varsigma^3(i)} = \cos\angle x_{\varsigma^3(i)}0v$ and $\angle x_{\varsigma^3(i)}0v = \angle v0x_{\varsigma(i)}$, so $|x_{\varsigma^3(i)}|\cos(\angle v0x_{\varsigma^3(i)}) < |x_i|\cos(\angle v0x_i)$ by the same argument as the case $j = \varsigma(i)$.

Thus the map $t \mapsto |\chi_t(x_i) - x_j|$ is increasing with respect to t for all $j \neq i$, which completes our claim that $\tau(\chi_t(x)) \geq \frac{1}{3}$ for all $t \in [0,1]$, $x \in S_\varsigma$.

The map $t \mapsto \Theta(\chi_t(x))$ is not necessarily constant, so χ_t may not preserve $s\left(\overline{\mathrm{Conf}}_{4,\frac{1}{3}}\right)$. Thus we define a modified flow $\bar{\chi}_t(x) = (-\Theta(\chi_t(x))) \cdot \chi_t(x)$. This flow retains all the previous properties due to invariance of distance and angles under rotation, and moreover $\Theta(\bar{\chi}_t(x)) = -\Theta(\chi_t(x)) + \Theta(\chi_t(x)) = 0$. Thus $\bar{\chi}_t(x) \in S_\varsigma$ for all $x \in S_\varsigma$. It can be verified that $\bar{\chi}_t|_{S'_\varsigma} = \mathrm{id}_{S'_\varsigma}$ for all $t \in [0,1]$ and $\bar{\chi}_1(S_\varsigma) = S'_\varsigma$. Therefore $(\chi_t)_{t\in[0,1]}$ is a strong deformation retraction of S_ς onto S'_ς. □

Lemma 4.3.3. *T_ς is a strong deformation retract of S'_ς.*

Proof. Let $V = \{x \in \mathrm{Conf}_4 \mid \forall_{\lambda\geq 0}\forall_{i\neq j} x_i \neq \lambda x_j\} \supset S'_\varsigma$, so that V consists of all configurations in Conf_4 in which no point is at the origin and no two points lie on the same radius of the unit disc. $V' \coloneqq \left\{x \in \mathrm{Conf}_4 \colon\ \forall_i\ |x_i| = \frac{2}{3}\right\} \supset T_\varsigma$ can be shown to be a strong deformation retract of V by the following flow, defined for $t \in [0,1]$.

$$\phi_t(x_1,x_2,x_3,x_4) = \left(\left(1 - t + \frac{2t}{3|x_i|}\right)x_i\right)_{i\in\{1,2,3,4\}}$$

Here, each point of the configuration flows along the radius it lies on at constant velocity, until it has magnitude $\frac{2}{3}$ (and hence the cyclic order of the points is unchanged).

$\Theta(\phi_t(x))$ may not be constant with respect to t, so we define a modified flow $\bar{\phi}_t(x) = (-\Theta(\phi_t(x))) \cdot \phi_t(x)$, Then $\Theta(\bar{\phi}_t(x)) = 0$ for all $x \in V$, $t \in [0,1]$, so in particular, $\bar{\phi}_t$ preserves the section $s\left(\overline{\mathrm{Conf}}_{4,\frac{1}{3}}\right)$. Moreover, for all $t \in [0,1]$ and $x \in S'_\varsigma$, and all distinct $i,j \in \{1,2,3,4\}$, we have $\varepsilon \leq |x_i| \leq |\bar{\phi}_t x_i| \leq \frac{2}{3}$ and $|x_i - x_j| \geq \frac{2}{3}$; therefore by Lemma 4.0.2, $|\bar{\phi}_t x_i - \bar{\phi}_t x_j| \geq \frac{2}{3}$ – that is, $\bar{\phi}_t x \in S'_\varsigma$. Therefore $(\bar{\phi}_t|_{S'_\varsigma})_{t\in[0,1]}$ is a strong deformation retraction from S'_ς onto $V' \cap S'_\varsigma = T_\varsigma$. □

Lemma 4.3.4. *$\{s_\varsigma\}$ is a strong deformation retract of T_ς.*

Proof. Let $\tilde{T_\varsigma} = \{x \in \tau^{-1}\left[\frac{1}{3}, \infty\right) \mid \forall_i |x_i| = \frac{2}{3},$ the points have cyclic order $\varsigma\} \supset T_\varsigma$. For any $x \in \tilde{T_\varsigma}$, let $\alpha = \angle x_1 0 x_{\varsigma(1)}$, $\beta = \angle x_1 0 x_{\varsigma^2(1)}$, $\gamma = \angle x_1 0 x_{\varsigma^3(1)}$. Denote by R_θ the S^1-action on the plane given by anticlockwise rotation about the origin through angle θ, and consider the following flow on $\tilde{T_\varsigma}$, defined for $t \in [0,1]$.

$$\psi_t(x_1, x_{\varsigma(1)}, x_{\varsigma^2(1)}, x_{\varsigma^3(1)}) = \left(x_1, R_{t\left(\frac{\pi}{2}-\alpha\right)} x_{\varsigma(1)}, R_{t(\pi-\beta)} x_{\varsigma^2(1)}, R_{t\left(\frac{3\pi}{2}-\gamma\right)} x_{\varsigma^3(1)}\right)$$

ψ_t fixes x_1, while causing each of the remaining x_i to flow along an arc of radius $\frac{2}{3}$ centred on the origin until it lies on the correct corner of the square which has x_1 as a vertex.

We want to prove that ψ_t is well-defined, that is, that $\psi_t(x) \in \tilde{T_\varsigma}$ for all $t \in [0,1],\ x \in \tilde{T_\varsigma}$. Given that $|\psi_t(x_i)| = \frac{2}{3}$ for all $t \in [0,1]$ and all i, it remains to check $|\psi_t(x_i) - \psi_t(x_j)| \geq \frac{2}{3}$ for all $i \neq j$, or equivalently $\angle \psi_t(x_i) 0 \psi_t(x_{\varsigma(i)}) \geq \frac{\pi}{3}$ for all i and all $t \in [0,1]$ (this condition also ensures that the cyclic order of the points is unchanged). This is immediate for $i = 1$, since either $\alpha > \frac{\pi}{2}$, in which case $\angle \psi_t(x_1) 0 \psi_t(x_{\varsigma(1)}) = \angle x_1 0 R_{t(\pi/2-\alpha)}(x_{\varsigma(1)}) \geq \frac{\pi}{2}$ for all $t \in [0,1]$, or else $\angle \psi_t(x_1) 0 \psi_t(x_{\varsigma(1)})$ is increasing with respect to t. But by considering instead the flow $(t, x) \mapsto (t(\alpha - \frac{\pi}{2})) \cdot \psi_t(x)$, we obtain a rotation of our original flow, where now $x_{\varsigma(1)}$ is stationary; since distances are invariant under rotation, we may argue in the same way that the desired property holds also for $i = \varsigma(1)$, and similarly for the remaining values of i.

$\Theta(\psi_t(x))$ is not necessarily constant with respect to t, so we instead use the modified flow $\bar{\psi}_t(x) = (-\Theta(\psi_t(x))) \cdot \psi_t(x)$. Then $\Theta(\bar{\psi}_t(x)) = 0$ for all $t \in [0,1]$, so in particular $\bar{\psi}_t$ preserves the section $s\left(\overline{\mathrm{Conf}}_{4,\frac{1}{3}}\right)$, where $T_\varsigma = \tilde{T_\varsigma} \cap s\left(\overline{\mathrm{Conf}}_{4,\frac{1}{3}}\right)$. Given that $\bar{\psi}_t(s_\varsigma) = s_\varsigma$ for all $t \in [0,1]$ and $\bar{\psi}_1(x) = s_\varsigma$ for all $x \in T_\varsigma$, it follows that $(\bar{\psi}_t|_{T_\varsigma})_{t\in[0,1]}$ is a strong deformation retraction from T_ς onto $\{s_\varsigma\}$. □

The following proposition is the key ingredient in Thm. 4.0.1, and is demonstrated visually in Fig. 4.5.

Proposition 4.3.5. *Let Y be the cell complex containing:*

- *a set, V_1, of 0-cells, indexed over the 6 vertices of an octahedron*
- *a set, V_2, of 0-cells, indexed over the 8 faces of an octahedron*

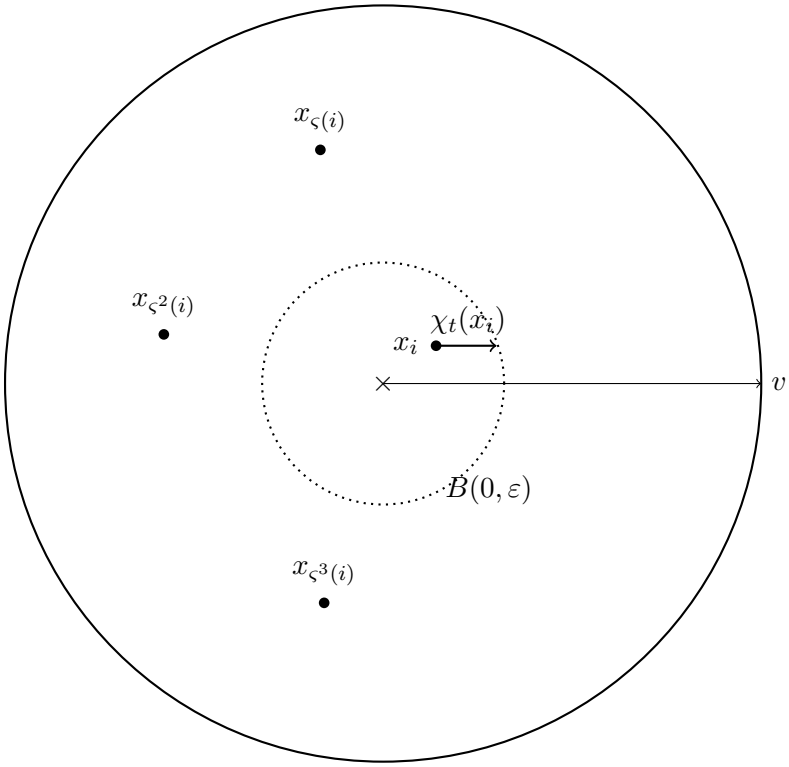

Figure 4.4: The flow χ_t on $\mathrm{Conf}_{4,\frac{1}{3}}$ from Lemma 4.3.2. v bisects the sector containing x_i, bounded by $x_{\varsigma(i)}$ and $x_{\varsigma^3(i)}$, where x_i is the unique point of x with $|x_i| \leq \varepsilon$. x_i flows in the v-direction.

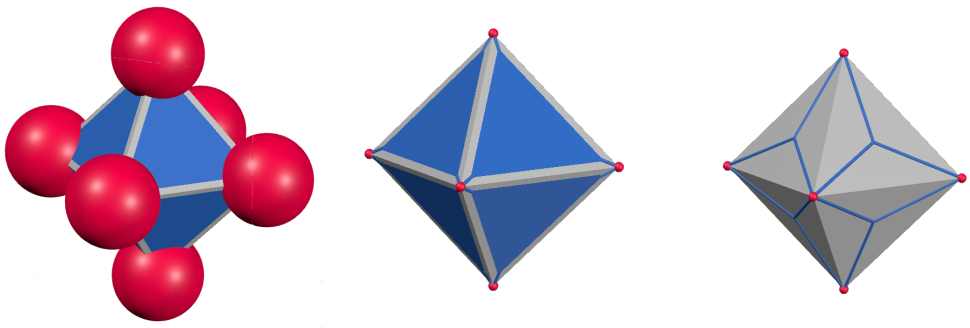

Figure 4.5: A graphical representation of Prop. 4.3.5. The left-hand picture, repeated from Fig. 4.2, shows the structure of $\mathrm{Conf}_{4,\frac{1}{3}}/S^1$. We contract the non-critical components (red) to points (shown in the middle picture), and then retract each critical component (blue) onto a Y-shaped skeleton (right).

- *a set, E, of 1-cells, in which $v_1 \in V_1$ and $v_2 \in V_2$ bound a 1-cell if and only if the vertex corresponding to v_1 is on the boundary of the face corresponding to v_2.*

Then $\overline{\mathrm{Conf}}_{4,\frac{1}{3}} \simeq Y$.

Since each face is bounded by three vertices, $|E| = 8 \times 3 = 24$. The theorem will require a theorem of Borsuk [12, Thm. 1], and we must first demonstrate some properties of $s\left(\overline{\mathrm{Conf}}_{n,r}\right)$.

Lemma 4.3.6. *$s\left(\overline{\mathrm{Conf}}_{n,r}\right)$ is a metric space.*

Proof. First, note that D^2 is a metric space under the Euclidean metric. Thus, $\left(D^2\right)^n$ is a metric space. Since $s\left(\overline{\mathrm{Conf}}_{n,r}\right)$ is a subspace of $\left(D^2\right)^n$, the result follows. □

Lemma 4.3.7. *$s\left(\overline{\mathrm{Conf}}_{n,r}\right)$ is an absolute neighbourhood retract.*

Proof. First, note that we may describe this space as

$$s\left(\overline{\mathrm{Conf}}_{n,r}\right) = \Big\{(x_1,\ldots,x_n) \in \left(\mathbb{R}^2\right)^n \mid \forall_i\ |x_i| \leq 1-r,\ \forall_{i\neq j}|x_i - x_j| \geq 2r,\\ \left((x_3-x_2)\cdot(1,0)\right)^2 = |x_3-x_2|^2, (x_3-x_2)\cdot(1,0) > 0\Big\}$$

Given that it is described by a finite set of polynomial equations and inequalities under the identification $\left(\mathbb{R}^2\right)^n = \mathbb{R}^{2n}$, $s\left(\overline{\mathrm{Conf}}_{n,r}\right)$ is a semi-algebraic (and thus semi-analytic) set as defined in [25, §1]. Thus there is a homeomorphism between $s\left(\overline{\mathrm{Conf}}_{n,r}\right)$ and a locally finite simplicial complex L [25, Thm. 1.c]. Therefore, in particular, $s\left(\overline{\mathrm{Conf}}_{n,r}\right)$ is ε-dominated by L for any $\varepsilon > 0$ as defined in [20, §6], and L is an absolute neighbourhood retract [20, Cor. 3.5]. Thus $s\left(\overline{\mathrm{Conf}}_{n,r}\right)$ is an absolute neighbourhood retract [20, Thm. 7.2.b]. □

Proof of Prop. 4.3.5. First, we have that S_ς is closed in $s\left(\overline{\mathrm{Conf}}_{n,r}\right)$ by Prop. 4.2.1. Furthermore, $s\left(\overline{\mathrm{Conf}}_{n,r}\right)$ is a metric space by Lemma 4.3.6 and an absolute neighbourhood retract by Lemma 4.3.7. Therefore $\left(s\left(\overline{\mathrm{Conf}}_{n,r}\right), S_\varsigma\right)$ has the homotopy extension property with respect to $s\left(\overline{\mathrm{Conf}}_{n,r}\right)$ by Borsuk's condition [12, Thm. 1].

Now let $\sim$ be an equivalence on $s\left(\overline{\mathrm{Conf}}_{n,r}\right)$, given by $x \sim y$ if and only if there is some cyclic ordering ς such that $x, y \in S_\varsigma$. Since S_ς is contractible by Prop. 4.3.1 and $\left(s\left(\overline{\mathrm{Conf}}_{n,r}\right), S_\varsigma\right)$ has HEP, we may contract each S_ς to a point inside $s\left(\overline{\mathrm{Conf}}_{n,r}\right)$ continuously by [22, Prop 0.17]. Therefore $s\left(\overline{\mathrm{Conf}}_{4,\frac{1}{3}}\right) \simeq s\left(\overline{\mathrm{Conf}}_{4,\frac{1}{3}}\right) / \sim$. The points

S_ς compose the set V_1. Since the contractions of S_ς to a point also contract alternate edges of each critical component, $C_{i,\rho'}$, these become triangles, connected to the points of V_1 at their vertices. Thus $s\left(\overline{\mathrm{Conf}}_{4,\frac{1}{3}}\right)/\sim$ consists of eight triangular faces, where each face is joined to three others at each of its vertices –it is an octahedron with the edges (but not the vertices) cut out.

Now, choose a point in the interior of each $C_{i,\rho'}$, and connect each of these points to the three vertices of its triangle by a line segment. These points compose V_2, and the line segments compose E. Now, we have chosen a Y-shape inside each $C_{i,\rho'}$, consisting of a 0-cell from V_2 at the centre, three 1-cells from E, and bounded by three 0-cells from V_1. We may retract every $C_{i,\rho'}$ onto this simultaneously. Therefore, by Prop. 4.1.1,

$$\overline{\mathrm{Conf}}_{4,\frac{1}{3}} \cong s\left(\overline{\mathrm{Conf}}_{4,\frac{1}{3}}\right) \simeq s\left(\overline{\mathrm{Conf}}_{4,\frac{1}{3}}\right)/\sim \simeq Y$$

□

Proof of Thm: 4.0.1. $\mathrm{Conf}_{4,r} \simeq \mathrm{Conf}_{4,\frac{1}{3}}$ by Fact 1.2.5 and Prop. 2.0.10. $\mathrm{Conf}_{4,\frac{1}{3}} \cong \overline{\mathrm{Conf}}_{4,\frac{1}{3}} \times S^1$ by Prop. 4.1.1. Finally, $\overline{\mathrm{Conf}}_{4,\frac{1}{3}} \times S^1 \simeq Y \times S^1$ by Prop. 4.3.5. □

4.4 The homotopy groups of $\mathrm{Conf}_{4,\frac{1}{3}}$: a comparison to Conf_4

Extending Thm. 3.1.1, we want to understand how precisely $\mathrm{Conf}_{4,\frac{1}{3}}$ has changed from Conf_4, for which we compare their homotopy groups. Using Thm. 4.0.1, we are able to calculate the homotopy groups of $\mathrm{Conf}_{4,\frac{1}{3}}$. We start with the following observation.

Corollary 4.4.1 (Corollary to Thm. 4.0.1)**.**

$$\pi_n\left(\mathrm{Conf}_{4,\frac{1}{3}}\right) = \begin{cases} \pi_1(Y)\times\mathbb{Z} & : \quad n=1 \\ 0 & : \quad n>1 \end{cases}$$

Proof. $\pi_n(\mathrm{Conf}_{4,\frac{1}{3}}) = \pi_n(Y\times S^1) = \pi_n(Y)\times\pi_n(S^1)$ by [22, Prop. 4.2]. For $n=1$, $\pi_1(S^1)=\mathbb{Z}$. For $n>1$, note that both Y, S^1 are a path-connected 1-dimensional cell complex. For any path-connected 1-dimensional cell complex Z, we have that the universal cover, $\tilde{Z}$, of Z is a tree and thus contractible by [22, Ex. 1B.1]; thus $\pi_n(\tilde{Z}) = \pi_n(Z) = 0$ by [22, Prop. 4.1]. □

That is, $\mathrm{Conf}_{4,\frac{1}{3}}$ is aspherical, sharing this property with Conf_4. In this section, we will first try to understand $\pi_1(Y)$ treating Y as an arbitrary graph. Following this, we will

explore the how the elements of $\pi_1(Y) \times \mathbb{Z} = \pi_1(\mathrm{Conf}_{4,\frac{1}{3}})$ behave as braids in $\pi_1(\mathrm{Conf}_4)$ when we push them forward under the natural inclusion $\mathrm{Conf}_{4,\frac{1}{3}} \to \mathrm{Conf}_4$.

In order to calculate $\pi_1(Y)$, first choose a vertex of the octahedron (this is also a vertex of Y) as a basepoint. We label the faces and edges of the octahedron as follows:

1. Take the four faces incident to the basepoint vertex, and label them F_1, F_2, F_3, F_4 in clockwise order, taking the index set to be $\mathbb{Z}/4\mathbb{Z}$.
2. Label the remaining faces F_i', $i \in \mathbb{Z}/4\mathbb{Z}$, so that F_i' is the face sharing an edge with F_i. Label this shared edge B_i.
3. For each $i \in \mathbb{Z}/4\mathbb{Z}$, label the edge between between F_i and F_{i-1} as A_i.
4. For each $i \in \mathbb{Z}/4\mathbb{Z}$, label the edge between between F_i' and F_{i-1}' as C_i.

Then the edges of F_i are A_i, B_i, A_{i+1} clockwise from the basepoint, and the edges of F_i' (clockwise) are B_i, C_{i+1}, C_i.

Then we can define elements $a_i, b_i, c_i \in \pi_1(Y)$, $i \in \mathbb{Z}/4\mathbb{Z}$ (see Fig. 4.6).

- a_i is the shortest loop winding once anticlockwise around A_i,
- b_i goes to the centre of F_i, then loops once anticlockwise around B_i, then back to the basepoint, and
- c_i goes to the other vertex of A_i via F_i, then loops once anticlockwise about C_i, then returns to the basepoint via F_i.

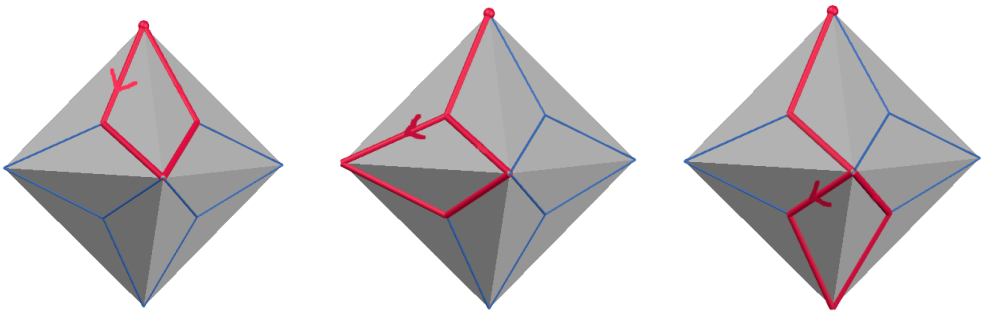

Figure 4.6: The loops $a_i, b_i, c_i \in \pi_1(Y)$ (shown in bold red on the left, centre and right octahedra). Here, on each octahedron, the basepoint is the top vertex, and the upper two visible faces are F_i (left) and F_{i-1} (right).

Proposition 4.4.2.

$$\begin{aligned}\pi_1(Y) &= \langle a_1, a_2, a_3, a_4, b_1, b_2, b_3, b_4, c_1, c_2, c_3 \rangle \\ &= \langle a_i, b_i, c_i \mid i \in \mathbb{Z}/4\mathbb{Z},\ a_1c_1b_1a_2c_2b_2a_3c_3b_3a_4c_4b_4 = e \rangle\end{aligned}$$

While this group presentation is pleasingly symmetric and corresponds to some simple braids, it will often be easier to use the alternative generators given below. Indeed, the alternative group presentation in the next lemma will be required to prove Prop. 4.4.2.

Consider the spanning tree T of Y (see Fig. 4.7) containing:

- The two edges on F_i which share a vertex with A_i, for each $i \in \mathbb{Z}/4\mathbb{Z}$,
- The edge on F_i' which shares a vertex with A_i, for each $i \in \mathbb{Z}/4\mathbb{Z}$, and
- The edge on F_4' which shares a vertex with every C_i.

Then the edges of $Y \backslash T$ are:

- One edge on F_i for each $i \in \mathbb{Z}/4\mathbb{Z}$, which we label a_{i+1}'',
- One edge on F_i' which shares a vertex with B_i for each $i \in \mathbb{Z}/4\mathbb{Z}$, which we label b_i'', and
- One edge on F_i' which shares a vertex with every C_j ($j \in \mathbb{Z}/4\mathbb{Z}$), for each $i \in \{1, 2, 3\}$, which we label c_i''.

We may then define some loops in Y which start at the basepoint and pass through exactly one of these edges (see Fig. 4.8), by following T to one end of the chosen edge, traversing the edge, then following T back to the basepoint. We give these loops the same name (a_i', b_i', c_i') as the unique edge of $Y \backslash T$ they contain, except we remove one prime symbol ($'$). We choose the orientation of the loops a_i' and b_i' to be anticlockwise, and c_i' to go out through faces F_i, F_i' and return through faces F_4', F_4.

Lemma 4.4.3. $\pi_1(Y) = \langle a_1', a_2', a_3', a_4', b_1', b_2', b_3', b_4', c_1', c_2', c_3' \rangle$

This is directly taken from [22, Prop. 1A.2]. We lay out a brief proof below as it helps explain how we can write the homotopy class of an arbitrary loop in terms of these generators in practice.

Proof. (Y, T) is a CW-pair, so it has the homotopy extension property by [22, Prop.

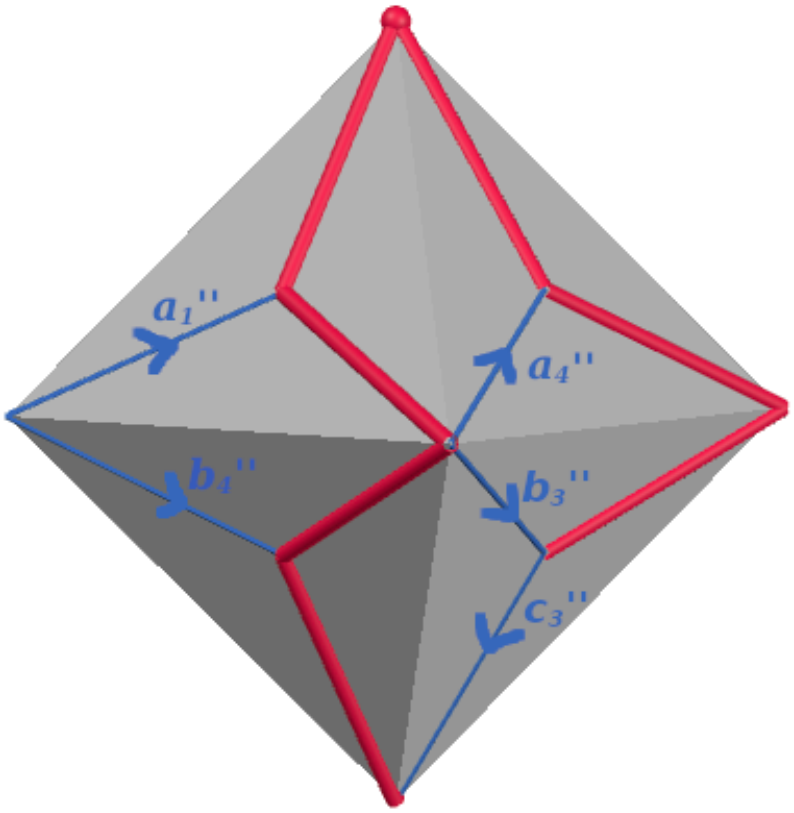

Figure 4.7: A spanning tree on Y (red bold). Here, the upper visible faces of the octahedron are F_4 (left), F_3 (right) and the faces below them are F_4', F_3'. The choice of edges of Y to be included in T on $F_1 \cup F_1'$ and $F_2 \cup F_2'$ is exactly the same as the choice on $F_3 \cup F_3'$. The orientation and label given to each edge of $Y \backslash T$ is written.

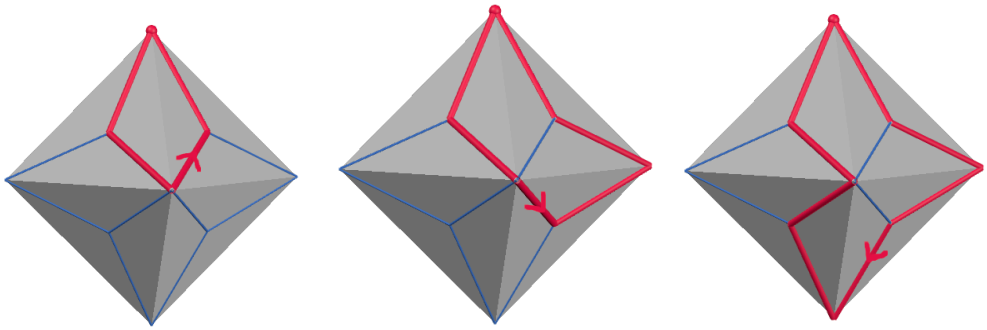

Figure 4.8: The loops $a_4', b_3', c_3' \in \pi_1(Y)$ (shown in bold red on the left, centre and right octahedra). Here, on each octahedron, the basepoint is the top vertex, and the upper two visible faces are F_4 (left) and F_3 (right). These naturally generate $\pi_1(Y)$, and we use them to prove the existence of the more symmetric group presentation depicted in Fig. 4.6 in Prop. 4.4.2.

0.16], so the projection $Y \to Y/T$ is a homotopy equivalence by [22, Prop. 0.17], which induces an isomorphism $\pi_1(Y) \to \pi_1(Y/T)$. This projection collapses each loop $l \in \{a'_1, a'_2, a'_3, a'_4, b'_1, b'_2, b'_3, b'_4, c'_1, c'_2, c'_3\}$ to its unique edge l' of $Y \backslash T$ and collapses all vertices to one vertex, so that Y/T is a wedge of circles, and thus $\pi_1(Y/T)$ is generated freely by $\{a''_1, a''_2, a''_3, a''_4, b''_1, b''_2, b''_3, b''_4, c''_1, c''_2, c''_3\}$. Thus by isomorphism, $\pi_1(Y)$ is generated freely by $\{a'_1, a'_2, a'_3, a'_4, b'_1, b'_2, b'_3, b'_4, c'_1, c'_2, c'_3\}$. □

It follows that any loop in $\pi_1(Y)$ can be expressed in terms of the generators a'_i, b'_i, c'_i by checking which edges of $Y \backslash T$ it passes through (and in which direction).

Proof of Prop. 4.4.2. We can write the non-primed generators in terms of the primed generators from Lemma 4.4.3 as follows:

- $a_i = a'_i$ for all $i \in \mathbb{Z}/4\mathbb{Z}$,
- $b_i = b'_i (a'_{i+1})^{-1}$ for all $i \in \mathbb{Z}/4\mathbb{Z}$,
- $c_1 = (b'_4)^{-1} c'_1$,
- $c_2 = (b'_1)^{-1} (c'_1)^{-1} c'_2$,
- $c_3 = (b'_2)^{-1} (c'_2)^{-1} c'_3$.

Working inductively through this list, each successive equation contains a primed generator not found in the previous equations, so $\pi_1(Y)$ contains no relations between these 11 elements. We may show that $\pi_1(Y)$ is generated (and thus generated freely) by these 11 elements by rearranging the equations as follows:

- $a'_i = a_i$ for all $i \in \mathbb{Z}/4\mathbb{Z}$,
- $b'_i = b_i a_{i+1}$ for all $i \in \mathbb{Z}/4\mathbb{Z}$,
- $c'_1 = b'_4 c_1 = b_4 a_1 c_1$,
- $c'_2 = c'_1 b'_1 c_2 = b_4 a_1 c_1 b_1 a_2 c_2$,
- $c'_3 = c'_2 b'_2 c_3 = b_4 a_1 c_1 b_1 a_2 c_2 b_2 a_3 c_3$.

That is to say,

$$\langle a_1, a_2, a_3, a_4, b_1, b_2, b_3, b_4, c_1, c_2, c_3 \rangle = \langle a'_1, a'_2, a'_3, a'_4, b'_1, b'_2, b'_3, b'_4, c'_1, c'_2, c'_3 \rangle = \pi_1(Y) \quad .$$

We complete the proof by observing that

$$c_4 = (b_3')^{-1}(c_3')^{-1} = (c_3'b_3')^{-1} = (b_4a_1c_1b_1a_2c_2b_2a_3c_3b_3a_4)^{-1} \quad . \qquad \square$$

For the remainder of this section, we will choose our basepoint to be s_ς (as defined for Prop. 4.3.1), where $\varsigma = [1\ 2\ 3\ 4]$, and label our faces such that F_i corresponds to $C_{i,[\hat{\varsigma}_i]}$ (the face of the octahedron where D_i is at the centre and the remaining discs inherit their cyclic order from ς). The example below illustrates how we will express loops in $s\left(\overline{\mathrm{Conf}}_{4,r}\right) \subset \mathrm{Conf}_{4,r}$, where $\frac{1}{4} < r \leq \frac{1}{3}$, in terms of the group presentations in Lemma 4.4.3 and Prop. 4.4.2: we find a homotopic loop inside $\mathrm{Conf}_{4,\frac{1}{3}}$, retract it onto Y, and check which edges of $Y \backslash T$ the loop passes through.

Example 4.4.4. Consider the loop from Thm. 3.1.1, shown in Fig. 3.2. By construction, this lies in $s\left(\overline{\mathrm{Conf}}_{4,r}\right)$ for any $r \leq \frac{1}{2+\sqrt{2}}$. Fig. 4.9 depicts a loop in $s\left(\overline{\mathrm{Conf}}_{4,\frac{1}{3}}\right)$ whose image under the inclusion $s\left(\overline{\mathrm{Conf}}_{4,\frac{1}{3}}\right) \hookrightarrow s\left(\overline{\mathrm{Conf}}_{4,r}\right)$ is homotopic to the loop from Fig. 3.2. This new loop passes through F_2 into the vertex corresponding to $S_{[1\ 3\ 4\ 2]}$; then through F_1' into $S_{[1\ 4\ 3\ 2]}$; then through F_4' into $S_{[1\ 2\ 4\ 3]}$; then through F_3 back to s_ς. The edges of $Y \backslash T$ in this loop are b_1'' and c_1'' in F_1', and a_4'' in F_3. Thus the loop is $a_4'c_1'b_1' = a_4b_4a_1c_1b_1a_2$.

More generally, in order to understand a loop $\gamma \in \pi_1(\mathrm{Conf}_{4,r}) = \pi_1(Y) \times \mathbb{Z}$, we calculate $s_*(q_*(\gamma)) \in \pi_1\left(s\left(\overline{\mathrm{Conf}}_{4,r}\right)\right) = \pi_1(Y)$ and find the winding number, $n = \Theta_*(\gamma) \in \pi_1(S^1) = \mathbb{Z}$, of x_3 about x_2. Then $\gamma = (s_*(q_*(\gamma)), n)$.

We complete this section by understanding the elements of $\pi_1(\mathrm{Conf}_{4,\frac{1}{3}}) = \pi_1(Y) \times \mathbb{Z}$ as thick braids, by looking at the image of these classes under the map $\pi_1(\mathrm{Conf}_{4,\frac{1}{3}}) \to \pi_1(\mathrm{Conf}_4)$ induced by the inclusion map. We can generate $\pi_1(\mathrm{Conf}_{4,\frac{1}{3}})$ with thirteen elements: an element (g, n_g) for each $g \in \{a_1, a_2, a_3, a_4, b_1, b_2, b_3, b_4, c_1, c_2, c_3, c_4\}$, for any choice of $n_g \in \mathbb{Z}$, and the element $(e, 1)$ where e is the identity of $\pi_1(Y)$.

For the purposes of calculating the braid corresponding to a given generator, we first remind ourselves that $Y \simeq \overline{\mathrm{Conf}}_{4,\frac{1}{3}}$. We denote $S_{\varsigma'}' = s^{-1}(S_{\varsigma'}) \subset \overline{\mathrm{Conf}}_{4,\frac{1}{3}}$ and $C_{i,\rho}' = s^{-1}(C_{i,\rho})$. Each $g \in \{a_1, a_2, a_3, a_4, b_1, b_2, b_3, b_4, c_1, c_2, c_3, c_4\}$ is a directed subgraph of Y (where we allow some edges to have both directions), and we will choose a representative loop $\alpha_g \colon (S^1, *) \to (\mathrm{Conf}_{4,\frac{1}{3}}, s_\varsigma)$ of g as follows.

First, split g into blocks consisting of two edges, where the first edge of the block goes

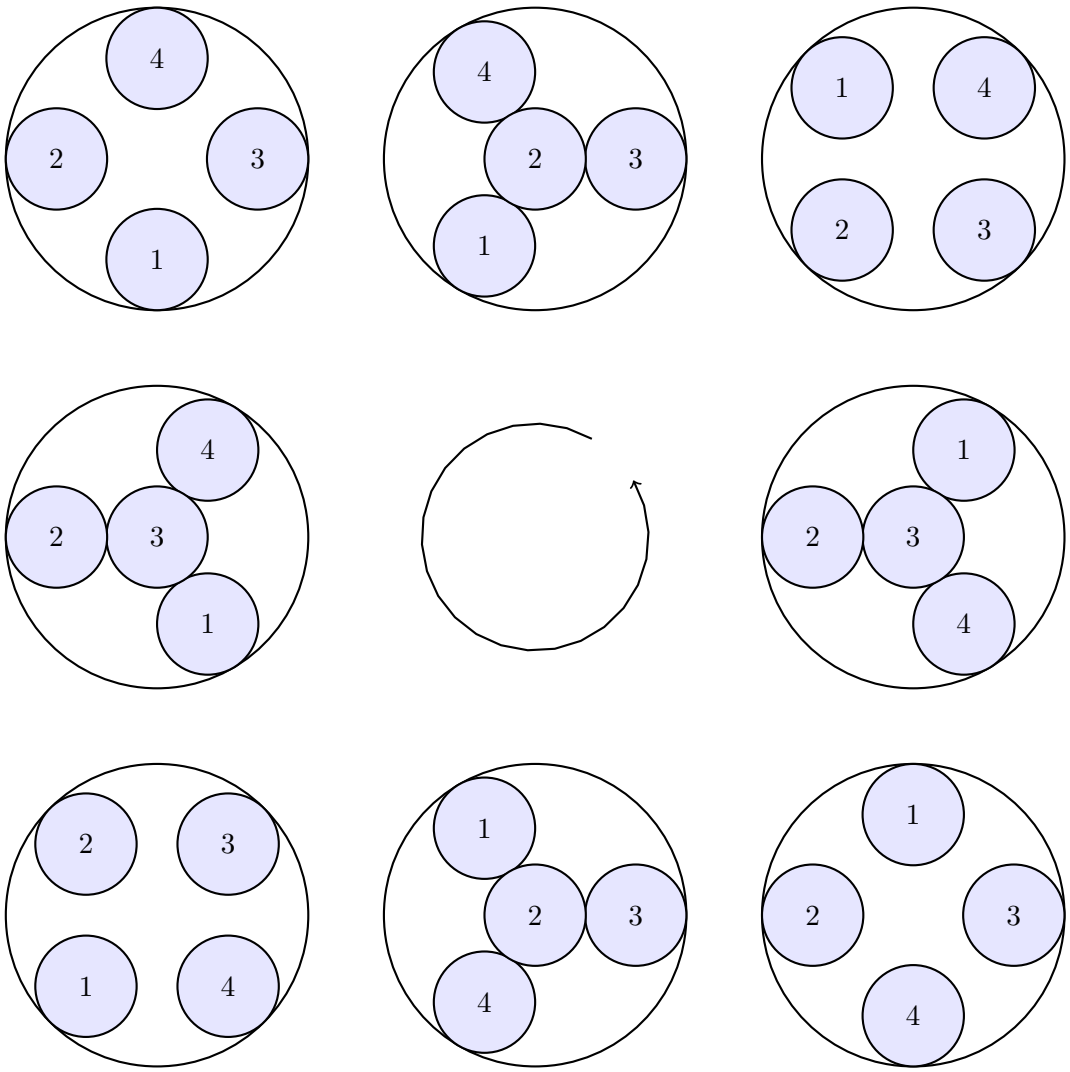

Figure 4.9: A loop in $s\left(\overline{\mathrm{Conf}}_{4,\frac{1}{3}}\right)$ which is homotopic to the loop given in Thm. 3.1.1 and Fig. 3.2. The four corner configurations correspond to the configurations in the same position on Fig. 3.2, and the configurations on the edges are the half-way points of the four braid actions.

from the vertex corresponding to some $S'_{\varsigma'}$ to the vertex corresponding to some $C'_{i,\rho}$, and the second edge goes from $C'_{i,\rho}$ to some $S'_{\varsigma''}$. Then it follows by Prop. 4.2.2 that $\rho = \left[\hat{\varsigma'}_i\right] = \left[\hat{\varsigma''}_i\right]$; that is, if $\varsigma' = [i\ j\ k\ l]$, then there are two cases: either $\varsigma'' = [i\ k\ l\ j]$ or $\varsigma'' = [i\ l\ j\ k]$. Then (see Fig. 4.10) we construct a path in $\mathrm{Conf}_{4,\frac{1}{3}}$ corresponding to this block:

1. Along the first edge of the block, D_i moves radially to the centre.
2. Inside the vertex $C'_{i,\rho}$, one of the other three discs rolls along the boundary, moving through a total angle of $\frac{\pi}{2}$ about the origin.
   - In the first case, this is D_j, which rolls clockwise into the space vacated by D_i.
   - In the second case, this is D_l, which rolls anticlockwise.
3. Along the second edge, D_i moves radially into the space vacated by D_j or D_l.

On this path, the positions of the two non-participating discs (D_k and either D_l or D_j) are fixed. This path is exactly the braid which swaps D_i and D_j clockwise in the first case, or D_i and D_l anticlockwise in the second case. In the first case, this braid is σ_1^{-1}, σ_2^{-1}, σ_3^{-1} or $(\sigma_1\sigma_3^{-1}\sigma_2\sigma_3\sigma_1^{-1})^{-1}$, depending on the starting position of D_i; and similarly in the second case, this braid is $\sigma_1\sigma_3^{-1}\sigma_2\sigma_3\sigma_1^{-1}$, σ_1, σ_2 or σ_3. Here, $\sigma_1\sigma_3^{-1}\sigma_2\sigma_3\sigma_1^{-1}$ is the braid which swaps the discs in positions 1 and 4 anticlockwise in the natural way. Geometrically, we would expect it to commute with σ_2, and indeed

$$\begin{aligned}
\sigma_2\sigma_1\sigma_3^{-1}\sigma_2\sigma_3\sigma_1^{-1} &= \sigma_2\sigma_3^{-1}\sigma_1\sigma_2\sigma_1^{-1}\sigma_3 \\
&= \sigma_2\sigma_3^{-1}\sigma_2^{-1}\sigma_1\sigma_2\sigma_3 \\
&= \sigma_3^{-1}\sigma_2^{-1}\sigma_3\sigma_1\sigma_2\sigma_3 \\
&= \sigma_3^{-1}\sigma_2^{-1}\sigma_1\sigma_3\sigma_2\sigma_3 \\
&= \sigma_3^{-1}\sigma_2^{-1}\sigma_1\sigma_2\sigma_3\sigma_2 \\
&= \sigma_3^{-1}\sigma_1\sigma_2\sigma_1^{-1}\sigma_3\sigma_2 \\
&= \sigma_1\sigma_3^{-1}\sigma_2\sigma_3\sigma_1^{-1}\sigma_2 \quad .
\end{aligned}$$

We construct the path for each block of g in sequence, taking the final configuration of one block to be the start of the next. After the final block, we will be at $(-\theta_g)\cdot s_\varsigma$ for some $\theta_g \in S^1$. We close the loop α_g by rotating D^2 through the angle θ_g (that is, by

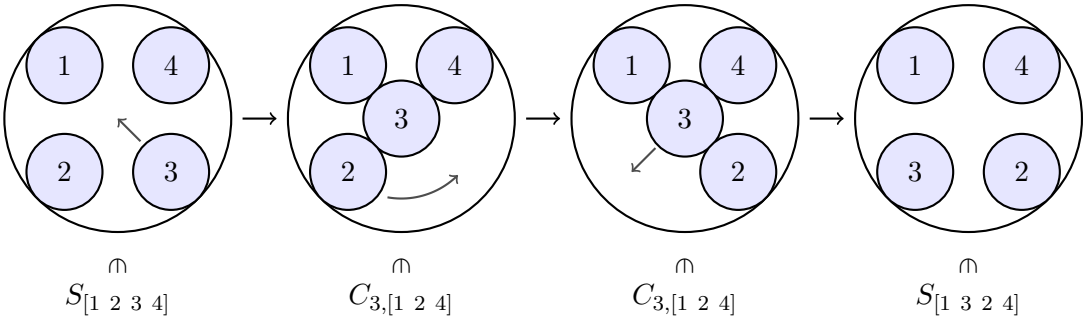

Figure 4.10: A path in $\mathrm{Conf}_{4,\frac{1}{3}}$, and the corresponding vertices in Y under the map $\mathrm{Conf}_{4,\frac{1}{3}} \xrightarrow{q} \overline{\mathrm{Conf}}_{4,\frac{1}{3}} \xrightarrow{\simeq} Y$. D_1 and D_4, which do not participate in this braid, have fixed position. Each generator of $\pi_1(Y)$ can be split into paths of the form $S_\varsigma \rightsquigarrow C_{i,\rho} \rightsquigarrow S_{\varsigma'}$, and we lift each of these paths to $\mathrm{Conf}_{4,\frac{1}{3}}$ in the manner depicted here.

acting on our configuration by θ_g). We will find that $\theta_{a_i} = \theta_{c_i} = 0$ and $\theta_{b_i} = \frac{\pi}{2}$ for all $i \in \mathbb{Z}/4\mathbb{Z}$. The action by $\frac{\pi}{2}$ is a quarter-rotation anticlockwise, corresponding to the braid $\sigma_1\sigma_2\sigma_3$ (see Fig. 4.11). α_{b_1} is given in Fig. 4.12 as an example.

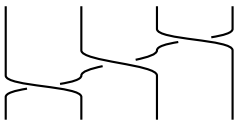

Figure 4.11: The braid corresponding to an anticlockwise rotation by $\frac{\pi}{2}$ of D_2. Each disc moves to the position of the next, yielding the braid $\sigma_1\sigma_2\sigma_3$.

In order to achieve $[\alpha_g] = (g, n_g)$, we require that n_g be the winding number of x_3 about x_2 in the loop α_g. By definition, this is $\frac{1}{2\pi}$ times the total change in $\Theta(\mathcal{D})$ along α_g. According to our construction algorithm for α_g, $\Theta(\mathcal{D})$ can change along the edges, at the $C'_{i,\rho}$ vertices, or at the final rotation by θ_g. Let m_g be the number of two-edge blocks in g, and let $\underline{\Theta}(g) \coloneqq (\theta_{11}, \theta_{12}, \theta_{13}; \ldots; \theta_{m_g 1}, \theta_{m_g 2}, \theta_{m_g 3}; \theta_g) \in (\mathbb{R}^3)^{m_g} \times \mathbb{R}$ be the element such that $(\theta_{i1}, \theta_{i2}, \theta_{i3})$ gives the changes in $\Theta(\mathcal{D})$ along the first edge, the $C'_{i,\rho}$ vertex, and the second edge of the i-th block. The sum of these values will be $2\pi n_g$.

There are two generators corresponding to s_{14}. x_2 and x_3 are fixed throughout α_{a_1}, so

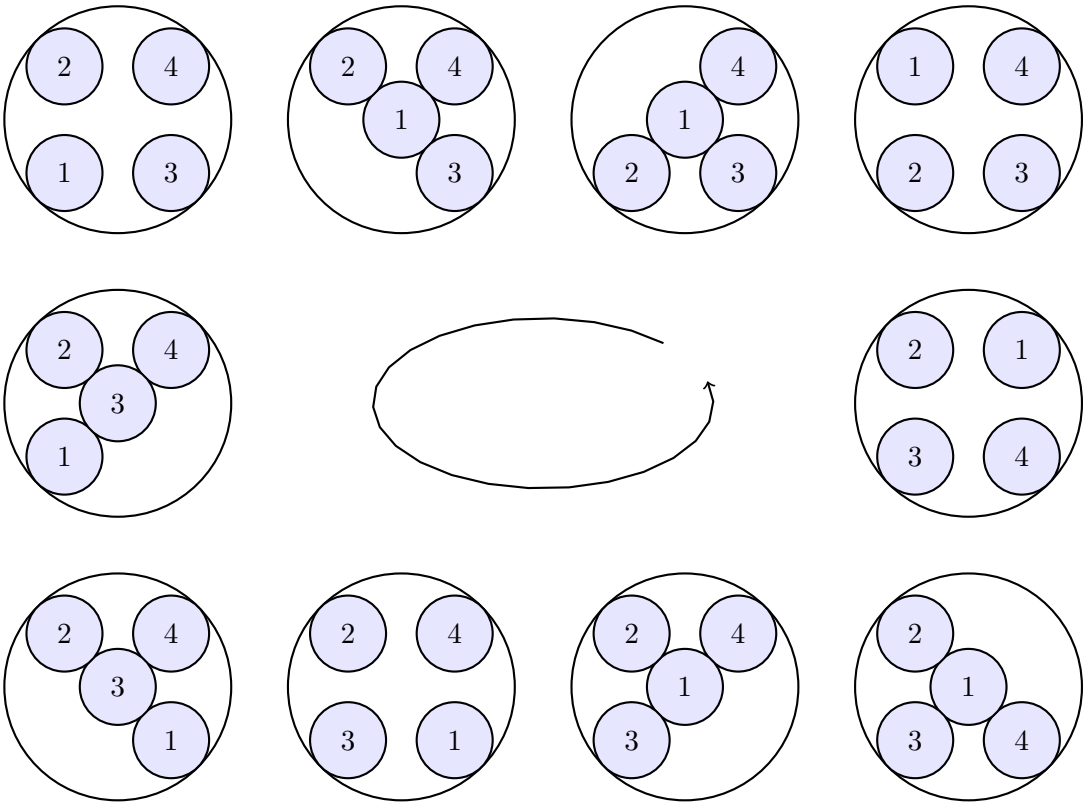

Figure 4.12: The loop α_{b_1} in $\mathrm{Conf}_{4,\frac{1}{3}}$starting at the top right. α_{b_1} is constructed to have the property $q_*([\alpha_{b_1}]) = b_1$, where $q_*\colon \pi_1(\mathrm{Conf}_{4,\frac{1}{3}}) \to \pi_1(\overline{\mathrm{Conf}}_{4,\frac{1}{3}})$. As we move to each successive diagram in the figure, the angle anticlockwise from the horizontal to $x_3 - x_2$ changes by $0, -\frac{\pi}{4}, 0, 0, 0, -\frac{\pi}{4}, 0, 0, 0, \frac{\pi}{2}$. Since these sum to $0 = 0 \times 2\pi$, it follows that $\Theta_*([\alpha_{b_1}]) = 0 \in \mathbb{Z} = \pi_1(S_1)$.

$\underline{\Theta}(a_1) = (0,0,0;0,0,0;0)$. Then we have

$$\begin{aligned}(a_1, 0) &\mapsto (\sigma_3^{-1}\sigma_1\sigma_2\sigma_3\sigma_1^{-1})^2 \\ &= \sigma_3^{-1}\sigma_1\sigma_2^2\sigma_3\sigma_1^{-1} \\ &= s_{14} \quad .\end{aligned}$$

In α_{c_3}, x_1 and x_4 are fixed along the first two edges and the last two edges, and x_2 and x_3 are fixed along the middle four edges. Then $\underline{\Theta}(c_3) = (\frac{\pi}{4}, \frac{\pi}{2}, \frac{\pi}{4}; 0,0,0; 0,0,0; -\frac{\pi}{4}, -\frac{\pi}{2}, -\frac{\pi}{4}; 0)$, so

$$\begin{aligned}(c_3, 0) &\mapsto \sigma_2^{-1}(\sigma_3^{-1}\sigma_1\sigma_2\sigma_3\sigma_1^{-1})^2\sigma_2 \\ &= s_{14} \quad .\end{aligned}$$

Thus $(a_1, 0)$ and $(c_3, 0)$ are undifferentiated as braids. However, they are differentiated as thick braids. In $(a_1, 0)$, the only weave is given by the rotation of D_1 and D_4 around each other; whereas in $(c_3, 0)$, there is a half-rotation of D_2 and D_3 around each other before the rotation of D_1 and D_4, and another half-rotation of D_2 and D_3 in the opposite direction afterwards. As braids, these half-rotations of D_2 and D_3 commute with the rotation of D_1 and D_4 and then cancel out; but as thick braids, they do not commute with the rotation of D_1 and D_4, due to geometric reasons arising from the relative size of the discs to the unit disc.

We fill out the remaining generators in Tables 4.1 and 4.2. We see that the pattern continues in the same way with a_i and c_{i+2} corresponding to the same braid for all $i \in \mathbb{Z}/4\mathbb{Z}$. Furthermore, we see that b_i has the same underlying braid as b_{i+2} (specifically, $s_{i,i+2}$) for $i \in \{1, 2\}$. Here, the distinction between them as thick braids is based on which of the two discs D_i or D_{i+2} moves to the origin first.

Finally, $(e, 1)$ describes one complete rotation of D^2. Since this is four consecutive quarter-rotations, $(e, 1) \mapsto (\sigma_1\sigma_2\sigma_3)^4 = s_{12}s_{23}s_{13}s_{34}s_{24}s_{14}$. This element generates the centre of Br_4 (see [18, Thm. 7] and Appendix A), and is thus an element of the centre of PBr_4.

In summary, $\pi_1(\mathrm{Conf}_{4,\frac{1}{3}})$ contains two generators for every generator of PBr_4, and there is only one relation between them as opposed to the 11 relations of PBr_4. In addition, $\pi_1(\mathrm{Conf}_{4,\frac{1}{3}})$ has a 13th generator $(e, 1)$, which cannot be written as a product of the

Generator g of $\pi_1(Y)$	$\underline{\Theta}(g)$	n_g
a_1	$(0,0,0;0,0,0;0)$	0
c_3	$(\frac{\pi}{4},\frac{\pi}{2},\frac{\pi}{4};0,0,0;0,0,0;-\frac{\pi}{4},-\frac{\pi}{2},-\frac{\pi}{4};0)$	0
a_2	$(-\frac{\pi}{4},0,0;0,\frac{\pi}{4},0;0)$	0
c_4	$(0,\frac{\pi}{4},0;0,0,-\frac{\pi}{4};0,\frac{\pi}{4},0;0,-\frac{\pi}{4},0;0)$	0
a_3	$(\frac{\pi}{4},\frac{\pi}{2},\frac{\pi}{4};\frac{\pi}{4},\frac{\pi}{2},\frac{\pi}{4};0)$	1
c_1	$(0,0,0;\frac{\pi}{4},\frac{\pi}{2},\frac{\pi}{4};\frac{\pi}{4},\frac{\pi}{2},\frac{\pi}{4};0,0,0;0)$	1
a_4	$(0,\frac{\pi}{4},0;0,0,-\frac{\pi}{4};0)$	0
c_2	$(-\frac{\pi}{4},0,0;0,\frac{\pi}{4},0;-\frac{\pi}{4},0,0;0,0,\frac{\pi}{4};0)$	0
b_1	$(0,-\frac{\pi}{4},0;0,0,-\frac{\pi}{4};0,0,0;\frac{\pi}{2})$	0
b_3	$(\frac{\pi}{4},0,0;0,\frac{\pi}{4},0;-\frac{\pi}{4},-\frac{\pi}{2},-\frac{\pi}{4};\frac{\pi}{2})$	0
b_2	$(-\frac{\pi}{4},-\frac{\pi}{2},-\frac{\pi}{4};0,\frac{\pi}{4},0;0,0,\frac{\pi}{4};\frac{\pi}{2})$	0
b_4	$(0,0,0;-\frac{\pi}{4},0,0;0,-\frac{\pi}{4},0;\frac{\pi}{2})$	0

Table 4.1: A summary of the change in $\Theta(\mathcal{D})$ along the loops $\alpha_g \subset \mathrm{Conf}_{4,\frac{1}{3}}$ for the generators g of Y, given by $\underline{\Theta}(g)$, and their winding numbers n_g, which are calculated by adding the elements of $\underline{\Theta}(g)$ and dividing by 2π. α_g is constructed so that $q_*([\alpha_g]) = g \in \pi_1\left(\overline{\mathrm{Conf}}_{4,\frac{1}{3}}\right)$.

Generator of $\pi_1(\mathrm{Conf}_{4,\frac{1}{3}})$	Image in Br_4, PBr_4	
$(a_1, 0)$	$(\sigma_3^{-1}\sigma_1\sigma_2\sigma_3\sigma_1^{-1})^2$	$= s_{14}$
$(c_3, 0)$	$\sigma_2^{-1}(\sigma_3^{-1}\sigma_1\sigma_2\sigma_3\sigma_1^{-1})^2\sigma_2$	$= s_{14}$
$(a_2, 0)$	σ_1^2	$= s_{12}$
$(c_4, 0)$	$\sigma_3^{-1}\sigma_1^2\sigma_3$	$= s_{12}$
$(a_3, 1)$	σ_2^2	$= s_{23}$
$(c_1, 1)$	$(\sigma_1\sigma_3^{-1}\sigma_2\sigma_3\sigma_1^{-1})^{-1}\sigma_2^2\sigma_1\sigma_3^{-1}\sigma_2\sigma_3\sigma_1^{-1}$	$= s_{23}$
$(a_4, 0)$	σ_3^2	$= s_{34}$
$(c_2, 0)$	$\sigma_1^{-1}\sigma_3^2\sigma_1$	$= s_{34}$
$(b_1, 0)$	$\sigma_1\sigma_2\sigma_3\sigma_3^{-1}\sigma_2\sigma_1^{-1}$	$= s_{13}$
$(b_3, 0)$	$\sigma_1\sigma_2\sigma_3\sigma_1^{-1}(\sigma_3^{-1}\sigma_1\sigma_2\sigma_3\sigma_1^{-1})\sigma_3^{-1}$	$= s_{13}$
$(b_2, 0)$	$\sigma_1\sigma_2\sigma_3(\sigma_3^{-1}\sigma_1\sigma_2\sigma_3\sigma_1^{-1})^{-1}\sigma_3\sigma_2^{-1}$	$= s_{24}$
$(b_4, 0)$	$\sigma_2\sigma_3\sigma_2^{-1}\sigma_1(\sigma_3^{-1}\sigma_1\sigma_2\sigma_3\sigma_1^{-1})^{-1}$	$= s_{24}$

Table 4.2: A list of generators of $\mathrm{Conf}_{4,\frac{1}{3}}$ and their associated braids. Full calculations for the braids corresponding to $(b_i, 0)$ are found in Appendix A.

other generators, but its image in PBr_4 can. Given that $\mathrm{Conf}_{4,\frac{1}{4}} \simeq \mathrm{Conf}_4$, further work on this space could start by attempting to glue the critical set at $r = \frac{1}{4}$ onto $\mathrm{Conf}_{4,\frac{1}{3}}$, in order to understand how the attachment of further cells causes some pairs of loops, such as $(a_1, 0)$ and $(c_3, 0)$, to become homotopic.

Chapter 5

Persistence under deformation of the unit disc

Given the rotational symmetry of D^2, $\tau\colon \mathrm{Conf}_n \to \mathbb{R}$ behaves as a Morse-Bott function (a generalisation of a Morse function in which critical points may not be isolated, defined in [19, §2.5]), with each critical radius corresponding not to a single critical configuration, but to an S^1 of critical configurations. Under a well-chosen small perturbation, we would thus expect, generically, a critical level r_0 to split into two critical radii, say $r_- < r_+$ near r_0. This is shown in the case of the first critical radius $\frac{1}{n}$ in the following proposition and lemma. We recall the stress graph $N(x)$ from Def. 1.2.3.

Lemma 5.0.1. (Adapted from [14, §2.5]) *Let $E \subset \mathbb{R}^2$ be an ellipse of semi-major radius a and eccentricity e, centred at the origin, whose major axis lies along the x-axis, and $p = (p_1, 0)$ a point on the major axis of E. If $|p_1| > ae^2$, then* $\mathrm{dist}(p, \partial E) = a - |p_1|$, *and this is achieved at either $(-a, 0)$ or $(a, 0)$; otherwise,* $\mathrm{dist}(p, \partial E) = \sqrt{\left(a^2 - \frac{p_1^2}{e^2}\right)(1 - e^2)}$, *and this is achieved at* $\left(\frac{p_1}{e^2}, \pm\sqrt{\left(a^2 - \frac{p_1^2}{e^4}\right)(1 - e^2)}\right)$.

Proof. $\partial E = \left\{(x, y) \in \mathbb{R} \mid \frac{x^2}{a^2} + \frac{y^2}{b^2} = 1\right\}$, where $b = a\sqrt{1 - e^2}$. Since ∂E is compact, there is some $(x', y') \in \partial E$ such that $\mathrm{dist}(p, \partial E) = |p - (x', y')| = \sqrt{(x' - p_1)^2 + (y')^2}$. Furthermore, we know that p lies on the normal line to ∂E at (x', y'), which has parametric form $x = x'(1 + \frac{t}{a^2})$, $y = y'(1 + \frac{t}{b^2})$, $t \in \mathbb{R}$. Then in particular, at p, we have $0 = y'(1 + \frac{t}{b^2})$; that is, either $y' = 0$ or $t = -b^2$.

In the first case, we have $(x', y') = (\pm a, 0)$, hence $|(x', y') - p| = a - |p_1|$.

In the second case, we have $p_1 = x'\left(1 - \frac{b^2}{a^2}\right) = x'e^2$, that is $x' = \frac{p_1}{e^2}$, and therefore $1 = \frac{p_1^2}{a^2e^4} + \frac{(y')^2}{b^2}$, or equivalently

$$\begin{aligned}(y')^2 &= b^2\left(1 - \frac{p_1^2}{a^2e^4}\right)\\ &= b^2 - \frac{p_1^2}{e^4} + \frac{p_1^2}{e^4} - \frac{b^2p_1^2}{a^2e^4}\\ &= b^2 - \frac{p_1^2}{e^4} + \frac{p_1^2}{e^2}\\ &= a^2(1-e^2) - \frac{p_1^2}{e^4}\left(1-e^2\right)\\ &= \left(a^2 - \frac{p_1^2}{e^4}\right)\left(1-e^2\right) \quad .\end{aligned}$$

Then

$$\begin{aligned}|(x', y') - p|^2 &= (x' - p_1)^2 + (y')^2\\ &= p_1^2\left(\frac{1}{e^2} - 1\right)^2 + \left(a^2 - \frac{p_1^2}{e^4}\right)\left(1-e^2\right)\\ &= \frac{p_1^2}{e^4} - \frac{2p_1^2}{e^2} + p_1^2 + a^2(1-e^2) - \frac{p_1^2}{e^4} + \frac{p_1^2}{e^2}\\ &= -\frac{p_1^2}{e^2} + p_1^2 + a^2(1-e^2)\\ &= \left(a^2 - \frac{p_1^2}{e^2}\right)\left(1-e^2\right) \quad .\end{aligned}$$

Since $p \in E$, we have $|x'| < a$, and therefore this case only applies in the case $|p_1| < ae^2$. In this case, we have

$$\begin{aligned}\left(a^2 - \frac{p_1^2}{e^2}\right)\left(1-e^2\right) &= a^2 - a^2e^2 - \frac{p_1^2}{e^2} + p_1^2\\ &= a^2 - 2ap_1 + p_1^2 - \left(a^2e^2 - 2ap_1 + \frac{p_1^2}{e^2}\right)\\ &= (a-p_1)^2 - \left(ae - \frac{p_1}{e}\right)^2\\ &\leq (a-p_1)^2 \quad ,\end{aligned}$$

so $\operatorname{dist}(p, \partial E) = \sqrt{\left(a^2 - \frac{p_1^2}{e^2}\right)\left(1-e^2\right)}$. Otherwise $\operatorname{dist}(p, \partial E) = a - |p_1|$. □

Proposition 5.0.2. *Take $n \in \mathbb{N}$, and let C denote the set of critical configurations of Conf_n with radius $\frac{1}{n}$ where the points lie in number order along the diameter. Consider the family of ellipses E_e with semi-major radius 1 indexed by eccentricity $e \in \left[0, \sqrt{\frac{n-1}{n}}\right)$. There are exactly two continuous families, $\left(x^{e,+}\right)_e$ and $\left(x^{e,-}\right)_e$, of configurations such that*

- $x^{e,+}, x^{e,-}$ *are critical configurations of* $\mathrm{Conf}_n(E_e)$,
- $x^{0,+}, x^{0,-} \in C$.

Proof. Let $(x^e)_e$ be a family of configurations such that x^e is a critical configuration of E_e and $x^0 \in C$. We choose coordinates such that E_e is defined by the equation $x^2 + \frac{y^2}{1-e^2} = 1$.

First, let $e \in \left(0, \sqrt{\frac{n-1}{n}}\right)$ be such that $N(x^e) \cong N(x^0)$. Then we deduce by Lemmas 2.0.3 and 2.0.4 that each of these edges of $N(x^e)$ must have positive weight and all the edges must be collinear – that is, $N(x^e)$ is a straight line. Furthermore, $N(x^e)$ is a normal to the boundary at both points of intersection. The normal at a point (p, q) is $2\left(p, \frac{q}{1-e^2}\right)$. Since the normal at the other intersection point must be parallel to this, the intersection point must be $(-p, -q)$. Then it follows that $(p, q) - (-p, -q) = \lambda\left(p, \frac{q}{1-e^2}\right)$ for some $\lambda \in \mathbb{R}$, which has solutions only if $p = 0$ or $q = 0$. Therefore $N(x^e)$ is either the major axis or the minor axis of E_e. We denote the configurations of this form $x^{e,+}$ and $x^{e,-}$ respectively. The points of these configurations are defined by $x_i^{e,+} = \left(\frac{2i-n-1}{n}, 0\right)$ and $x_i^{e,-} = \left(0, \frac{2i-n-1}{n}\sqrt{1-e^2}\right)$.

Now suppose for a contradiction there is $e' \in \left[0, \sqrt{\frac{n-1}{n}}\right)$ such that $N(x^{e'}) \ncong N(x^0)$, and let $e^* = \inf\left\{e \in \left[0, \sqrt{\frac{n-1}{n}}\right) \mid N(x^e) \ncong N(x^0)\right\}$. $N(x^{e'})$ cannot be a strict subgraph of $N(x^0)$, since any strict subgraph of $N(x^0)$ has an interior vertex of degree 1 on every component, and thus cannot be balanced by Lemma 2.0.3.

Let $f\colon \mathrm{Conf}_n \to \mathbb{R}$ be any distance function from the definition of τ – that is, $f(x)$ takes the form $\frac{1}{2}|x_i - x_j|$ for some distinct i, j, or $\mathrm{dist}(x_i, \partial D^2)$ for some i. Let $g\colon \left[0, \sqrt{\frac{n-1}{n}}\right) \to \mathbb{R},\ e \to \frac{f(x^e)}{\tau(x^e)}$. Then g is continuous, and the edge corresponding to f is found in $N(x^e)$ if and only if $g(e) = 1$. Since g is constant on $[0, e^*)$, it follows by continuity that $g(e^*) = g(0)$ for all choices of f, and thus $N(x^{e^*}) \cong N(x^0)$, which lies along either the major axis or the minor axis of E.

Hence by assumption, there exists some edge which lies in $N(x^{e'})$ but not in $N(x^{e^*})$. There are two possibilities: either the points $x_1^{e'}$ or $x_n^{e'}$ are adjacent to more than one boundary vertex, or there is some choice of f such that $g(e^*) > g(e') = 1$. Denote $B_e = B\left(0, \sqrt{1-e^2}\right)$. First, if $x^{e'}$ lies along the major axis, we have $|x_1^{e'}| = |x_n^{e'}| = \frac{n-1}{n} > (e')^2$, thus $\mathrm{dist}(x_1^{e'}, \partial E_{e'})$ and $\mathrm{dist}(x_n^{e'}, \partial E_{e'})$ are each achieved at a unique point by Lemma

5.0.1. On the other hand, if $x^{e'}$ lies along the minor axis, we see that $x_1^{e'}, x_n^{e'} \in B_{e'} \subset E_{e'}$, where $B_{e'}$ intersects $\partial E_{e'}$ only on the line containing $\bigcup x^{e'}$. $\operatorname{dist}\left(x_1^{e'}, \partial B_{e'}\right)$ is achieved only at the point of intersection closer to x_1; this is therefore also the unique point where $\operatorname{dist}(x_1^{e'}, \partial E_{e'})$ is achieved. The same argument holds for $\operatorname{dist}(x_n^{e'}, \partial E_{e'})$.

Now only one possibility remains: there is some choice of f such that $g(e^*) > g(e') = 1$. We consider each distance functions f for which $g(e^*) > 1$:

- For $j - i \geq 2$, $\frac{1}{2}|x_j^{e^*} - x_i^{e^*}| = (j-i)\tau\left(x^{e^*}\right) \geq 2\tau\left(x^{e^*}\right)$.
- For $x^{e^*} = x^{e^*,-}$ and $1 < i < n$, we note that $x_i^{e^*} \in B_{e^*} \subset E_{e^*}$. Then $\operatorname{dist}(x_i^{e^*}, \partial E_{e^*}) \geq \operatorname{dist}\left(x_i^{e^*}, \partial B_{e^*}\right) = \sqrt{1-(e^*)^2} - |x_i^{e^*}| \geq \frac{3}{n}\sqrt{1-(e^*)^2} = 3\tau\left(x^{e^*}\right)$
- For $x^{e^*} = x^{e^*,+}$ and $1 < i < n$ such that $|x_i^{e^*}| \geq (e^*)^2$, we have $\operatorname{dist}(x_i^{e^*}, \partial E_{e^*}) = 1 - |x_i^{e^*}| \geq \frac{3}{n} = 3\tau\left(x^{e^*}\right)$ by Lemma 5.0.1.
- For $x^{e^*} = x^{e^*,+}$ and $1 < i < n$ such that $|x_i^{e^*}| < (e^*)^2$, we have $\frac{|x_i^{e^*}|^2}{(e^*)^2} < |x_i^{e^*}|$. Then $\operatorname{dist}(x_i^{e^*}, \partial E_{e^*}) = \sqrt{\left(1 - \frac{|x_i^{e^*}|^2}{(e^*)^2}\right)(1-(e^*)^2)} > \sqrt{\left(1-|x_i^{e^*}|\right)\frac{1}{n}} > \sqrt{\frac{3}{n}\cdot\frac{1}{n}} = \frac{\sqrt{3}}{n} = \sqrt{3}\tau\left(x^{e^*}\right)$ by Lemma 5.0.1.

For each of these distance functions f, by continuity of g, there exists $\delta_f > 0$ such that for all $e \in [e^*, e^* + \delta_f)$, we have $g(e) > g(e^*) - \frac{1}{2} \geq \sqrt{3} - \frac{1}{2} > 1$. Therefore $N(x^e)$ does not contain the edge corresponding to f. Set $\delta = \min_f \delta_f$. Then $N(x^e) \cong N(x^{e^*})$ for all $e \in [e^*, e^* + \delta)$, contradicting the definition of e^*.

Therefore $x^e = x^{e,+}, x^{e,-}$ are the unique families of configurations $(x^e)_e$ such that x^e is a critical configuration of E_e and $x^0 \in C$. □

Provided the perturbation is small, we would expect the topology just above r_+ in the perturbed case to be the same as the topology just above r_0 in the unperturbed case. By contrast, the homotopy type on the region with radius just above r_- may have different topology, and this is where the π_{n-2}-class of Baryshnikov et al. [11, §5.2] lives (if you consider an infinite strip as the limit of an ellipse with fixed semi-minor radius as eccentricity approaches 1).

In this section, we investigate the topology beyond r_+, by considering the persistence of our homotopy class from §3.2 under perturbations of D^2. First, we consider arbitrary small perturbations. Then, following Remark 3.2.6, we consider to what extent it is

necessary to use the full unit disc by investigating the persistence of this homotopy class as we replace D^2 with an ellipse of decreasing semi-minor radius.

This section will use the map ang from Def. 3.1.2.

Theorem 5.0.3. *Take $r \in (0, \infty)$, $n \geq 4$, and $U \subset \mathbb{R}^2$. Suppose there are discs $C_1, C_2 \subset \mathbb{R}^2$ of radius $(n-1)\,r$ and strictly less than nr respectively, such that $C_1 \subset U$ and any disc of radius r in U is contained in C_2. Then there is some non-zero $\gamma \in \pi_{n-3}(\mathrm{Conf}_{n,r}(U))$ such that $\iota_*(\gamma) = 0$ in $\pi_{n-3}(\mathrm{Conf}_n(U))$.*

In particular, this shows that the non-trivial π_{n-3}-class remains in $\mathrm{Conf}_{n,r}(U)$ for $\frac{1}{n} < r < \frac{1}{n-1}$ when U is a deformation of D^2, provided that the deformation is small enough that: 1) we can fit a disc of radius $(n-1)\,r$ inside U, and 2) every disc of radius r in U lies in the unit disc. The first condition means the boundary of U cannot be deformed very far towards the origin. On the other hand, these conditions place no restrictions on the area of U, nor do they require U to be bounded – consider, for example, the deformation of D^2 in which we remove the segment of D^2 with y-coordinate greater than $1 - \varepsilon$ for some small $\varepsilon > 0$, and then take the union of the remaining region with the semi-infinite strip $[-\varepsilon, \varepsilon] \times [0, \infty)$.

Proof. The conditions on C_1, C_2 yield $\mathrm{Conf}_{n,r}(C_1) \subset \mathrm{Conf}_{n,r}(U) \subset \mathrm{Conf}_{n,r}(C_2)$. Denote the inclusion maps by i_1, i_2 respectively. Furthermore, it is impossible for n discs of radius r to lie on a straight line inside C_2, so $\mathrm{ang}(\mathrm{Conf}_{n,r}(C_2)) \subset T^{n-2}\backslash\{0\}$.

By Thm. 3.1.1 and 3.2.1, there is some non-contractible sphere $\mathcal{S} \subset \mathrm{Conf}_{n,r}(C_1)$ such that $\iota_*([\mathcal{S}]) = 0$ in $\pi_{n-3}(\mathrm{Conf}_n(C_1))$. In particular, this is proven by showing that $\mathrm{ang}(\mathcal{S})$ is non-contractible in $T^{n-2}\backslash\{0\}$. We claim $\gamma \coloneqq (i_1)_*([\mathcal{S}])$ satisfies the desired properties.

First, note that $\mathrm{ang} = \mathrm{ang} \circ i_2 \circ i_1$. Since $(\mathrm{ang} \circ i_2)_* \circ (i_1)_*([\mathcal{S}]) = (\mathrm{ang})_*[\mathcal{S}] \neq 0$ in $\pi_{n-3}(T^{n-2}\backslash\{0\})$, it follows that $\gamma \neq 0$ in $\pi_{n-3}(\mathrm{Conf}_{n,r}(U))$.

To finish, let $i_3 \colon \mathrm{Conf}_n(C_1) \hookrightarrow \mathrm{Conf}_n(U)$ be the inclusion map. Then $\iota \circ i_1 = i_3 \circ \iota$ and therefore

$$\iota_*(\gamma) = \iota_*((i_1)_*([\mathcal{S}])) = (i_3)_*(\iota_*([\mathcal{S}])) = (i_3)_*(0) = 0 \quad . \qquad \square$$

Following Remark 3.2.6, it is apparent we shouldn't need the full extent of the unit

disc in Thm. 3.2.1. Indeed, if a small enough angle is used in place of $\frac{2\pi}{n}$ in the given construction of the $(n-3)$-sphere, the discs should remain within some narrow strip parallel to (and centred on) the x-axis. The following result shows that this homotopy class in §3 remains when we deform the unit disc into an ellipse with semi-major radius 1, provided that the semi-minor radius is greater than $\frac{1}{\sqrt{n}}$. This result also enables us to generalise Thm. 5.0.3 by replacing C_1 with a suitable ellipse.

Under this deformation, the first critical level $\frac{1}{n}$ splits into two critical levels. The lower of these is $\frac{\sqrt{1-e^2}}{n}$, where the numerator is the semi-minor radius. This theorem concerns the upper critical level, $\frac{1}{n}$, which is related to the semi-major radius.

Theorem 5.0.4. *Let $n \in \mathbb{N}$, and let E be an ellipse of semi-major radius 1 and eccentricity $e \in \left[0, \sqrt{\frac{n-1}{n}}\right)$ (equivalently, the semi-minor radius of E lies in $\left(\frac{1}{\sqrt{n}}, 1\right]$). Then there is some $\varepsilon > 0$ such that, for $r \in \left(\frac{1}{n}, \frac{1}{n} + \varepsilon\right]$, $\mathrm{Conf}_{n,r}(E)$ contains a non-contractible $(n-3)$-sphere.*

To prove this, we will construct a sphere in $\mathrm{Conf}_{n,r}(E)$, and prove that the disc centres in each configuration lie in some smaller ellipse E'. The following lemma defines the necessary relationship between the dimensions of E and E' which ensures that, if a disc has its centre in E', then the disc is contained in E.

Lemma 5.0.5. *Take $\mathcal{D} \in \mathrm{Conf}_{n,r}(\mathbb{R}^2)$, $a > r$. Let E' be an ellipse with semi-major radius $a - r$ and eccentricity e' such that the centre of every disc of $\mathcal{D}$ lies in $\overline{E'}$. Let E be a concentric, coaxial ellipse of semi-major radius a and eccentricity $e \leq \sqrt{\left(1 - \frac{r}{a}\right)\left(1 - \sqrt{1-(e')^2}\right)}$. Then $\bigcup \mathcal{D} \subset E$.*

Proof. It is sufficient to check this for $e = \sqrt{\left(1 - \frac{r}{a}\right)\left(1 - \sqrt{1-(e')^2}\right)}$, since the associated ellipse is contained inside the ellipses of smaller eccentricity. For this proof, we use the equivalent definition $e = \sqrt{\frac{a-r-b'}{a}}$, where $b' = (a-r)\sqrt{1-(e')^2}$ is the semi-minor radius of E'. Since E and E' are concentric and coaxial, we choose coordinates so that the shared centre is the origin, and the shared major axis is the x-axis. Take $q = (q_1, q_2) \in \overline{E'}$ to be the centre of some disc in $\mathcal{D}$ and assume by symmetry that q lies in the first quadrant. We need to show that $\mathrm{dist}(q, \partial E) \geq r$. We will achieve this by finding a suitable point on the x-axis and using the triangle inequality.

Let $q_3 = \min\{q_1, ae^2\}$ and $q' = (q_3, 0)$. Since $q_3 \leq ae^2$, we have $\mathrm{dist}(q', \partial E) =$

$\sqrt{\left(a^2 - \frac{q_3^2}{e^2}\right)(1-e^2)}$ by Lemma 5.0.1. This inequality also yields $a^2 - \frac{q_3^2}{e^2} \geq a^2(1-e^2)$, so that $\operatorname{dist}(q', \partial E)^2 \geq a^2(1-e^2)^2 = a^2(1 - \frac{a-r-b'}{a})^2 = (r+b')^2$.

Then it remains to show $|q-q'| \leq b'$. If $q_1 \leq ae^2$, then $|q-q'| = q_2 \leq b'$, where the second inequality arises from the fact that b' is the semi-minor radius. Otherwise, $q' = (ae^2, 0)$, and $\sup\{|q-q'| \colon q = (q_1, q_2) \in \overline{E'}, q_1 > ae^2\}$ is achieved by some $(q_1, q_2) \in \partial E'$ with $q_1 \geq ae^2$. Since $ae^2 \leq (a-r)(e')^2$, Lemma 5.0.1 applied to q' and E' shows that $\partial E' \to \mathbb{R}$, $q \mapsto |q-q'|$ has its local minima at $\left(\frac{p_1}{e^2}, \pm\sqrt{\left(a^2 - \frac{p_1^2}{e^4}\right)(1-e^2)}\right)$, and therefore has local maxima at $(\pm(a-r), 0)$. When we restrict to $q_1 \geq ae^2$, this supremum must be achieved at either: 1) $q_1 = ae^2$, where $|q-q'| \leq b'$ by the first case; or 2) $(a-r, 0)$, where $|q-q'| = a - r - ae^2 = b'$.

Thus $\operatorname{dist}(q, \partial E) \geq \operatorname{dist}(q', \partial E) - |q-q'| \geq \operatorname{dist}(q', \partial E) - b' \geq r$ as required. □

Remark 5.0.6. The inequality $e \leq \sqrt{\left(1 - \frac{r}{a}\right)\left(1 - \sqrt{1-(e')^2}\right)}$ is asymptotically sharp as $e' \to 1$. To see this, note that when $e' = 1$, we have $e > \sqrt{1 - \frac{r}{a}}$ if and only if $a - r < ae^2$. Hence, by Lemma 5.0.1, $\operatorname{dist}((a-r, 0), \partial D^2)$ is not achieved at $(a, 0)$, so $\operatorname{dist}((a-r, 0), \partial E) < |(a,0) - (a-r, 0)| = r$, so the disc of radius r centred at $(a-r, 0) \in \overline{E'}$ is not contained in E. This is the case of interest in the following proof.

Proof of Theorem 5.0.4. Take some angle $0 < \xi < \frac{\pi}{n-2}$ such that $1 - r > e^2$, where $r = \frac{1}{n - 4\sin^2\frac{\xi}{4}}$, and let $S = \partial\left([-\xi, \xi]\right)^{n-2} \subset T^{n-2}$. Let $e' = \sqrt{1 - \left(1 - \frac{e^2}{1-r}\right)^2}$, $z_1 = (-e'(1-r), 0)$, $z_2 = (e'(1-r), 0)$. Note that $\frac{e^2}{1-r} < 1$ and $\frac{e^2}{1-r} \to 1$ as $e \to \sqrt{\frac{n-1}{n}}^-$, $\xi \to 0$. Thus $e' < 1$ and $e' \to 1$ as $e \to \sqrt{\frac{n-1}{n}}^-$, $\xi \to 0$. We construct some $\mathcal{S} \colon S \to \operatorname{Conf}_{n,r}(\mathbb{R}^2)$ by the following algorithm on each $(\phi_2, \ldots, \phi_{n-1}) \in S$:

1. Place D_1 at the origin of the plane and D_2 in contact with it, centred at $(2r, 0)$.
2. Place each subsequent disc D_i for $i \leq n$ in contact with D_{i-1} such that x_i lies on the ray from x_{i-1} at angle ϕ_{i-1} (Figure 3.3).
3. Translate and rotate the configuration so that x_1 and x_n lie on the x-axis, equidistant from the origin.

This is continuous and the discs are non-overlapping by the arguments in the proof of Theorem 3.2.1.

We now show that the centre of every disc in each configuration in $\mathcal{S}$ fits inside the ellipse with semi-major radius $1-r$ and foci z_1, z_2, which has eccentricity e'. By remark 3.2.5, we see that, at stage 2,

$$\begin{aligned}
|x_1 - x_n|^2 &= 4r^2 \left| \left(\sum_{i=1}^{n-1} \cos\theta_i \ , \ \sum_{i=1}^{n-1} \sin\theta_i \right) \right|^2 \\
&= 4r^2 \left(\left(\sum_{i=1}^{n-1} \cos\theta_i \right)^2 + \left(\sum_{i=1}^{n-1} \sin\theta_i \right)^2 \right) \\
&= 4r^2 \left(\sum_{i=1}^{n-1} (\cos^2\theta_i + \sin^2\theta_i) + 2 \sum_{i=2}^{n-1} \sum_{j=1}^{i-1} (\cos\theta_i \cos\theta_j + \sin\theta_i \sin\theta_j) \right) \\
&= 4r^2 \left(n - 1 + 2 \sum_{i=2}^{n-1} \sum_{j=1}^{i-1} \cos(\theta_i - \theta_j) \right)
\end{aligned}$$

where $|\theta_i - \theta_j| = |\sum_{k=i+1}^{j} \phi_k| \leq (j-i)\xi \leq (n-2)\xi$. Denoting $\theta = (n-2)\xi < \pi$, we see that $\cos(\theta_i - \theta_j) \geq \cos\theta$, and thus

$$\begin{aligned}
|x_1 - x_n|^2 &\geq 4r^2 \left(n - 1 + 2 \sum_{i=2}^{n-1} \sum_{j=1}^{i-1} \cos\theta \right) \\
&= 4r^2 \left(n - 1 + (n-1)(n-2)\cos\theta \right) \\
&= 4r^2 \left((n-1)^2 - (n-1)(n-2)(1-\cos\theta) \right) \quad .
\end{aligned}$$

That is, at step 3, the x-coordinate of x_n will be at least

$$r\sqrt{(n-1)^2 - (n-1)(n-2)(1-\cos\theta)} \to \frac{n-1}{n} \text{ as } \xi \to 0.$$

Since

$$\begin{aligned}
e'(1-r) &= \sqrt{(1-r)^2 - (1-r-e^2)^2} \\
&= \sqrt{2(1-r)e^2 - e^4} \\
&< \sqrt{2\left(1 - \frac{1}{n}\right)e^2 - e^4} \\
&= \sqrt{\left(1 - \frac{1}{n}\right)^2 - \left(1 - \frac{1}{n} - e^2\right)^2} \\
&< 1 - \frac{1}{n} \\
&= \frac{n-1}{n}
\end{aligned}$$

and $\sqrt{2\left(1-\frac{1}{n}\right)e^2 - e^4}$ is independent of ξ, it follows that

$$r\sqrt{(n-1)^2 - (n-1)(n-2)(1-\cos\theta)} > e'(1-r)$$

for sufficiently small ξ. Then x_1, x_n are further from the origin than z_1, z_2 for small ξ, so we can find $t \in (0,1)$ such that $z_1 = tx_1 + (1-t)x_n$ and $z_2 = (1-t)x_1 + tx_n$.

Using this, we find that for any i,

$$\begin{aligned}|x_i - z_1| + |x_i - z_2| &\leq t|x_i - x_1| + (1-t)|x_i - x_n| + (1-t)|x_i - x_1| + t|x_i - x_n| \\ &= |x_i - x_1| + |x_i - x_n| \\ &\leq 2r\left(n - 1 - 4\sin^2\frac{\xi}{4}\right) \quad ,\end{aligned}$$

where the last line follows from Lemma 3.2.2. That is, each x_i lies inside the closed ellipse with foci z_1, z_2 and semi-major radius $(n - 4\sin^2\frac{\xi}{4})r - r = 1 - r$ as required.

Therefore, since $e = \sqrt{(1-r)\left(1 - \sqrt{1-(e')^2}\right)}$, we observe that for all $\Phi \in S$, $\bigcup \mathcal{S}(\Phi) \subset E$ by Lemma 5.0.5. Thus $\mathcal{S}$ is a local section of $\mathrm{ang}\colon \mathrm{Conf}_{n,r}(E) \to T^{n-2}$.

We finish by observing that $E \subset D^2$, and moreover $[S] \neq 0 \in \pi_{n-3}(T^{n-2}\backslash\{0\})$, where $0 \in T^{n-2}$ corresponds to all discs lying in a straight line. Therefore $\mathcal{S}$ represents a non-trivial class in $\mathrm{Conf}_{n,r}(E)$ by Lemma 3.1.3. □

While $\frac{1}{\sqrt{n}}$ is the best semi-minor radius we can achieve while keeping the semi-major radius equal to 1, we would hope to achieve better, since, as made clear in Remark 3.2.6, the maximal distance of our configurations from the y-axis is arbitrarily close to $\frac{1}{n}$. We achieve this semi-minor radius in the next theorem. However, in order to achieve this, we must allow our semi-major radius, and thus too the area of the ellipse, to approach infinity.

Theorem 5.0.7. *Let $n \in \mathbb{N}$, and let E be an ellipse with eccentricity $e \in \left[\sqrt{1-r}, 1\right)$ and semi-minor radius $b = \sqrt{\frac{(1-r)^2(1-e^2)}{e^2} + r^2}$, where $r = \frac{1}{n} + \varepsilon$ for some sufficiently small $\varepsilon > 0$. Then $\mathrm{Conf}_{n,r}(E)$ contains a non-contractible $(n-3)$-sphere.*

Under these hypotheses, b takes all values in $(r, \sqrt{r}]$. The semi-major radius is $b\left(1-e^2\right)^{-\frac{1}{2}} = \sqrt{\frac{(1-r)^2}{e^2} + \frac{r^2}{1-e^2}}$, which takes all values in $[1, \infty)$.

Proof. For a sufficiently small angle $\xi > 0$, let $S = \partial\left[-\xi, \xi\right]^{n-2} \subset T^{n-2}$ and take $\frac{1}{n} < r \leq \frac{1}{n - 4\sin^2\frac{\xi}{4}}$. Take the length-preserving coordinate system in which E is centred at the origin and its major axis coincides with the x-axis. We define a local section $\mathcal{S}\colon S \to \mathrm{Conf}_{n,r}(E)$ to ang by constructing each $\mathcal{S}(\phi_2, \ldots, \phi_{n-1})$ as follows:

1. Place D_1 at the origin of the plane and D_2 in contact with it at $(2r, 0)$.
2. Place each subsequent disc D_i in contact with D_{i-1}, such that x_i lies on the ray from x_{i-1} at angle ϕ_{i-1}.
3. Translate all discs by $-\frac{x_1+x_n}{2}$.
4. Rotate the configuration about the origin so that x_1 and x_n lie on the x-axis.

There is no overlap between discs and $\mathcal{S}$ is continuous by the arguments of Thm. 3.2.1, so we simply need to show $\bigcup \mathcal{S}(\Phi) \subset E$ for all $\Phi \in S$. By Remark 3.2.6, x_i is arbitrarily close to $(\frac{2i-n-1}{n}, 0)$ at step 3. In particular, $x_1 \to (-\frac{n-1}{n}, 0)$ and $x_n \to (\frac{n-1}{n}, 0)$ as $\xi \to 0$, so the size of the rotation in step 4 tends to 0, which means this limit position holds after step 4 as well. This limit is the first critical configuration, consisting of the n discs of radius $\frac{1}{n}$ lined up along the horizontal diameter of D^2, such that D_i touches D_{i-1} and D_{i+1} if they exist, and D_1 and D_n touch the boundary.

More precisely, for each $\frac{1}{n} < r \leq \frac{1}{n-4\sin^2\frac{\xi}{4}}$, there is some $s > r$ (where $s \to \frac{1}{n}$ as $\xi \to 0$) such that, for $2 \leq i \leq n-1$, $D_i \subset B\left(\left(\frac{2i-n-1}{n}, 0\right), s\right)$. Therefore

$$\bigcup_{i=2}^{n-1} D_i \subset F_1 \coloneqq \left[-\frac{n-3}{n} - s, \frac{n-3}{n} + s\right] \times [-s, s] \quad .$$

We have fixed the centres of D_1 and D_n to lie on the x-axis, and Lemma 3.2.2 gives us $|x_1|, |x_n| \leq (n - 1 - 4\sin^2\frac{\xi}{4})r \leq 1 - r$. Thus

$$D_1 \cup D_n \subset F_2 \coloneqq B((-1+r, 0), r) \cup ([-1+r, 1-r] \times [-r, r]) \cup B((1-r, 0), r) \quad .$$

For sufficiently small ξ, we have $s < \frac{3}{2n}$. Then $\frac{n-3}{n} + s < \frac{2n-3}{2n} < 1 - r$, and so

$$\bigcup \mathcal{S}(\Phi) \subset F_1 \cup F_2 \subset F \coloneqq B((-1+r, 0), r) \cup ([-1+r, 1-r] \times [-s, s]) \cup B((1-r, 0), r)$$

for all $\Phi \in S$ (see Fig. 5.1).

Next, we show that $F \subset E$ by showing that all points of F satisfy the inequality which defines E,

$$x^2(1-e^2) + y^2 \leq b^2 = \frac{(1-r)^2(1-e^2)}{e^2} + r^2 \quad .$$

First, if $(x, y) \in [-1+r, 1-r] \times [-s, s]$, then $x^2(1-e^2) + y^2 \leq (1-r)^2(1-e^2) + s^2$. As $\xi \to 0$, then $s, r \to \frac{1}{n}$, and therefore $s^2 - r^2 \to 0$. Since the lower bound on e is always

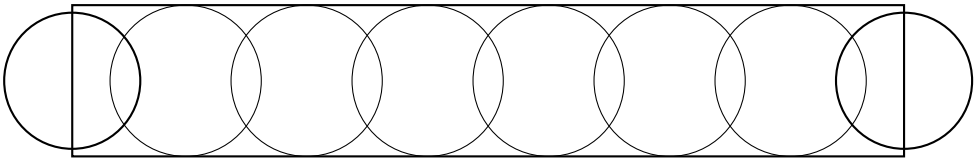

Figure 5.1: The outer boundary shows a thickening of the first critical configuration, constructed in such a way that it contains the configurations of the non-contractible sphere $\mathcal{S}$, and is in turn contained in the ellipse E, in Theorem 5.0.7.

less than $\sqrt{\frac{n-1}{n}}$, we may assume e to be fixed. Therefore $s^2 - r^2 \leq \frac{1}{4}(1-e^2)\left(\frac{1}{e^2}-1\right) \leq (1-r)^2(1-e^2)\left(\frac{1}{e^2}-1\right)$ for sufficiently small ξ. Hence

$$\begin{aligned} x^2(1-e^2) + y^2 &\leq (1-r)^2(1-e^2) + r^2 + (1-r)^2(1-e^2)\left(\frac{1}{e^2}-1\right) \\ &= \frac{(1-r)^2(1-e^2)}{e^2} + r^2 \quad . \end{aligned}$$

Second, if $(x,y) \in B((1-r,0),r)$, then $(x-1+r)^2 + y^2 \leq r^2$. Thus

$$\begin{aligned} x^2(1-e^2) + y^2 &\leq x^2(1-e^2) + r^2 - (x-1+r)^2 \\ &= -e^2x^2 + 2(1-r)x + 2r - 1 \\ &= -\left(ex - \frac{1-r}{e}\right)^2 + \frac{(1-r)^2}{e^2} + 2r - 1 \\ &\leq \frac{(1-r)^2}{e^2} + 2r - 1 \\ &= \frac{(1-r)^2(1-e^2)}{e^2} + (1-r)^2 + 2r - 1 \\ &= \frac{(1-r)^2(1-e^2)}{e^2} + r^2 \quad . \end{aligned}$$

Symmetrically, we see the same for $(x,y) \in B((-1+r,0),r)$. Therefore $\bigcup \mathcal{S}(\Phi) \subset F \subset E$ for all $\Phi \in S$, which completes the proof that $\mathcal{S}$ is a local section of ang.

Finally, let $\Delta = \{B(p,r) \colon p \in \mathbb{R}^2,\ B(p,r) \subset E\}$ be the set of all discs of radius r contained in E. We want to show that every such disc also lies in D^2. It is clear geometrically that $\sup\{|p| \colon B(p,r) \in \Delta\}$ is achieved on the major axis of E, which is the x-axis. We may assume the x-coordinate of p to be positive by symmetry. Then, by checking that these coordinates satisfy the equations defining both sets, we note that $\partial B((1-r,0),r)$ intersects ∂E at $p_\pm = \left(\frac{1-r}{e^2}, \pm\sqrt{r^2 - (1-r)^2(e^{-2}-1)^2}\right)$, so the x-coordinate of p cannot be greater than $1-r$ – that is, $\sup\{|p| \colon B(p,r) \in \Delta\} \leq 1-r$. This is equivalent to the claim.

Now $[S] \neq 0 \in \pi_{n-3}(T^{n-2}\backslash\{0\})$, and if $\mathrm{ang}(\mathcal{D}) = 0$, then all the disc centres are collinear. Thus $\mathcal{S}$ represents a non-trivial element of $\pi_{n-3}(\mathrm{Conf}_{n,r}(E))$ by Lemma 3.1.3, as required. □

We note that there is no discontinuity in the ranges of the semi-minor and semi-major radii between Theorems 5.0.4 and 5.0.7; indeed, when $e = \sqrt{1-r}$, both settings yield the ellipse of semi-major radius 1 and semi-minor radius $\sqrt{r}$. Hence there exists a continuous family of ellipses, indexed over the semi-minor radius on the range $\left(\frac{1}{n}, 1\right]$, which contain this non-contractible sphere class.

Chapter 6

Exploring the lower homotopy classes beyond the first critical radius

Consider the inclusion $\iota\colon \mathrm{Conf}_{n,r} \to \mathrm{Conf}_n$. In §3, we show that there exists $\gamma \in \pi_{n-3}(\mathrm{Conf}_{n,r})$ such that $\iota_*(\gamma) = 0 \in \pi_{n-3}(\mathrm{Conf}_n)$ for r just beyond the first critical radius. This shows that ι_* is not injective in dimension $n-3$. This suggests some related questions: is ι_* surjective in dimension $n-3$? Is ι_* injective or surjective in any other dimensions?

We will consider here the dimensions $k \leq n-3$. We hope for a theorem akin to Lefschetz' Hyperplane Theorem [27, Cor. 7.4], taking inspiration from the proof originally laid out in [8].

Theorem 6.0.1 (Lefschetz' Hyperplane Theorem)**.** *Let V be an algebraic variety of complex dimension n and P a hyperplane of $\mathbb{C}^n$. Then for $m < n$, we have $\pi_m(V, V \cap P) = 0$.*

Here, given topological spaces $A \subset X$ and $x_0 \in A$, the elements of the m-th relative homotopy group $\pi_m(X, A)$ (or homotopy set in the case $m = 1$) are homotopy classes of maps of triples $(D^m, \partial D^m = S^{m-1}, *) \to (X, A, x_0)$ (see [22, pp. 343-344]). In the case $A = \{x_0\}$, S^{m-1} is mapped to a point – thus the map is equivalent to a map of pairs $(D^m/S^{m-1} = S^m, *) \to (X, x_0)$ and we regain the homotopy group $\pi_m(X)$. Due to the

long exact sequence on homotopy groups, the Lefschetz Hyperplane Theorem implies $\pi_m(V \cap P) \cong \pi_m(V)$ for $m < n-1$ and $\pi_{n-1}(V \cap P) \to \pi_{n-1}(V)$ is surjective.

The proof uses the notion of an upward (or stable) manifold: given a manifold M, a flow $(\phi_t \colon M \to M)_{t\in(-\infty,\infty)}$ on M, and a differentiable map $f \colon M \to \mathbb{R}$ with critical point p, the upward manifold of p is the submanifold $\mathscr{U}_p = \{x \in M \mid \phi_t(x) \to p \text{ as } t \to -\infty\}$, consisting of all points which tend to p as they flow downwards along the flow.

Sketch proof. The authors choose a map $f \colon V \to [0,\infty)$ such that $f(x) = 0$ if and only if $x \in V \cap P$. f further has the property that, for each critical point $p \in V$, $\dim \mathscr{U}_p \leq n$, where they use the flow given by the gradient vector field ∇f. Then, by the Transversality Theorem [23, Thm. 2.1], any map $g \colon (D^m, S^{m-1}, *) \mapsto (V, V \cap P, x_0)$ can be perturbed so that $g(D^m)$ is transverse to $\mathscr{U}_p$ for all critical points p; in particular, since $\dim g(D^m) + \dim \mathscr{U}_p \leq m + n < 2n = \dim V$, the two sets are disjoint. Thus after perturbation, we can retract $g(D^m)$ onto $f^{-1}(0) = V \cap P$ along the gradient field. Since the entire $g(D^m)$ now lies in $V \cap P$, it can be contracted to the basepoint inside $V \cap P$, so $[g] = 0 \in \pi_m(V, V \cap P)$. □

This sketch suggests a route towards a similar theorem for showing that $\pi_m(\mathrm{Conf}_n, \mathrm{Conf}_{n,r}) = 0$ for small m. We use the tautological function τ defined in §1.2, and hope to show, for any map of triples $g \colon (D^m, S^{m-1}, *) \to (\mathrm{Conf}_n, \mathrm{Conf}_{n,r}, s_0)$, that we can flow $g(D^m)$ upwards into $\tau^{-1}[r,\infty) = \mathrm{Conf}_{n,r}$. In order to achieve this, we will need to:

1. Define the flow ϕ_t on Conf_n, ideally gradient-like for τ.
2. Find the downward manifolds $\mathscr{D}_p = \{x \in M \mid \phi_t(x) \to p \text{ as } t \to \infty\}$ for each stationary point of the flow and determine their dimension.
3. Use the maximum dimension of these downward manifolds to determine the maximum value of m for which the theorem holds. Since we are using the idea that transversality implies disjointness, these two maxima will add up to $\dim \mathrm{Conf}_n - 1 = 2n - 1$.

In the case just beyond the first critical radius, $r = \frac{1}{n} + \varepsilon$ for small ε, the only stationary points of a gradient-like flow for τ with $\tau(x) < r$ will be the configurations associated to the critical radius $\frac{1}{n}$. In these configurations, the points lie on

some shared diameter of D^2. Naively, we might expect to define our flow so that $\mathscr{D}_p = \{x \in \mathrm{Conf}_n \mid \exists_{v\in\mathbb{R}^2}\forall_{i\neq j}\exists_{\lambda\in\mathbb{R}}\ x_j - x_i = \lambda v\}$ is the set consisting of all configurations in which all the points lie on some common chord of D^2. The chord is uniquely defined by the position of its centre, which is an element of D^2. Then the position on the chord of each x_i is defined by one coordinate. Thus $\dim \mathscr{D}_p = n + 2$. Using $(2n-1) - (n+2) = n - 3$ leads us to the following conjecture.

Conjecture 6.0.2. *Take* $r \in \left(\frac{1}{n}, \frac{1}{n-1}\right]$. *Then* $\pi_m(\mathrm{Conf}_n, \mathrm{Conf}_{n,r}) = 0$ *for all* $m \leq n-3$. *Therefore the inclusion* $\iota\colon \mathrm{Conf}_{n,r} \to \mathrm{Conf}_n$ *induces an isomorphism on homotopy groups in dimensions* $m < n-3$ *and a surjection in dimension* $m = n-3$.

6.1 Proof of concept: the case $n = 3$

Here, we develop a gradient-like flow for τ in the case $n = 3$. There is no definition for a relative homotopy group in dimension 0, so there is no conjecture to prove here. However, we hope to find that our downward manifold has codimension $n - 2 = 1$, as this would provide a template for our proposed proof. The Transversality Theorem implies that any submanifold of codimension m can be disjoined from any submanifold of dimension less than m.

Recall the stress graph, $N(x)$, of a configuration $x \in \mathrm{Conf}_n$ from Def. 1.2.3. Configurations with a balanced stress graph (Def. 1.2.4) act as critical points, at which there is no canonical choice of τ-increasing flow. Let Γ_{n+1} denote the set of graphs on $n+1$ labelled vertices, with vertex set $V = \{v_1, \ldots, v_{n+1}\}$. Then abstractly, we can think of the map $x \mapsto N(x)$ as a map $N\colon \mathrm{Conf}_n \to \Gamma_{n+1}$, where:

- Given $1 \leq i, j \leq n$, $N(x)$ contains an edge v_iv_j if and only if $|x_j - x_i| = 2\tau(x)$, and
- Given $1 \leq i \leq n$, $N(x)$ contains an edge v_iv_{n+1} if and only if $\mathrm{dist}(x_i, \partial D^2) = \tau(x)$.

(Here, the entire boundary is encoded by a single vertex. For arbitrary $\mathrm{Conf}_n(U)$, there could be one or more discs with multiple points of contact with the boundary (for example, by Lemma 5.0.1, if U is an ellipse and there is some x_i on the major axis, adjacent to the boundary, with $|x_i| < ae^2$). Then the second condition would be replaced by 'Given $1 \leq i \leq n$, $N(x)$ contains an edge v_iv_{n+1} for each $p \in \partial U$ such that $|x_i - p| = \tau(x)$', which in general yields a multigraph. Alternatively, we could partition

the boundary into more than one piece, each corresponding to its own vertex.)

Then for each $G \in \Gamma_{n+1}$ we can define the stratum $N_G = \{x \in \mathrm{Conf}_n \mid N(x) = G\}$, the set of all configurations whose stress graph is G. We will define a continuous flow on the closure $\overline{N_G}$, in which the configurations in ∂N_G are stationary; and for $x \in N_G$, the vertices of degree 0 in G remain stationary, while the other vertices flow in such a way that the edges of the stress graph increase in length at the same rate. Eventually, this flow will meet either a critical configuration or the boundary ∂N_G, at which point the flow ends. The flow meets the boundary when some pair (or pairs) of vertices which are not adjacent in G become adjacent in $N(x)$ – that is, $\partial N_G \subset \bigcup_{G' \supset G} N_{G'}$. Choose a total order $G_1 \leq G_2 \leq \ldots \leq G_k$ on the set of graphs on $n+1$ vertices such that if G is a subgraph of G', then $G \leq G'$. We will retract the strata onto their boundaries one at a time using this order. The below propositions imply that these flows induce homotopy-equivalence.

Lemma 6.1.1. *Take $G \in \Gamma_{n+1}$. Then N_G is open in $\bigcup_{G' \not\subset G} N_{G'}$.*

Here, although we typically let $A \subset B$ include equality, the notation $G' \not\subset G'$ means that G' is not a strict subgraph of G.

Proof. Take $x \in N_G$ and consider the set

$$L = \left(\left\{ \frac{1}{2}|x_i - x_j| \mid 1 \leq i < j \leq n \right\} \cup \left\{ \mathrm{dist}(x_i, \partial D^2) \mid 1 \leq i \leq n \right\} \right) \backslash \{\tau(x)\} \quad .$$

Let $\delta = \frac{1}{2}(\min(L) - \tau(x))$ and take $y \in \bigcup_{G' \not\subset G} N_{G'}$ such that $|y_i - x_i| < \delta$ for all i. Then if $N(x)$ contains the edge $v_i v_j$, where $i, j \leq n$, we have

$$|y_i - y_j| \leq |y_i - x_i| + |x_i - x_j| + |x_j - y_j| < 2\tau(x) + 2\delta = \min(L) + \tau(x) \quad .$$

Thus $\tau(y) < \frac{1}{2}(\min(L) + \tau(x))$.

Next suppose G does not contain the edge $v_i v_j$, where $i, j \leq n+1$. If $j = n+1$, then

$$\mathrm{dist}(y_i, \partial D^2) \geq \mathrm{dist}(x_i, \partial D^2) - |x_i - y_i| > \min L - \delta = \frac{1}{2}\left(\min L + \tau(x)\right) > \tau(y)$$

otherwise if $i, j \leq n$, then

$$|y_i - y_j| \geq -|y_i - x_i| + |x_i - x_j| - |x_j - y_j| > 2\min(L) - 2\delta = \min(L) + \tau(x) > 2\tau(y) \quad .$$

Thus in each case, $N(y)$ does not contain the edge $v_i v_j$. Therefore $N(y) \subset G$, hence $N(y) = G$. □

Proposition 6.1.2. *Let ϕ_t ($t \in I$ for some interval $I \subset \mathbb{R}$) be a continuous flow on $\overline{N_G}$ which fixes the boundary. Then ϕ_t extends to a continuous flow $\bar{\phi}_t$ on $\bigcup_{G' \not\subset G} N_{G'}$ which fixes all points outside N_G.*

Proof. Let $t \in I$ and $x \in \overline{N_G}$. Take $\varepsilon > 0$. By continuity at (t, x), there is $\delta > 0$ such that, if $y \in \overline{N_G}$ and $|y_i - x_i| < \delta$ for all i, then $|\phi_t y_i - \phi_t x_i| < \varepsilon$ for all i. We now consider $\bar{\phi}_t$. Since $\bar{\phi}_t$ is either the identity or equal to ϕ_t, it is immediate that ϕ is continuous at (t, x) with respect to t. It remains to check continuity with respect to x.

Take $x \in N_G$. By Lemma 6.1.1, there is $\delta' > 0$ such that if $y \in \bigcup_{G' \not\subset G} N_{G'}$ and $|y_i - x_i| < \delta'$ for all i, then $y \in N_G$. $\bar{\phi}_t$ agrees with ϕ_t on N_G. Therefore, if $|y_i - x_i| < \min\{\delta, \delta'\}$ for all i, then $|\bar{\phi}_t y_i - \bar{\phi}_t x_i| = |\phi_t y_i - \phi_t x_i| < \varepsilon$ for all i. Thus $\bar{\phi}_t$ is continuous at (t, x).

Next take $x \in \partial N_G$. Then $\bar{\phi}_t x_i = x_i$. Hence if $|y_i - x_i| < \min\{\delta, \varepsilon\}$ for all i, we have either $\bar{\phi}_t y_i = y_i$ or $y_i \in \overline{N_G}$. Therefore $|\phi_t y_i - \phi_t x_i| < \varepsilon$ for all i. Thus $\bar{\phi}_t$ is continuous at (t, x).

Otherwise, $x \in \bigcup_{G' \not\subset G} N_{G'} \backslash \overline{N_G}$, which is open in $\bigcup_{G' \not\subset G} N_{G'}$. Then there is $\delta' > 0$ such that if $y \in \bigcup_{G' \not\subset G} N_{G'}$ and $|y_i - x_i| < \delta'$ for all i, then $y \notin N_G$. $\bar{\phi}_t$ acts as the identity outside of N_G. Therefore, if $|y_i - x_i| < \min\{\delta', \varepsilon\}$ for all i, then $|\phi_t y_i - \phi_t x_i| = |y_i - x_i| < \varepsilon$ for all i. □

We define the flow on connected components of the stress graph. If G has more than one non-trivial component, each component will follow its defined flow, in such a way that the edge lengths of the components increase at the same rate. If a component has no boundary edges, we enlarge it about the centre of mass of its vertices. If a component has one boundary edge, we enlarge it about the boundary vertex.

In the case $n = 3$, there are only six possible components with at least two boundary vertices. For convenience, we will use the labels x_1, x_2, x_3, but any permutations are defined in the same way.

1. The component where x_1 and x_2 are adjacent to each other and to the boundary. We choose the unique flow (up to reparametrisation) in which the angle between $x_2 - x_1$ and the x-axis is held constant. In the case that this angle is 0 and the discs have positive y-coordinate, we can describe this flow explicitly in terms of the radius $r = \tau(x)$ as $(x_1, x_2) = ((-r, \sqrt{1 - 2r}), (r, \sqrt{1 - 2r}))$.

2. The component where x_1 and x_2 are adjacent to each other and to the boundary, and x_3 is adjacent to x_2. We flow x_1 and x_2 as described above and keep the angle between $x_2 - x_1$ and $x_3 - x_1$ constant.

3. The graph G^* where x_1 is adjacent to x_2 and the boundary, and x_3 is adjacent to x_2 and the boundary, and the three graphs which have this as a subgraph. Since this stratum contains the critical configurations at radius $\frac{1}{3}$, we will discuss this further.

We will choose our order on the set of graphs so that we retract the strata in the order discussed here. Then everything retracts onto the set of strata $\overline{N_{G^*}} = \bigcup_{G \supset G^*} N_G$, numbered (3) above. We can describe this coordinate-wise by (r, θ, ϕ), where $r = \tau(x)$, 2θ is the angle between the radius containing x_1 and the radius containing x_3 (since both points have magnitude $1 - r$, neither is at the origin, so this is well-defined), and ϕ is the angle between the radius containing x_3 and the horizontal (see Fig. 6.1). If $x_3 = ((1-r)\cos\phi, (1-r)\sin\phi)$ and $x_1 = ((1-r)\cos(\phi + 2\theta), (1-r)\sin(\phi + 2\theta))$, then there are at most two possible positions for x_2.

We define a flow on this stratum, keeping ϕ constant. First, we determine the coordinate range for (r, θ). We will split the set of configurations into clockwise or anticlockwise, depending on the order of the points x_1, x_2, x_3 in the triangle whose vertices are these points. If they lie in a straight line, we count the configuration in both sets.

Proposition 6.1.3. *The coordinates (r, θ, ϕ) yield a configuration of $\overline{N_{G^*}}$ if and only if the following hold:*

1. *$r \leq (1-r)\sin\theta \leq 2r$, and*

2. *Either $(1-r)\cos\frac{\theta}{2} \geq r$ and the configuration is clockwise, or $(1-r)\sin\frac{\theta}{2} \geq r$ and the configuration is anticlockwise.*

Proof. First, by drawing the line between x_1 and x_3, we see that $\sin\theta = \frac{\frac{1}{2}|x_1 - x_3|}{1-r}$, thus $|x_1 - x_3| = 2(1-r)\sin(\theta)$. We must have $|x_1 - x_3| \geq 2\tau(x) = 2r$ by the definition of τ, and $|x_1 - x_3| \leq |x_1 - x_2| + |x_2 - x_3| = 4r$. These are sufficient to be able to place a point x_2 at a distance $2r$ from both points.

Now, assume without loss of generality that $\phi = 0$. Then $x_3 = (1 - r, 0)$. Since x_2 is equidistant from x_1 and x_3, it lies on the line through the origin which bisects

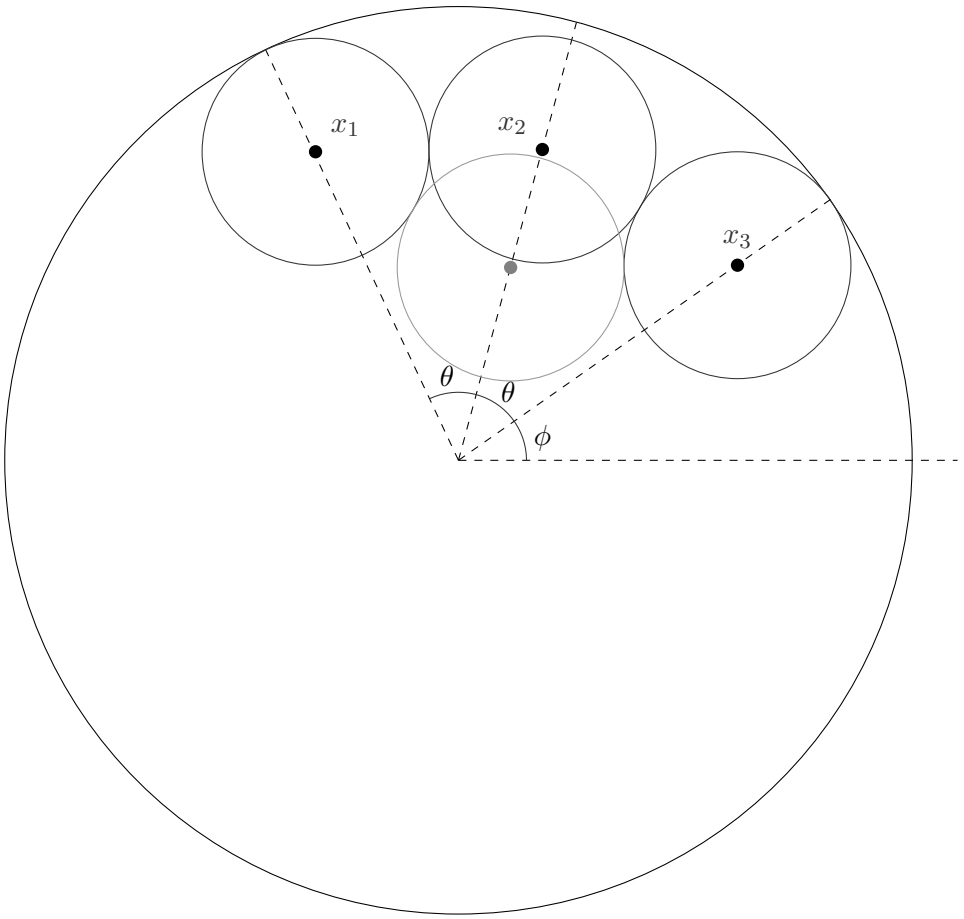

Figure 6.1: A configuration from the stratum $\overline{N_{G^*}} \subset \mathrm{Conf}_3$ with the angle coordinates θ, ϕ and the associated configuration of touching discs. The positions of x_1, x_3, which are defined by these angles and the value $r \coloneqq \tau(x)$, determine the position of x_2 up to a choice of two points: the labelled point, or the grey point. Then (r, θ, ϕ) determines a configuration of $\overline{N_{G^*}}$ up to a choice between two configurations.

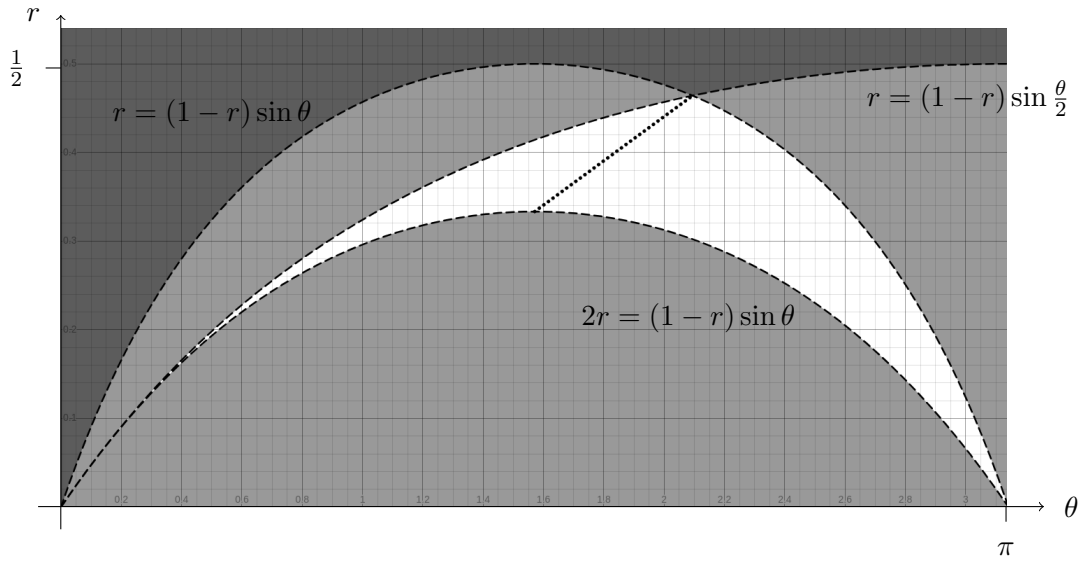

Figure 6.2: A cross-section, $\{\phi = \phi_0\}$, of the coordinate region corresponding to clockwise configurations of $\overline{N_{G^*}}$, for the coordinate system (r, θ, ϕ) given in Fig. 6.1. The region of possible coordinates is shown in white. A dotted line joins the points corresponding to the first and second critical configurations of Conf_3.

the angle $\angle x_1 0 x_3$, so $x_2 = (s\cos\theta, s\sin\theta)$ for some $s \in \mathbb{R}$. Then, we obtain a valid configuration of $\overline{N_{G^*}}$ if and only if $s^2 = |x_2|^2 \leq (1-r)^2$ and $(1-r-s\cos\theta)^2 + s^2\sin^2\theta = |x_3 - x_2|^2 = 4r^2$. Rearranging the latter, we get a pair of solutions $s_\pm = (1-r)\cos\theta \pm \sqrt{4r^2 - (1-r)^2\sin^2\theta}$. The configurations given by s_+ are the clockwise configurations, and s_- are anticlockwise. Then we have

$$\begin{aligned}
1 - r \geq s_+ &\Leftrightarrow (1-r)(1-\cos\theta) \geq \sqrt{4r^2 - (1-r)^2\sin^2\theta} \\
&\Leftrightarrow (1-r)^2(1-\cos\theta)^2 \geq 4r^2 - (1-r)^2\sin^2\theta \\
&\Leftrightarrow (1-r)^2(2-2\cos\theta) \geq 4r^2 \\
&\Leftrightarrow 4(1-r)^2\sin^2\frac{\theta}{2} \geq 4r^2 \\
&\Leftrightarrow (1-r)\sin\frac{\theta}{2} \geq r \quad .
\end{aligned}$$

(We can take the square root in the last step since $\frac{\theta}{2} \in \left(0, \frac{\pi}{2}\right)$, so all quantities are positive.) Similarly, $-(1-r) \leq s_-$ if and only if $(1-r)\cos\frac{\theta}{2} \geq r$. Finally, we have for all (r, θ) that $-(1-r)(1+\cos\theta) \leq \sqrt{4r^2 - (1-r)^2\sin^2\theta}$ and $(1-r)(1-\cos\theta) \geq -\sqrt{4r^2 - (1-r)^2\sin^2\theta}$, from which we deduce $s_+ > -(1-r)$ and $s_- < 1-r$ for all (r, θ). □

For each $\phi \in S^1$, the coordinate region relating to (r, θ) for the clockwise configurations of $\overline{N_{G^*}}$, restricted to the (r, θ)-plane, consists of the region shown in Fig. 6.2. The coordinate region for the anticlockwise configurations is found by reflection about the line $\theta = \frac{\pi}{2}$. In the full coordinate region, the clockwise and anticlockwise regions meet precisely along the surface $S = \{(r, \theta, \phi \mid 2r = (1 - r)\sin\theta\}$, which consists of the configurations in which x_2 lies on the line segment joining x_1 and x_3. The points of the form $\left(\frac{1}{3}, \frac{\pi}{2}, \phi\right) \in S$ correspond to the first critical radius.

We finish by recognising that we can easily define a continuous flow on $\overline{N_{G^*}}$ such that:

- All flow lines lie in a plane of constant ϕ,
- Configurations on S flow along on S to the first critical configuration,
- Configurations in the clockwise region flow near-parallel to S at small r, but converge towards the dotted line on Fig. 6.2 and follow it to the second critical radius, which corresponds to the configurations where the points form a triangle, with radius $2\sqrt{3} - 3$, and
- Configurations in the anticlockwise region behave in the same way.

$\dim \overline{N_{G^*}} = 3$ and $\dim S = 2$. Therefore S has codimension $3 - 2 = 1$, as required.

6.2 A candidate flow to generalise the proof for all n

In order to prove the conjecture for all n, we need to generalise our flow construction. The number of isomorphism classes of graphs on $n+1$ vertices quickly becomes prohibitively large, meaning we cannot define a flow on each isomorphism class individually as we did for the strata with more than two boundary vertices in §6.1. Instead, we will find a general formula for the flow. Using the notion that discs in contact push against each other from [11], we give to each edge of $N(x)$ a weight, so that the flow depends only on the direction and position of the edges of $N(x)$. We will first generalise, treating the stress graph as a special case of a *graph realisation* in D^2.

Definition 6.2.1. Let $G = (V \sqcup V', E)$ be a (not necessarily connected) graph, in which each vertex of V' is a leaf. A realisation of G inside D^2 is a pair of maps $(p\colon V \to D^2,\ p'\colon V' \to \partial D^2)$ such that each $v' \in V'$ has a unique neighbour, and this neighbour is an element of V and lies on the normal to ∂D^2 at v'.

Definition 6.2.2. Let $w = (w_e \colon (a,b) \to \mathbb{R})_{e \in E}$, $x = (x_v \colon (a,b) \to \overline{D^2})_{v \in V \sqcup V'}$ where $a \leq 0 \leq b$. Then x is a w-flow of (p, p') if all of the following hold:

1. $x(t)$ is a realisation of G inside D^2 for all $t \in (a,b)$
2. $x_v(0) = p(v)$ and $x_{v'}(0) = p'(v')$ for all $v \in V, v' \in V'$
3. $\dot{x}_v(t) = \sum_{uv \in E} w_{uv}(t)(x_v(t) - x_u(t))$ for all $v \in V$, $t \in \mathbb{R}$

The w-flow formalises the notion that the edges of G exert a force on the vertices at each end. Here, we are not using 'force' in the physical sense – the velocity (not the acceleration) of each vertex is proportional to the force on it. By definition, if there is a non-trivial map w such that $w_e \geq 0$ for all $e \in E$ and $\dot{x}_v(0) = 0$ for all $v \in V \sqcup V'$, then we regain the notion of a balanced stress graph. In this formalisation, there is also the possibility of a non-trivial map w such that $\dot{x}_v(0) = 0$ for all $v \in V \sqcup V'$, but there exists some $w_e < 0$. This motivates the idea of a *generalised balanced stress graph*, which we defined earlier in Def. 2.0.1. We have already calculated these for $n \leq 5$ in §2.

We want to define a w-flow such that $\dot{x}_v(0) = 0$ for all $v \in V \sqcup V'$ whenever the graph realisation with vertices at $\{x_v(0) \mid v \in V \sqcup V'\}$ is balanced. $\dot{x}_v(0) = 0$ for all $v \in V \sqcup V'$ if and only if $\sum_{v \in V \sqcup V'} |\dot{x}_v(0)|^2 = 0$, so we minimise this function over all non-trivial maps w. In order to avoid the trivial map, we choose some surface in $\mathbb{R}^E$ which avoids the origin. With a good choice of surface, we can also place restrictions on the behaviour of the edges of G away from the critical points.

Proposition 6.2.3. *Let P be be the hyperplane of $\mathbb{R}^E$ defined by $\sum_{e \in E} m_e \omega_e = 1$ for some $m_e \in [0, \infty)$, and let x be a w-flow for some $w \in P$. For each t, let*

$$f_{t,v} \colon \mathbb{R}^E \to T_{x_v(t)} D^2 \cong \mathbb{R}^2, \quad \omega \coloneqq (\omega_e)_{e \in E} \mapsto \sum_{uv \in E} \omega_{uv}(x_v(t) - x_u(t)) \quad ,$$

$$F_t = \sum_{v \in V} |f_{t,v}|^2$$

If $w(t)$ is a minimum of the restriction $F_t|_P$ for all t, then the lengths of the edges are increasing, and $m_{uu'} |x_v(t) - x_{v'}(t)|^2 - m_{vv'} |x_u(t) - x_{u'}(t)|^2$ is constant with respect to t for all $vv', uu' \in E$.

Remark 6.2.4. We have by definition $f_{t,v}(w(t)) = \dot{x}_v(t)$. Hence, if w fulfils the given condition, we will call it (G-)flow-minimising and x (G-)minimal. The flow is unchanged (except for speed) under rescaling, so the choice of hyperplane P is a normalisation.

Remark 6.2.5. Being a sum of squares, F_t is convex, so all stationary points are global minima, and the set of global minima is convex.

Remark 6.2.6. A stress graph has the property that, for all $uu', vv' \in E$,

$$\frac{|x_u - x_{u'}|^2}{|x_v - x'_v|^2} = \begin{cases} 1 & \text{if both edges are interior or both edges are boundary} \\ 4 & \text{if } uu' \text{ is interior and } vv' \text{ is boundary} \end{cases} .$$

Therefore, if we set $m_e = 1$ for all interior edges and $m_e = \frac{1}{4}$ for all boundary edges, then this ratio remains constant. Thus no edges disappear from the stress graph, so this is a well-defined flow on the stratum $\overline{N_G} \subset \mathrm{Conf}_n$ as understood in §6.1.

Proof of Prop. 6.2.3. Suppose $w(t)$ is a minimum of $F_t|_P$. Then, by the Lagrange multiplier theorem, there is $\lambda \in \mathbb{R}$ such that $\lambda \nabla P = \nabla F_t$ at $\omega = w(t)$. That is, for all $e = vv' \in E$,

$$\lambda m_e = \lambda \frac{\partial}{\partial \omega_e} \left(\sum_{e \in E} m_e \omega_e - 1 \right) = \frac{\partial F_t}{\partial \omega_e} \quad .$$

In the case $v, v' \in V$,

$$\begin{aligned} \frac{\partial F_t}{\partial \omega_e} &= \frac{\partial}{\partial \omega_e} \left(|f_{t,v}|^2 + |f_{t,v'}|^2 \right) \\ &= 2 \left(f_{t,v}(w(t)) \cdot \frac{\partial f_{t,v}}{\partial \omega_e} + f_{t,v'}(w(t)) \cdot \frac{\partial f_{t,v'}}{\partial \omega_e} \right) \\ &= 2 \left(\dot{x}_v(t) \cdot (x_v(t) - x_{v'}(t)) + \dot{x}_{v'}(t) \cdot (x_{v'}(t) - x_v(t)) \right) \\ &= 2 \left(\dot{x}_v(t) - \dot{x}_{v'}(t) \right) \cdot (x_v(t) - x_{v'}(t)) \\ &= \frac{\mathrm{d}}{\mathrm{d}t} |x_v(t) - x_{v'}(t)|^2 \quad . \end{aligned}$$

Otherwise, one end of e (say v') is in V', in which case

$$\begin{aligned} \frac{\partial F_t}{\partial \omega_e} &= \frac{\partial}{\partial \omega_e} |f_{t,v}|^2 \\ &= 2 f_{t,v}(w(t)) \cdot \frac{\partial f_{t,v}}{\partial \omega_e} \\ &= 2 \dot{x}_v(t) \cdot (x_v(t) - x_{v'}(t)) \quad . \end{aligned}$$

Since $x_v(t)$ lies on the normal to ∂D^2 at $x_{v'}(t)$ and $x_{v'}(s) \in \partial D^2$ for all s in the domain of x, it follows that $\dot{x}_{v'}(t) \cdot (x_v(t) - x_{v'}(t)) = 0$, so again, we have

$$\frac{\partial F_t}{\partial \omega_e} = 2 \left(\dot{x}_v(t) - \dot{x}_{v'}(t) \right) \cdot (x_v(t) - x_{v'}(t)) = \frac{\mathrm{d}}{\mathrm{d}t} |x_v(t) - x_{v'}(t)|^2 \quad .$$

This proves the second claim.

To show that the lengths are increasing, we need to show that $\frac{\mathrm{d}}{\mathrm{d}t}|x_v(t) - x_{v'}(t)|^2 \geq 0$, or equivalently that $\lambda \geq 0$. We have

$$\begin{aligned}\lambda &= \lambda \nabla P \cdot (\omega_e)_{e\in E} \\ &= \nabla F_t \cdot (\omega_e)_{e\in E} \quad .\end{aligned}$$

But since F_t is a positive semi-definite quadratic form, it can be orthogonally diagonalised with non-negative coefficients, by the Principal Axis Theorem: that is, there is an orthonormal coordinate system $(\gamma_e)_{e\in E}$ such that $F_t = \sum_{e\in E} c_e \gamma_e^2$, with $c_e \geq 0$. Thus we have

$$\lambda = \sum_{e\in E} 2c_e\gamma_e^2 \geq 0 \quad . \qquad \square$$

Remark 6.2.7. We observe from the proof that $m_{vv'}\lambda = \frac{\mathrm{d}}{\mathrm{d}t}|x_v(t) - x_{v'}(t)|^2$. In the case of a stress graph, weighted as in Remark 6.2.6, this yields $\lambda = \frac{\mathrm{d}}{\mathrm{d}t}4r^2$, $r = \tau(x)$.

We would hope to use this flow to retract maps $M \to \mathrm{Conf}_n$ onto $\mathrm{Conf}_{n,r}$ for low-dimensional manifolds M for the proof of Conjecture 6.0.2. In order to do this, we would need to address the following questions:

- Is the flow-minimising w-flow continuous on Conf_n, or do we need to retract it stratum by stratum as in §6.1? If the latter, are there any configurations which do not eventually flow towards a generalised critical configuration?
- Are there configurations which are not generalised balanced for which the minimum of $F_t|P$ is achieved at more than one ω? Will these give different flows, and if so, how do we make a consistent choice for $w(t)$?
- What do the downward manifolds of the phantom critical points look like? Are there phantom critical radii below the first critical radius (or in general, the critical radius of interest), and how much do they obstruct the flow?

We finish by giving an example of the flow on a stratum of Conf_4.

Example 6.2.8. Let $x \in \mathrm{Conf}_4$ be a configuration whose stress graph is a 4-cycle, with the points in anticlockwise order and with no boundary edges. Then in particular the stress graph is a rhombus of side length $2r$, $r = \tau(x)$. Let $\theta \in \left(\frac{\pi}{3}, \frac{2\pi}{3}\right)$ denote the internal

angle at x_1, and let w_i be the weight on the edge joining x_{i-1} to x_i ($i \in \mathbb{Z}/4\mathbb{Z}$). Then

$$\begin{aligned} f_{t,1}(\omega) &= \omega_1(x_1 - x_4) + \omega_2(x_1 - x_2) \quad , \\ f_{t,2}(\omega) &= \omega_2(x_2 - x_1) + \omega_3(x_2 - x_3) \quad , \\ f_{t,3}(\omega) &= \omega_3(x_3 - x_2) + \omega_4(x_3 - x_4) \quad , \text{ and} \\ f_{t,4}(\omega) &= \omega_4(x_4 - x_3) + \omega_1(x_4 - x_1) \quad . \end{aligned}$$

Thus

$$\begin{aligned} \lambda &= \frac{\partial}{\partial \omega_1} F_t \\ &= \frac{\partial}{\partial \omega_1} \left(|f_{t,1}|^2 + |f_{t,4}|^2 \right) \\ &= 2(x_1 - x_4) \cdot f_{t,1}(\omega) + 2(x_4 - x_1) \cdot f_{t,4}(\omega) \\ &= 2\omega_1 |x_1 - x_4|^2 + 2\omega_2 (x_1 - x_4) \cdot (x_1 - x_2) + 2\omega_4 (x_4 - x_1) \cdot (x_4 - x_3) + 2\omega_1 |x_4 - x_1|^2 \\ &= 8r^2(\omega_1 + \omega_2 \cos\theta - \omega_4 \cos\theta + \omega_1) \\ &= 8r^2(2\omega_1 + (\omega_2 - \omega_4)\cos\theta) \end{aligned}$$

and similarly

$$\begin{aligned} \lambda &= \frac{\partial}{\partial \omega_2} F_t \\ &= 8r^2(2\omega_2 + (\omega_1 - \omega_3)\cos\theta) \\ \lambda &= \frac{\partial}{\partial \omega_3} F_t \\ &= 8r^2(2\omega_3 + (\omega_4 - \omega_2)\cos\theta) \\ \lambda &= \frac{\partial}{\partial \omega_4} F_t \\ &= 8r^2(2\omega_4 + (\omega_3 - \omega_1)\cos\theta) \quad . \end{aligned}$$

The equations have a unique solution $\omega_1 = \omega_2 = \omega_3 = \omega_4 = \frac{\lambda}{16r^2}$, and normalisation gives $4\frac{\lambda}{16r^2} = 1$, that is $\frac{\mathrm{d}}{\mathrm{d}t} 4r^2 = \lambda = 4r^2$.

Thus we have $w(t) = \left(\frac{1}{4}, \frac{1}{4}, \frac{1}{4}, \frac{1}{4}\right)$ and $\dot{x}_i(t) = f_{t,i}(w(t))$ for all $i \in \{1, 2, 3, 4\}$. We can

use this to find $\frac{\mathrm{d}}{\mathrm{d}t}\cos\theta$.

$$\begin{aligned}
\frac{\mathrm{d}}{\mathrm{d}t}4r^2\cos\theta &= \frac{\mathrm{d}}{\mathrm{d}t}\left((x_1-x_4)\cdot(x_1-x_2)\right)\\
&= (\dot{x}_1-\dot{x}_4)\cdot(x_1-x_2)+(x_1-x_4)\cdot(\dot{x}_1-\dot{x}_2)\\
&= \frac{1}{4}\left((x_1-x_4)+(x_1-x_2)-(x_4-x_3)-(x_4-x_1)\right)\cdot(x_1-x_2)\\
&\quad +\frac{1}{4}(x_1-x_4)\cdot\left((x_1-x_4)+(x_1-x_2)-(x_2-x_1)-(x_2-x_3)\right)\\
&= \frac{4r^2}{4}\left(\cos\theta+1-1-(-\cos\theta)+1+\cos\theta-(-\cos\theta)-1\right)\\
&= 4r^2\cos\theta \quad .
\end{aligned}$$

Then

$$4r^2\cos\theta = \frac{\mathrm{d}}{\mathrm{d}t}4r^2\cos\theta = \cos\theta\frac{\mathrm{d}}{\mathrm{d}t}4r^2 + 4r^2\frac{\mathrm{d}}{\mathrm{d}t}\cos\theta = 4r^2\cos\theta + 4r^2\frac{\mathrm{d}}{\mathrm{d}t}\cos\theta$$

That is, $4r^2\frac{\mathrm{d}}{\mathrm{d}t}\cos\theta = 0$, hence θ is constant. The flow of the configuration is an enlargement.

Bibliography

[1] H. Alpert. Restricting cohomology classes to disk and segment configuration spaces. *Topology and its Applications*, 230(2):51–76, 2016.

[2] H. Alpert. Discrete configuration spaces of squares and hexagons. *Journal of Applied and Computational Topology*, 4(2):263–280, 2019.

[3] H. Alpert. Generalized representation stability for disks in a strip and no-k-equal spaces. *arXiv:2006.01240*, 2020.

[4] H. Alpert, U. Bauer, M. Kahle, R. MacPherson, and K. Spendlove. Homology of configuration spaces of hard squares in a rectangle. *Algebraic and Geometric Topology*, 23(6):2593–2626, 2023.

[5] H. Alpert, M. Kahle, and R. MacPherson. Configuration spaces of disks in an infinite strip. *Journal of Applied and Computational Topology*, 5(3):357–390, 2021.

[6] H. Alpert, M. Kahle, and R. Macpherson. Asymptotic betti numbers for hard squares in the homological liquid regime. *International Mathematics Research Notices*, 2024:8240–8263, 2024.

[7] H. Alpert and F. Manin. Configuration spaces of disks in a strip, twisted algebras, persistence, and other stories. *Geometry and Topology*, 28(2):641–699, 2021.

[8] A. Andreotti and T. Frankel. The lefschetz theorem on hyperplane sections. *Annals of Mathematics*, 69(3):713–717, 1959.

[9] L. Angelani, L. Casette, M. Pettini, G. Ruocco, and F. Zamponi. Topology and phase transitions: From an exactly solvable model to a relation between topology and thermodynamic. *Physical Review E*, 71(3):036152, 2005.

[10] V. I. Arnol'd. The cohomology ring of the coloured braid group. *Mathematical Notes of the Academy of Sciences of the USSR*, 5(2):138–140, 1969.

[11] Y. Baryshnikov, P. Bubenik, and M. Kahle. Min-type morse theory for configuration spaces of hard spheres. *International Mathematical Research Notices*, 2014(9):2577–2592, 2014.

[12] K. Borsuk. Sur les prolongements des transformations continues. *Fundamnta Mathmaticae*, 28(1):99–110, 1937.

[13] G. Carlsson, J. Gorham, M. Kahle, and J. Mason. Computational topology for configuration spaces of hard disks. *Physical Review E*, 85(1):011303, 2012.

[14] D. Eberly. Distance from a point to an ellipse, an ellipsoid, or a hyperellipsoid. `https://www.geometrictools.com/Documentation/Documentation.html`, 2013. Accessed: 4th September 2023.

[15] E. Fadell and L. Neuwirth. Configuration spaces. *Mathematica Scandinavica*, 10:111–118, 1962.

[16] M. Farber. *Invitation to Topological Robotics*, chapter 4, pages 87–123. European Mathematical Society, 2004.

[17] F. Fodor. The densest packing of 19 congruent circles in a circle. *Geometriae Dedicata*, 74:139–145, 1999.

[18] F. A. Garside. The braid group and other groups. *The Quarterly Journal of Mathematics*, 20(1):235–254, 1969.

[19] M. A. Guest. Morse theory in the 1990's. In M. R. Bridson and S. M. Salamon, editors, *Invitations to Geometry and Toplogy*, pages 146–207. Oxford University Press, Oxford, 2002.

[20] O. Hanner. Some theorems on absolute neighbourhood retracts. *Arkiv för Matematik*, 1(30):389–408, 1951.

[21] V. L. Hansen. *Braids and Coverings*, chapter I, pages 2–49. Cambridge University Press, 1989.

[22] A. Hatcher. *Algebraic Topology*. Cambridge University Press, 2001.

[23] M. W. Hirsch. *Differential Topology*, chapter 3.2, pages 74–84. Springer-Verlag, 1933.

[24] E.-K. Lee. A positive presentation for the pure braid group. *Journal of the Chungcheong Mathematical Society*, 23(3):555–561, 2010.

[25] S. Lojasiewicz. Triangulation of semi-analytic sets. *Annali della Scuola Normale Superiore di Pisa, Classe di Scienze 3 e série*, 18(4):449–474, 1964.

[26] H. Löwen. Fun with hard spheres. In K. R. Mecke and D. Stoyan, editors, *Statistical Physics and Spacial Physics*, pages 295–331. Springer, Berlin, Heidelberg, 2000.

[27] J. Milnor. *Morse Theory*, chapter I.2–3, pages 1–24. Cambridge University Press, 1989.

[28] L. Plachta. Configuration spaces of squares in a rectangle. *Algebraic and Geometric Topology*, 21(3):1445–1478, 2021.

[29] E. H. Spanier. *Algebraic Topology*, chapter I.4, pages 27–32. McGraw-Hill, 1966.

[30] E. Specht. The best known packings of equal circles in a circle (complete up to n = 2600). `http://hydra.nat.uni-magdeburg.de/packing/cci/cci.html`, 2021. Accessed: 9th March 2023.

[31] A. C. R. Teixeira and D. A. Stariolo. Topological hypothesis on phase transitions: The simplest case. *Physical Review E*, 70(1):016113, 2004.

[32] N. Wawrykow. On the symmetric group action on rigid disks on a strip. *Journal of Applied and Computational Topology*, 7(3):427–472, 2022.

[33] N. Wawrykow. Representation stability for disks in a strip. *Journal of Topology and Analysis*, 0(0), 2024.

[34] N. Wawrykow. The topological complexity of the ordered configuration space of disks in a strip. *Proceedings of the American Mathematical Society Series B*, 11:638–652, 2024.

Appendix A

Braid calculations for §4.4

Here, we give the full calculations of the underlying braids of b_i, as given in §4.4. For easier comprehension, we will sometimes use brackets to mark the generators to which the braid operations are applied on each line.

$$
\begin{aligned}
(b_1, 0) &\mapsto \sigma_1\sigma_2\sigma_3\sigma_3^{-1}\sigma_2\sigma_1^{-1} \\
&= \sigma_1\sigma_2\sigma_2\sigma_1^{-1} \\
&= s_{13} \quad , \\
(b_3, 0) &\mapsto \sigma_1\sigma_2\sigma_3\sigma_1^{-1}(\sigma_3^{-1}\sigma_1\sigma_2\sigma_3\sigma_1^{-1})\sigma_3^{-1} \\
&= \sigma_1\sigma_2\sigma_2\sigma_1^{-1} \\
&= s_{13} \quad , \\
(b_2, 0) &\mapsto \sigma_1\sigma_2\sigma_3(\sigma_3^{-1}\sigma_1\sigma_2\sigma_3\sigma_1^{-1})^{-1}\sigma_3\sigma_2^{-1} \\
&= \sigma_1\sigma_2\sigma_1\sigma_2^{-1}\sigma_3\sigma_1^{-1}\sigma_3\sigma_2^{-1} \\
&= \sigma_2\sigma_1\sigma_2\sigma_2^{-1}\sigma_3\sigma_1^{-1}\sigma_3\sigma_2^{-1} \\
&= \sigma_2\sigma_3\sigma_3\sigma_2^{-1} \\
&= s_{24} \quad ,
\end{aligned}
$$

$$
\begin{aligned}
(b_4, 0) &\mapsto \sigma_1\sigma_2\sigma_3\sigma_2^{-1}\sigma_1(\sigma_3^{-1}\sigma_1\sigma_2\sigma_3\sigma_1^{-1})^{-1} \\
&= \sigma_1\sigma_3^{-1}\sigma_2\sigma_3\sigma_1\sigma_3^{-1}\sigma_1\sigma_2^{-1}\sigma_3\sigma_1^{-1} \\
&= \sigma_1\sigma_3^{-1}\sigma_2\sigma_1\sigma_1\sigma_2^{-1}\sigma_1^{-1}\sigma_3 \\
&= \sigma_1\sigma_3^{-1}\sigma_2\sigma_1\sigma_2^{-1}\sigma_1^{-1}\sigma_2\sigma_3 \\
&= \sigma_1\sigma_3^{-1}\sigma_1^{-1}\sigma_2\sigma_1\sigma_1^{-1}\sigma_2\sigma_3 \\
&= \sigma_3^{-1}\sigma_2\sigma_2\sigma_3 \\
&= s_{24} \quad .
\end{aligned}
$$

In the main body, we cite [18, Thm. 7], which states that $(\sigma_1\sigma_2\sigma_3\sigma_1\sigma_2\sigma_1)^2$ generates the centre of Br_4. We claim that $(\sigma_1\sigma_2\sigma_3)^4$ also generates the centre. We can show the equivalence of these statements using the braid relations to show these are the same element:

$$
\begin{aligned}
(\sigma_1\sigma_2\sigma_3)^4 &= \sigma_1\sigma_2\sigma_3\sigma_1\sigma_2(\sigma_3\sigma_1)\sigma_2\sigma_3\sigma_1\sigma_2\sigma_3 \\
&= \sigma_1\sigma_2\sigma_3\sigma_1\sigma_2\sigma_1(\sigma_3\sigma_2\sigma_3)\sigma_1\sigma_2\sigma_3 \\
&= \sigma_1\sigma_2\sigma_3\sigma_1\sigma_2\sigma_1\sigma_2\sigma_3(\sigma_2\sigma_1\sigma_2)\sigma_3 \\
&= \sigma_1\sigma_2\sigma_3\sigma_1\sigma_2\sigma_1\sigma_2(\sigma_3\sigma_1)\sigma_2(\sigma_1\sigma_3) \\
&= \sigma_1\sigma_2\sigma_3\sigma_1\sigma_2\sigma_1\sigma_2\sigma_1(\sigma_3\sigma_2\sigma_3)\sigma_1 \\
&= \sigma_1\sigma_2\sigma_3\sigma_1\sigma_2\sigma_1(\sigma_2\sigma_1\sigma_2)\sigma_3\sigma_2\sigma_1 \\
&= \sigma_1\sigma_2\sigma_3\sigma_1\sigma_2\sigma_1\sigma_1\sigma_2(\sigma_1\sigma_3)\sigma_2\sigma_1 \\
&= \sigma_1\sigma_2\sigma_3\sigma_1\sigma_2\sigma_1\sigma_1\sigma_2\sigma_3\sigma_1\sigma_2\sigma_1 \\
&= (\sigma_1\sigma_2\sigma_3\sigma_1\sigma_2\sigma_1)^2 \quad .
\end{aligned}
$$

We claim also that $(e,1) \mapsto s_{12}s_{23}s_{13}s_{34}s_{24}s_{14}$ in PBr_4, which can be proven thus:

$$\begin{aligned}
(e,1) &\mapsto (\sigma_1\sigma_2\sigma_3)^4 \\
&= \sigma_1\sigma_2(\sigma_3\sigma_1)\sigma_2\sigma_3\sigma_1\sigma_2\sigma_3\sigma_1\sigma_2\sigma_3 \\
&= \sigma_1\sigma_2\sigma_1(\sigma_3\sigma_2\sigma_3)\sigma_1\sigma_2\sigma_3\sigma_1\sigma_2\sigma_3 \\
&= \sigma_1\sigma_2\sigma_1\sigma_2\sigma_3(\sigma_2\sigma_1\sigma_2)\sigma_3\sigma_1\sigma_2\sigma_3 \\
&= \sigma_1\sigma_2\sigma_1\sigma_2(\sigma_3\sigma_1)\sigma_2(\sigma_1\sigma_3)\sigma_1\sigma_2\sigma_3 \\
&= \sigma_1(\sigma_2\sigma_1\sigma_2)\sigma_1(\sigma_3\sigma_2\sigma_3)\sigma_1\sigma_1\sigma_2\sigma_3 \\
&= \sigma_1\sigma_1\sigma_2\sigma_1\sigma_1\sigma_2\sigma_3\sigma_2\sigma_1\sigma_1\sigma_2\sigma_3 \\
&= \sigma_1^2\sigma_2^2(\sigma_2^{-1}\sigma_1^2\sigma_2)\sigma_3^2(\sigma_3^{-1}\sigma_2^2\sigma_3)(\sigma_3^{-1}\sigma_2^{-1}\sigma_1^2\sigma_2\sigma_3) \\
&= s_{12}s_{23}s_{13}s_{34}s_{24}s_{14} \quad .
\end{aligned}$$